



IEAGHG Technical Report 2023-05

Classification of Total Storage Resources and Storage Coefficients

December 2023

Disclaimer

The GHG TCP, also known as the IEAGHG, is organised under the auspices of the International Energy Agency (IEA) but is functionally and legally autonomous. Views, findings and publications of the IEAGHG do not necessarily represent the views or policies of the IEA Secretariat or its individual member countries.

The views and opinions of the authors expressed herein do not necessarily reflect those of the IEAGHG, its members, the organisations listed below, nor any employee or persons acting on behalf of any of them. In addition, none of these make any warranty, express or implied, assumes any liability or responsibility for the accuracy, completeness or usefulness of any information, apparatus, product of process disclosed or represents that its use would not infringe privately owned rights, including any parties intellectual property rights. Reference herein to any commercial product, process, service or trade name, trade mark or manufacturer does not necessarily constitute or imply any endorsement, recommendation or any favouring of such products. IEAGHG expressly disclaims all liability for any loss or damage from use of the information in this document, including any commercial or investment decisions.

Copyright © IEA Environmental Projects Ltd. (IEAGHG) 2023. All rights reserved.

Acknowledgements & Citations

The report should be cited as follows: 'IEAGHG, "Classification of Total Storage Resources and Storage Coefficients", 2023-05, December 2023.'

This report describes work undertaken by the British Geological Survey (BGS) on behalf of IEAGHG. The principal researchers were H. Vosper, J.C. White, M.C. Akhurst, K.L. Kirk, G.A. Williams, L. Abel, and C.J. Vincent.

To ensure the quality and technical integrity of the research undertaken by IEAGHG each study is managed by an appointed IEAGHG manager. The report is also reviewed by a panel of independent technical experts before its release.

The IEAGHG manager for this report was Nicola Clarke. The expert reviewers for this report were Jamie Andrews – Equinor, David Bason - CO2CRC, George Koperna - Advanced Resources International, Wes Peck – EERC, Owain Tucker – Shell, and Peter Zweigel – Equinor.

Further information can be obtained by contacting IEAGHG at:

Email: mail@ieaghg.org **Phone:** +44 (0)1242 802911

Address: IEAGHG, Pure Offices, Hatherley Lane, Cheltenham, GL51 6SH, UK

About IEAGHG

Blazing the way to net zero with leading CCS research. *We advance technology to accelerate project development & deployment.*

We are at the forefront of cutting-edge carbon, capture and storage (CCS) research. We advance technology that reduces carbon emissions and accelerates the deployment of CCS projects by improving processes, reducing costs, and overcoming barriers. Our authoritative research is peer-reviewed and widely used by governments and industry worldwide. As CCS technology specialists, we regularly input to organisations such as the IPCC and UNFCCC, contributing to the global net-zero transition.

About the IEA

The International Energy Agency (IEA), an autonomous agency, was established in November 1974. Its primary mandate is twofold: to promote energy security amongst its member countries through collective response to physical disruptions in oil supply, and provide authoritative research and analysis on ways to ensure reliable, affordable and clean energy. The IEA created Technology Collaboration Programmes (TCPs) to further facilitate international collaboration on energy related topics.



CLASSIFICATION OF TOTAL STORAGE RESOURCES AND STORAGE COEFFICIENTS

(IEA/CON/22/286)

The CO₂ Storage Resources Management System (SRMS) is a classification scheme to quantify, classify and categorise CO₂ storage resources. It comprises ‘total storage resources’, which are understood as maximum (theoretical) storage quantities that could ever be accommodated in the subsurface. Comprising maximum mobile CO₂ in structural/stratigraphic traps, maximum residually trapped CO₂ in other parts of the formation, and maximum dissolution potential in remaining formation water. ‘Storable quantities’ are understood as accessible from one or several current or future projects. It is the sum of capacity, contingent and prospective resources. The concept of ‘storage coefficient’ ‘E’ is the ratio of the subsurface volume of CO₂ storable quantities to either the total storage resources or the pore volume. The calculation is arguably complicated as E is impacted by lithological heterogeneity, trapping structures, boundary conditions, injection rates, well spacing, fluid properties etc. Due to its complexity, there is much controversy on how to estimate E, with some arguing it should not be used at all and that reservoir simulation is a better path. However, estimates for E are used in most regional mapping studies. This study explores storage resource classification schemes and their evolution in understanding, the calculation of storage resources and the storage coefficient. This is explored in terms of calculating E for CO₂ storage sites, through flow modelling and analytical solutions.

Key Messages

- The classification of storage resources and associated schemes have become more complex over time and more aligned to the requirements of operational storage with the SRMS becoming the industry standard.
- Storage coefficients are vital for quantifying accessible storage resources, standard methodologies have been presented and examples of usage within national and international databases. 97% of global storage is of a prospective nature and having quick screening criteria are useful in initial basin screening.
- Data from CO₂ storage sites can be used to calculate storage efficiency through time by measuring plume area on time-lapse seismic data. These results can then be compared to numerical models and analytical approximations.
- Numerical simulations were run with key parameters identified through publicly available modelling studies with storage coefficients evaluated for each case.
 - Structure and injection rates have a significant influence on storage coefficients
 - The evolution of the storage coefficient through a 30 year injection period and 70 year post injection period was modelled and in the case of a dipping aquifer the storage coefficient peaks at 20-30 years and then gradually reduces whereas a structural closure sees a more stable post injection storage coefficient.
 - Water production did not impact the storage coefficient, but modelling an open system may have impacted the results.
 - Hysteresis may not impact storage coefficient significantly, but it does cause the distribution of CO₂ with more trapped in deeper layers of the reservoir increasing storage security.
- Analytical models from the literature have been modified to estimate storage coefficients and compared to modelled and data from the storage sites. At first pass they give a quick and easy estimate for lower stages of development but results slightly underperform. Another approach using dimensionless variables to emulate or build upon some of the numerical modelling



work may provide a way to estimate storage coefficients for a cheaper cost than using full dynamic simulations.

Background to the Study

The Society of Petroleum Engineers (SPE) have developed the SRMS, the CO₂ Storage Resources Management System, which was published in 2017. It is based on the concepts of Total Storage Resources and Storable Resources and establishes technically based capacity and resources evaluation standards.

The SRMS provides terms and clear definitions in order to classify storage quantities and provides context for investment. The structure of the SRMS involves classification and categorisation of a storage estimate. Classification is based on maturation of a project and major classifications are discovered (contingent storage resources) vs. undiscovered (prospective storage resources) and commercial vs. sub-commercial. The categorisation is based on certainty in an estimate and the major categorisations are low, most-likely (best) and high.

The SRMS provides a methodology for stakeholders to follow to compare between projects and could help reduce financial risks associated with estimates of storage.

Important concepts of the SRMS include ‘total storage resources’, which are understood as maximum (theoretical) storage quantities that could ever be accommodated in the subsurface. They can be decomposed into maximum mobile CO₂ in structural/stratigraphic traps, maximum residually trapped CO₂ in other parts of the formation, and maximum dissolution potential in remaining formation water. ‘Storable quantities’ are understood as accessible from one or several current or future projects. It sums to capacity, contingent and prospective resources. The concept of ‘storage coefficient’ is the ratio of the subsurface volume of CO₂ storable quantities to either the total storage resources or the pore volume.

The purpose of a storage coefficient is to assign a value to that fraction of a given pore volume in which CO₂ can be effectively stored (Gorecki et al, 2009). This work in 2009 developed storage coefficients to determine the storage resource in saline formations. Other work by Peck et al (2018) looked at quantifying CO₂ storage efficiency factors in hydrocarbon reservoirs using simulation models involving fluvial clastic and shallow shelf carbonate depositional environments and provides practical information that can be used to quantify CO₂ storage resource estimates in oil reservoirs during CO₂-EOR operations.

These two examples of work on storage resources and coefficients go some way in exploring total storage resources which is of utmost importance to site developers, operators and other stakeholders.

Scope of Work

The aim of the study is firstly to provide an up-to-date review of previous work on CO₂ storage resource estimation and storage coefficients and provide a platform to identify a set of realistic parameters for study. It aims to explore what storage resources and storage coefficients may look like in various types of geological formations in a saline aquifer and what the main impacting parameters are. Using flow simulations, the study will derive ranges of total storage resources and storage coefficients from a variety of development schemes, including with and without water extraction, in a range of parameterised geological formations. Analytical solutions are then to be found to approximate the physics, geology and geometry of the system.

Approach. The study was approached in the following ways.



The first part of the report details: the main methods of calculating CO₂ storage resources in saline and depleted hydrocarbon reservoirs; how resources are classified and how these have been developed and refined over time leading to the Storage Resource Management System (SRMS); and also how these methods have been applied to national programs of cataloguing CO₂ storage resources.

Storage efficiency was explored through a literature review of previous modelling studies and key parameters which impact how CO₂ accesses the pore space in a reservoir have been drawn out with the view to directing the modelling work in the second part of the report. Storage efficiency is shown to be influenced by the following key subsurface parameters: geometry of the reservoir, depth, temperature, relative permeability, boundary conditions, number of wells, injection rate and reservoir heterogeneity.

Storage efficiencies are then calculated in two ways, by using time-lapse seismic data from three CO₂ storage projects (Sleipner, Snøhvit and Ketzin) and by dynamic flow modelling (designed based on parameters identified from previous published studies) investigating the impact of structure, injection rate, water production and hysteresis on the resulting storage efficiencies over the span of a 30 year injection period and 70 year post injection period.

Analytical modelling work was then applied, calculating storage coefficients across a wide parameter space. This may be useful for assessing sites at low storage readiness levels where large amounts of site specific data are not yet available. Analytical expressions for the storage coefficient were derived for simple models of CO₂ injection for a flat and dipping caprock and compared with case studies and numerical modelling results.

Findings of the Study

Storage Resource Estimation Methodologies

Methods to assess CO₂ storage resources have been proposed and developed since 2007, initially by the Carbon Sequestration Leadership Forum Task Force (CSLF) and US Department of Energy (US DOE). These methods have been variably applied to national and regional storage potential screening assessments. Both groups present almost identical methodologies with only a few minor discrepancies for estimating storage resource in saline aquifers. However, in a review of methods to calculate national geological storage assessments Vincent et al (2017) conclude that the methods employed vary widely and the process is in constant evolution – their recommendations were that tabulated parameters (such as depth, porosity, formation thickness, net sandstone to gross thickness and temperature) be included, then as methods advance new calculations can be applied and allow the comparison of results on an equal basis.

Storage Resource Classifications

The classification of storage resources has evolved over time, starting with parallel work undertaken by the CSLF and by the US DOE and IEAGHG (with EERC), eventually leading to the incorporation of concepts from the hydrocarbon industry and the Petroleum Resources Management System and then leading the development under the SPE of the Storage Resource Management System in 2017 (SRMS). The early work was based on a resource pyramid whereby as you move upwards in understanding of the physical, technical, commercial constraints then storage resource will increase in certainty and potentially decrease in size (or access only a portion of the total available storage resource), but this is also subject to other factors such as site appraisal, regulations and economics. In the first instance the theoretical capacity as introduced by Bachu et al (2007) and later termed Total Storage Resource assumes the entire pore volume (minus the irreducible water saturation) is accessible to CO₂ storage, whereas the effective capacity is the theoretical capacity multiplied by a capacity co-efficient (or storage



efficiency co-efficient). Gorecki et al (2009) built on previous work with the addition of defining storage resource and storage capacity (whereby injection of CO₂ within a storage unit is viable under economic conditions, either current or future). Further refinement led to the SRMS, a two-axis system whereby the total storage resource is geologically defined and development scheme co-dependent, with technical uncertainty on the x-axis and commercial and regulatory uncertainty on the y-axis. It has better defined uncertainty in storage resource classification and is becoming the internationally standard scheme.

The SRMS however is a project based scheme and therefore the large majority of regional studies of storage resources will fall in the undiscovered category (Akhurst et al 2021). In their assessment of the availability of CO₂ storage resources the Oil and Gas Climate Initiative (OGCI, 2017) conclude that 97% of the global storage resource is prospective in nature. Storage Readiness Levels as defined by Akhurst et al (2021) can communicate to stakeholders technical understanding, progress toward regulatory requirements for CO₂ storage and injection, and planning of a site as a component of a commercial CO₂ storage project, particularly to those unfamiliar with CO₂ storage planning and permitting.

Storage Resource Calculations

The amount of CO₂ that is able to fill a storage reservoir is dependent upon many factors. Of the total available pore space in the host reservoir only a portion of this is accessible. This can be dependent on a number of factors including immiscible displacement physics, irreducible water saturation, segregation from CO₂ buoyancy/gravity forces, geological heterogeneity, reservoir compartmentalisation, limits to permissible pressurisation, distance from injection wells, and the presence of resident fluids amongst others.

Methods to calculate storage resources vary but all include a storage efficiency coefficient which provides a robust estimation of the storage potential of the geological domain under consideration. Put simply, the storage efficiency coefficient is a ratio or percentage of the volume of the CO₂ that can be stored/ total pore volume available to store CO₂. Efficiency factors can include net to total area, net to gross thickness, effective to total porosity, areal displacement efficiency, vertical displacement efficiency, gravity and microscopic displacement efficiency (IEAGHG 2009). Storage efficiency coefficients are expressed as a product of volumetric and dynamic components. Structural amplitude and reservoir thickness also have implications in structural traps.

Storage resource calculations are described in the report for saline reservoirs and depleted fields, and include open and closed systems. Storage efficiencies are defined in this report as the volumetric displacement efficiency, the ratio between the reservoir volume of injected CO₂ and the accessible pore volume of a reservoir defined by the propagating CO₂ plume (the area swept by the CO₂ plume and its trail).

Limitations of storage coefficients are discussed, and their usage as part of estimating resources for sites at low storage readiness levels where there is not a lot of site specific data. They can also be calculated at mature sites, as demonstrated in this study, with operational data. Factors to consider include: reservoir heterogeneity with depth, the limit of detectability of the leading edge of the plume, the impact of pressure- - particularly in closed systems, injectivity and the structure of the reservoir and seal.

Previous published studies and key parameters identified

Previous studies have modelled the impact of injecting CO₂ and assessing the impact on storage coefficients and storage resources in a variety of ways and with varying factors. These are briefly reviewed in the report and key parameters drawn out and identified as impacting the storage coefficient (Table 1). Notably these include simulations that utilise different time steps, temperature,



depth, permeabilities, heterogeneities, pressure, closed and open systems, density, number of wells etc.

Parameter	Studies with numerical modelling	Results
Geological structure – flat, dipping, dome	(IEAGHG, 2009)	Efficiency increases with curvature of structure
Depth	(IEAGHG, 2009; Kopp (2009)	Increases with depth (higher CO ₂ density)
Relative permeability	(IEAGHG, 2009; Haeiri et al., 2022; Okwen et al., 2014)	Complex, no clear relationship between S_{wirr} and E, no strong effect.
Permeability anisotropy (k_v/k_h)	(IEAGHG, 2009)	Low values give higher E
Temperature	(IEAGHG, 2009)	Not huge dependence, high temperature gives slightly higher E at shallow depths near critical point.
Injection rate	(IEAGHG, 2009; Kopp, 2009)	Higher injection rate gives higher E as deeper pore space is utilised before gravity effects dominate
Lithology type	(Gorecki et al., 2014; Gorecki et al., 2009; Haeiri et al., 2022; Okwen et al., 2014)	Can have a large effect on porosity/permeability and therefore efficiency
Boundary conditions – open or closed	(Bachu, 2015; Gorecki et al., 2009; Zhou, Q. et al., 2008)	Higher E in a more closed system (Zhou, Quanlin et al., 2008)
Number of injection wells	(Gorecki et al., 2014; Wang et al., 2013)	More wells mean higher E (subject to a maximum)
Heterogeneity – permeability distribution	(Tian et al., 2016; Wang et al., 2013)	E decreases with both λ (correlation length) and σ (log permeability standard deviation) of the heterogeneity (Tian et al., 2016)
Pauses in injection once BHP limit reached	(Wang et al., 2013)	Little added benefit
Porosity	(Wang et al., 2013)	No significant results
Time dependency of storage coefficients	(Bachu, 2015; Gorecki et al., 2014; Okwen et al., 2014)	E increases with time up to a plateau. Can take long time period to approach volumetric values.
Water production	(Gorecki et al., 2014; IEAGHG, 2018)	Water production greatly increases E in closed systems, increases E a bit in open systems



Net-to-Gross	(Kopp et al., 2009b)	Not a good measure
S_{wirr}	(Haeri et al., 2022)	Irreducible water saturation determines the microscopic displacement efficiency.

Table 1: Key parameters as identified in the literature review and the impact of each on the CO₂ storage capacity estimation

Opportunities for further modelling identified

As a result of the literature review the following areas were highlighted by the authors as warranting further study and development.

- Storage coefficient will be calculated in a series of geological geometries: a flat caprock, a dipping aquifer and a structural dome.
- The storage coefficient will be calculated at realistic time steps through an injection and post-injection period.
- Water production and the relationship between storage coefficients will be explored.
- Hysteresis and residual trapping will be investigated.
- Time steps and storage coefficients are calculated from available data in three CO₂ storage projects.
- Impact of gridding.

Case Studies – Operational Data

Time-lapse geophysical data were evaluated from three CO₂ storage projects: Sleipner and Snøhvit in Norway and Ketzin in Germany in order to calculate storage efficiencies at time steps through their operation. These highlight variability through time and the authors look at reasons for differences between observed values.

- Sleipner: the plume outline of nine individual stacked layers in the 200m thick Utsira formation were mapped on four vintages of seismic (2001, 2004, 2006, and 2008). An ellipse was fitted to the overall extent of the seismic anomaly in each case and used to calculate the storage efficiency of the reservoir. Values of ~2% are consistent through time, where the growth of the plume layers migrate beneath partially sealing units.
- Snøhvit: the plume outline of CO₂ accumulation within the Stø formation was plotted and an ellipse fitted for the years 2011 and 2012. Higher storage efficiency values (7.8-10.2%) were calculated than Sleipner, potentially a function of lower permeability and plume growth though a greater proportion of the vertical extent of the reservoir.
- Ketzin: the plume extent of CO₂ accumulation within the 70m thick Stuttgart Formation was fitted with an ellipse on seismic datasets from 2009 and 2021. The reservoir varies in quality, with high quality sandstones overlying lower porosity and permeable units. The storage efficiency is calculated on the full thickness of the reservoir (3.9-6.6%), and the quality sandstone thickness (7.4 – 12.5%). Ketzin provides an estimate of the evolution of time-lapse storage efficiencies in gaseous phase CO₂ injection into medium quality reservoir units.

Modelling

Numerical flow models are used to simulate CO₂ injection into a saline aquifer, for a structural dome and a simple dipping aquifer in order to study the evolution of storage coefficients over time, through injection and post injection periods. Modelling was performed using PFLOTTRAN-OGS reservoir simulator 16 simulations were performed with variations of injection and production well locations, injection rate, water production rate, and hysteresis. The results were inspected for quality, injection



and production rates and pressure values. Maps of the extent of the CO₂ saturation were output after 1, 10, 20, 30 and 100 years for each case with which to calculate the area of the plume and derive the storage coefficient.

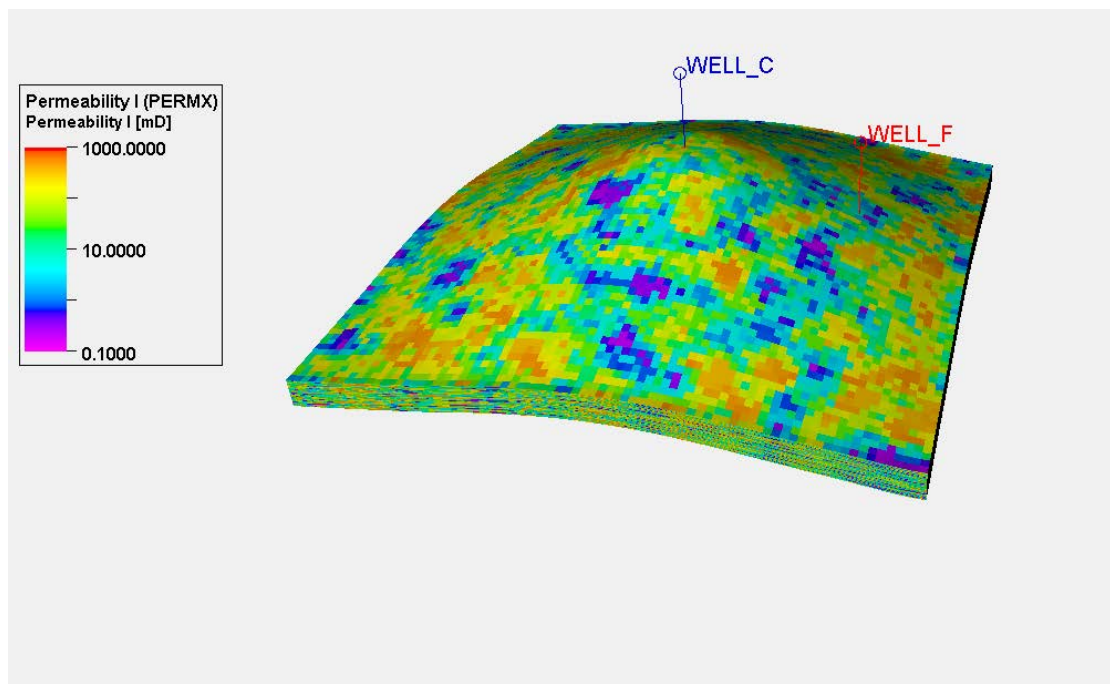


Figure 1: Horizontal permeability of the static model. Vertical exaggeration is 5 times. WELL_C is used for CO₂ injection/water production from the crest, and WELL_F is used for CO₂ injection/water production from the flank. Values correspond to P50 Deltaic environment of (Gorecki et al., 2009) and are directly linked to porosity.

Structural dome:

- Regional anticline with four-way dip closure, similar to the Triassic Bunter Sandstone salt cored domes of the United Kingdom Southern North Sea (UKSNS) (Figure 1).
- The apex of the dome is located at a depth of 1300 m below Mean Sea Level (MSL) in the model, and the reservoir thickness is 200 m.
- The simulation grid covers an area of 20x20 km with 80 250 m grid cells in the X and Y directions and 80 2.5 m grid cells along the vertical axis of the model.
- Open boundary conditions have been applied to all sides of the model domain, using large pore volume multipliers.
- The reservoir formation is assumed to be saturated with brine containing 100,000 ppm NaCl prior to CO₂ injection.
- Values of permeability correspond to P50 deltaic environment after Gorecki et al 2009 and are directly linked to porosity. Mean porosity is 0.15, mean permeability 230 mD and permeability range 0.13-522 mD – the distribution is stochastic. An additional model was created using shallow shelf environment.
- Injection into apex of the dome (for structural case) and only flanks (for dipping aquifer).
- CO₂ injection into the flank reaches the top of the structure after 100 years and begins to pool after 200 years.

Reservoir Flow Properties

- Relative permeability curves used in this model are based on a compilation of measurements for western Canadian sandstone units (Bachu, 2015) and were calculated using a modified



Brooks-Corey model. In experimental data relative permeability can be low and irreducible water saturation relatively high, however flow rate has been demonstrated to increase end point relative permeability and decrease residual water saturation thereby allowing higher CO₂ saturations – thus higher flow rates in commercial scale storage projects are likely to result in higher displacement efficiency. Upscaled relative permeability curves are used to reflect flow conditions of a commercial scale.

- Simulation runs incorporated effects of relative permeability hysteresis and capillary trapping after Burnside and Naylor (2014) and Carlson’s relative permeability hysteresis model for water-wet brine-gas system.
- The trapped gas saturation (S_{gt}) is defined as the horizontal interval between the drainage and scanning curves at the non-wetting phase relative permeability for the current gas saturation (S_{gc}) in the model cell (after Snippe & Tucker, 2014). Maximum trapped gas saturation used is 0.3 in all model runs after mean and median published values (Burnside and Naylor, 2014).
- CO₂-brine capillary pressure curves have been generated from data from Wu et al (2018), with a best fit Brooks-Corey capillary pressure model used in the simulations.
- Additional simulations were run to test the dependence of the results on the size of the numerical grid used.

Injection and production schedule

- Injection schedule is designed to be realistic and simple: a single well injects 1Mt/yr for 30 years, with simulations running for 70 years post injection – 100 years total. Selected simulations ran for 1000 years.
- A higher rate of injection 2Mt/yr and lower rate 0.5Mt/yr were also performed.
- Water production: an equivalent (density-corrected) pore volume of formation brine was produced from the production well. In some runs 2x amount of water was produced.

Results

The storage coefficient was calculated in the same way as the operational data and time steps, based on the volume of injected CO₂ at reservoir conditions and the volume of reservoir based on an ellipse and total thickness of the reservoir (Table 2). CO₂ spreads radially from the perforation interval, rises buoyantly towards the top of the reservoir where it begins to spread laterally under the caprock and the store efficiency reaches a peak. Post injection the CO₂ continues to migrate and spread increasing the volume of total pore space and thereby reducing the storage efficiency.

Sim #	Case	Storage coefficient at time [years]				
		1	10	20	30	100
1	Inject into crest of dome, 1Mt/yr, no water production	1.99%	6.82%	9.66%	11.96%	11.74%
2	Inject into flank of dome, 1Mt/yr, no water production	2.26%	7.78%	9.32%	9.14%	6.02%
3	Inject into flank of dome, 2Mt/yr, no water production	3.18%	9.69%	11.65%	13.18%	8.48%
4	Inj into flank of dome, 0.5Mt/yr, no water production	1.32%	5.59%	7.24%	7.31%	4.59%



5	1:1 Down dip water production 1Mt/yr	1.84%	7.13%	9.54%	12.09%	11.88%
6	1:1 Up dip water production 1Mt/yr	2.29%	7.65%	9.32%	9.17%	5.90%
7	2:1 Down dip water production 1Mt/yr	1.82%	7.12%	9.79%	12.16%	11.94%
8	2:1 Up dip water production 1Mt/yr	2.31%	7.61%	9.34%	9.95%	6.13%
9	As #1 no hysteresis	2.04%	6.99%	9.89%	11.96%	11.74%
10	As #2 no hysteresis	2.36%	7.78%	9.32%	9.14%	5.52%
11	As #3 no hysteresis	3.26%	9.75%	11.65%	12.76%	7.89%
12	As #4 no hysteresis	1.33%	5.67%	7.20%	7.31%	4.35%
13	As #5 no hysteresis	1.88%	7.16%	9.88%	12.40%	11.99%
14	As #6 no hysteresis	2.33%	7.93%	9.09%	9.96%	5.65%
15	As #7 no hysteresis	1.83%	7.22%	9.82%	11.97%	11.50%
16	As #8 no hysteresis	2.36%	7.80%	9.09%	10.60%	5.81%

Table 2: Summary table of model runs showing the value of the storage coefficient at given time steps for each simulated case. Water production ratio is the ratio of reservoir volume of water produced to reservoir volume of CO₂ injected.

- Structure has significant impact on the lateral behaviour of a CO₂ plume, injection into a structural dome leads to higher storage efficiency whereby more of the thickness of the reservoir is filled (up to 12%) compared to a dipping aquifer (~9%) and produces a more stable plume leading to a constant storage efficiency post injection.
- Injection rates: higher injection rates force CO₂ to utilise more of the deeper pore space leading to higher storage coefficients. Up to 13% storage efficiency is achieved by injecting 2Mt/y into the flanks of the dome but just over half the efficiency for 0.5Mt/yr.
- Water production in these runs do not show a marked difference in storage coefficients as calculated by this approach as there is little to no impact on the dispersion of the plume, although distribution of the plume in deeper layers when water is produced up dip is demonstrated by the models. This contrasts previous studies and limitations include modelling an open system and not accounting for pressure. Further work is required.
- Hysteresis: all models were repeated without hysteresis to model its effects. Hysteresis works to residually trap gas in the deeper layers of the model and leaves less gas in the mobile layer at the top, therefore a smaller lateral area is swept by the plume leading to slightly higher storage efficiencies when hysteresis is included in the dipping aquifer (see Figure 2). Hysteresis as modelled demonstrates the residual trapping through the trailing edge of the plume, and does not carry the same risk as leakage as the more mobile buoyant CO₂ demonstrating a compelling safety case. No significant impact to efficiency with injection into the crest of the structural dome was seen. Figure 3 shows the total volume of injected CO₂ and the volume which is mobile, dissolved and residually trapped in the model where injection is in the flank of the dome.



- Porosity/Permeability: higher storage efficiency values are calculated in a dipping aquifer model using shallow shelf properties after Gorecki et al (2009). Whereas the storage efficiency is higher for both injection into the dome and flank of the deltaic environment for the structural dome model than shallow shelf.
- Shape fitting: the shape used to define the plume impacts the storage coefficient, an ellipse giving higher values than a rectangle. Usage within published works should be critically assessed on how the volume of the pore space is calculated.

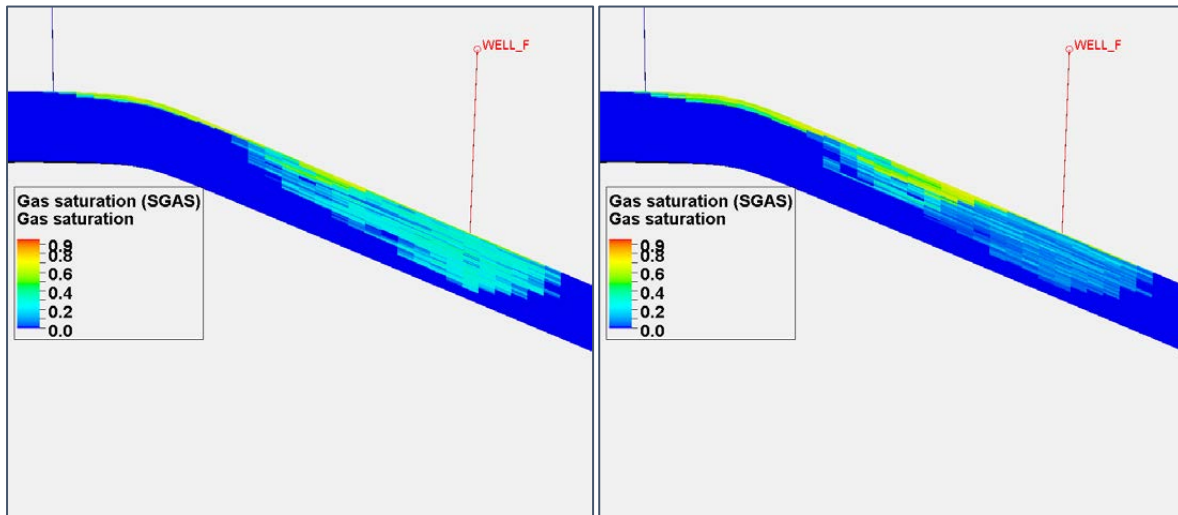


Figure 2: Cross-sectional view of the gas saturation after 100 years of simulation (a) with hysteresis and (b) without hysteresis.

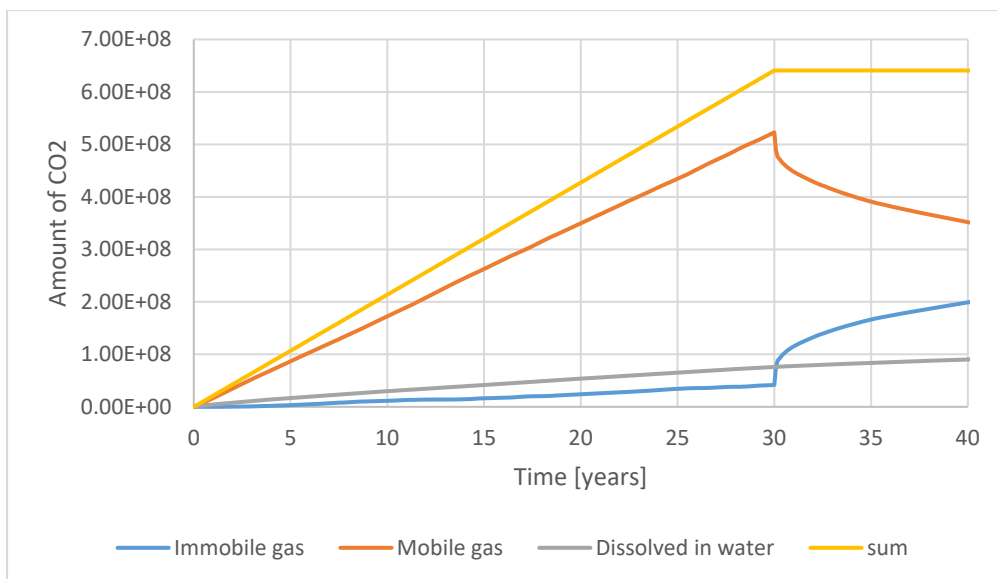


Figure 3: Breakdown of the trapping states of CO₂ for injection into flank of structural dome.

Analytical approximations of storage coefficients

An analytical approximation as applied to storage coefficients is derived from existing models of analytical methods which predict the size, shape and position of a plume of buoyant CO₂ injected into a porous reservoir under an impermeable caprock. A basic model is set up under a flat caprock with axisymmetric radially spreading buoyant CO₂ into a brine (immiscible).

A constant has been derived



$$E = \frac{1}{H\pi 1.15^2} \sqrt{\frac{Q\mu}{kg\Delta\rho}}$$

E = storage efficiency

Q is the rate of CO₂ injection (kg/s)

Δρ the density difference between the brine and CO₂

H is the thickness of the reservoir

k is the permeability of the porous medium,

g the gravitational acceleration 9.81 ms⁻²

μ the dynamic viscosity of the CO₂

In this simplified case:

- Storage efficiency is not expected to change with time
- Thickness of the reservoir is influential with a thick reservoir giving low efficiency
- Efficiency increases with the square root of the injection rate – as seen in the modelled cases.
- Parameters input from the three case studies demonstrate that the analytically derived efficiency factor underperforms compared to storage coefficient measured due in part to greater heterogeneity in the reservoirs with layers and compartments increasing the storage efficiency (table 3).

Case study	Analytically derived storage coefficient (year)		Storage coefficient from seismic data (year)			
Sleipner	1.2%		1.8% (2001)	2.1% (2004)	1.9% (2006)	1.8% (2008)
Snøhvit	3.7%		7.8% (2011)	10% (2012)		
Ketzin (70m thick)	2.0% (2009)	2.1% (2012)	3.9% (2009)	6.6% (2012)		
Ketzin (37m thick)	3.73% (2009)	4.02% (2012)	7.5% (2009)	12.5% (2012)		

Table 3: Comparison of storage coefficients measured from operational data and analytical approximation for three case studies.

A derivation is also given for a dipping caprock where asymptotic scaling factors are applied for the buoyant CO₂ plume travelling up-dip.

$$E = \frac{Q^{2/3} \mu (\phi \tan \theta)^{1/3}}{H\pi k g \Delta\rho \sin \theta} t^{-1/3}$$

In this case

- As time increases the area of the plume increases driven by continued injection and buoyancy forces acting to migrate CO₂ up-dip.
- Thickness of the plume after ~2.5 years decreases with time, as observed in numerical simulations.
- The thinning of the CO₂ layer and up-dip migration means that the storage efficiency decreases with time.
- Increasing the angle of dip (θ) results in a lower storage efficiency, as would be expected.



- Values calculated are significantly lower than numerically modelled, potentially due to the location of the CO₂ injection (single point below caprock in the analytical model).

Conclusions

The classification of storage resources and associated schemes have become more complex over time and more aligned to the requirements of operational storage with the SRMS becoming the industry standard.

Storage coefficients are vital for quantifying accessible storage resources, standard methodologies have been presented and examples of usage within national and international databases. 97% of global storage is of a prospective nature and having quick screening criteria are useful in initial basin screening.

Data from CO₂ storage sites can be used to calculate storage efficiency through time by measuring plume area on time-lapse seismic data. These results can then be compared to numerical models and analytical approximations.

Numerical simulations were run with key parameters identified through publicly available modelling studies with storage coefficients evaluated for each case.

- Structure and injection rates have a significant influence on storage coefficients
- The evolution of the storage coefficient through a 30 year injection period and 70 year post injection period was modelled and in the case of a dipping aquifer the storage coefficient peaks at 20-30 years and then gradually reduces whereas a structural closure sees a more stable post injection storage coefficient.
- Water production did not impact the storage coefficient in this study, but modelling an open system may have impacted the results. In closed systems water production impacts pressure and the total amount of CO₂ that can be injected, but is unlikely to impact location of the plume.
- Hysteresis may not impact storage coefficient significantly, but it does cause the distribution of CO₂ with more trapped in deeper layers of the reservoir increasing storage security.

Analytical models from the literature have been modified to estimate storage coefficients and compared to modelled and data from the storage sites. At first pass they give a quick and easy estimate for lower stages of development but results slightly underperform.

Expert Review

Six expert reviewers were involved in providing comment to the draft report, these have given constructive feedback to the authors. There was concern over the use of the term capacity and storage resource and its consistency. The use of the ellipse fitting was welcomed and some useful feedback with supplementary data was supplied.

There was feedback that the modelling work didn't factor in the range of parameters outlined in the original scope or produce the outputs requested,

The final report has addressed the reviewers broader comments, there has been some restructuring to enhance the flow and further clarification where needed and attention to definitions where required, and a recommendations for further work section has been added.

New work has been added, notably:



- Sensitivity to gridding
- Additional porosity/permeability model.
- An additional modelling run using shallow shelf facies to explore impact of facies.
- Output on the proportion of CO₂ in mobile, residually trapped and dissolved states, including graphs showing how this varies with time.

Recommendations

Having reviewed a series of national databases that assess storage potential on a regional or basin scale, it would be useful if the project-based SRMS could be extended to incorporate an internationally recognised classification scheme that is relevant for a wider range of Storage Readiness Levels (particularly regional/undiscovered resources). There is a requirement for additional funding to ensure that large scale characterisation studies in developed and developing countries are utilised and brought into alignment with one another globally. This would provide a clear framework when evaluating storage resource and expanding CCS more widely around the globe.

Wherever possible numerical models form the basis of storage resource estimations and are more reliable than volumetric or analytical approximations of storage coefficients.

Storage coefficients calculated from CO₂ storage sites could be used to inform achievable estimates for sites earlier in their development, extending this work to include the Otway Stage 3 demonstration site is a possibility and using more recent seismic data from Sleipner for example.

Further work using analytical methods could be attempted from a different angle to that approached in this study. The use of dimensionless variables to emulate or build upon some of the numerical modelling work may provide a way to estimate storage coefficients for a cheaper cost than using full dynamic simulations.



British
Geological
Survey

Classification of Total Storage Resources and Storage Coefficients

Decarbonisation and Resource Management Programme

Commercial Report CR/22/061

BRITISH GEOLOGICAL SURVEY

DECARBONISATION AND RESOURCE MANAGEMENT PROGRAMME

COMMERCIAL REPORT CR/22/061

The National Grid and other
Ordnance Survey data
© Crown Copyright and
database rights 2023.
Ordnance Survey Licence
No. 100021290 EUL.

Bibliographical reference

H VOSPER, J WHITE, M
AKHURST, K KIRK, G WILLIAMS,
L ABEL, C VINCENT2023.
Classification of Total Storage
Resources and Storage
Coefficients. *British
Geological Survey
Commercial Report,
CR/22/061*. 104pp.

Copyright in materials derived
from the British Geological
Survey's work is owned by
UK Research and Innovation
(UKRI) and/or the authority
that commissioned the work.
You may not copy or adapt
this publication without first
obtaining permission. Contact
the BGS Intellectual Property
Rights Section, British
Geological Survey, Keyworth,
e-mail ipr@bgs.ac.uk. You
may quote extracts of a
reasonable length without
prior permission, provided a
full acknowledgement is given
of the source of the extract.

Maps and diagrams in this
book use topography based
on Ordnance Survey
mapping.

Classification of Total Storage Resources and Storage Coefficients

H Vosper, J White, M Akhurst, K Kirk, G Williams, L Abel, C
Vincent

Editors

H Vosper, J White

BRITISH GEOLOGICAL SURVEY

The full range of our publications is available from BGS shops at Nottingham, Edinburgh, London and Cardiff (Welsh publications only) see contact details below or shop online at www.geologyshop.com

The London Information Office also maintains a reference collection of BGS publications, including maps, for consultation.

We publish an annual catalogue of our maps and other publications; this catalogue is available online or from any of the BGS shops.

The British Geological Survey carries out the geological survey of Great Britain and Northern Ireland (the latter as an agency service for the government of Northern Ireland), and of the surrounding continental shelf, as well as basic research projects. It also undertakes programmes of technical aid in geology in developing countries.

The British Geological Survey is a component body of UK Research and Innovation.

British Geological Survey offices

**Nicker Hill, Keyworth,
Nottingham NG12 5GG**

Tel 0115 936 3100

BGS Central Enquiries Desk

Tel 0115 936 3143

email enquiries@bgs.ac.uk

BGS Sales

Tel 0115 936 3241

email sales@bgs.ac.uk

**The Lyell Centre, Research Avenue South,
Edinburgh EH14 4AP**

Tel 0131 667 1000

email scotsales@bgs.ac.uk

**Natural History Museum, Cromwell Road,
London SW7 5BD**

Tel 020 7589 4090

Tel 020 7942 5344/45

email bgs_london@bgs.ac.uk

**Cardiff University, Main Building, Park Place,
Cardiff CF10 3AT**

Tel 029 2167 4280

**Maclean Building, Crowmarsh Gifford,
Wallingford OX10 8BB**

Tel 01491 838800

**Geological Survey of Northern Ireland, Department of
Enterprise, Trade & Investment, Dundonald House,
Upper Newtownards Road, Ballymiscaw,
Belfast, BT4 3SB**

Tel 01232 666595

www.bgs.ac.uk/gsni/

**Natural Environment Research Council, Polaris House,
North Star Avenue, Swindon SN2 1EU**

Tel 01793 411500

Fax 01793 411501

www.nerc.ac.uk

**UK Research and Innovation, Polaris House,
Swindon SN2 1FL**

Tel 01793 444000

www.ukri.org

Website www.bgs.ac.uk

Shop online at www.geologyshop.com

Acknowledgements

This report describes research and review sponsored by the IEAGHG and was prepared by the British Geological Survey (BGS).

The principal researchers were:

- H. Vosper
- J.C. White
- M.C. Akhurst
- K.L. Kirk
- G.A. Williams
- L. Abel
- C.J. Vincent

The report was compiled and edited by: H. Vosper and J.C. White

To ensure the quality and technical integrity of the research undertaken by the IEAGHG, each study is managed by an appointed IEAGHG manager. The report is also reviewed by a panel of independent technical experts before its release.

The IEAGHG manager for this report was: Nicola Clarke.

The expert reviewers for this report were:

- Jamie Andrews, Equinor
- David Bason, CO2CRC
- George Koperna, Advanced Resources International
- Wes Peck, EERC
- Owain Tucker, Shell
- Peter Zweigel, Equinor

The report should be cited in literature as follows:

'IEAGHG, "Classification of Total Storage Resources and Storage Coefficients", 2023-05, December 2023.'

Further information or copies of the report can be obtained by contacting the IEAGHG:
IEAGHG, Pure Offices, Cheltenham Office Park, Hatherley Lane, Cheltenham, Glos. GL51 6SH,
UK

Tel: +44 (0)1242 802911

E-mail: mail@ieaghg.org

www.ieaghg.org

THIS PAGE IS INTENTIONALLY BLANK

Contents

Acknowledgements	i
Contents	iii
Figures	v
Tables	viii
Summary	ix
1 Introduction 1	
1.1 Objectives of this report	1
1.2 Scope of this report	1
1.3 Report structure	2
2 Published storage resource assessments	3
2.1 Background	3
2.2 Storage resource estimation methodologies	3
2.3 CO ₂ storage Resource assessment methodologies	4
2.4 Storage Resource classifications	5
2.5 CO ₂ storage maturity of understanding, readiness indices and levels	11
3 Storage resource calculation	15
3.1 Volumetric storage resource calculation	15
3.2 Dynamic storage efficiency coefficients	18
3.3 Case studies: databases	23
3.4 Key parameters identified from the literature	26
3.5 Limitations of storage coefficients	27
3.6 Opportunities for further modelling	29
4 Cases studies: operational data	30
4.1 Sleipner	30
4.2 Snøhvit	32
4.3 Ketzin	34
5 Numerical flow modelling to estimate storage coefficients	38
5.1 Static models	38
5.2 Reservoir flow properties	43
5.3 Results	50
5.4 Sensitivity to grid size	66
5.5 Summary of the modelling study	67
6 Analytical approximations of storage coefficients	69
6.1 Storage coefficient under a flat caprock	69
6.2 Storage coefficient in a dipping aquifer	73
6.3 Discussion of structural traps	75
7 Discussion 76	
7.1 Further work	78

8	Conclusions.....	80
	References	82
Appendix A.	What makes a good geological storage site?	88
	Introduction	88
	A geological Storage site.....	88
Appendix B.	Techno-economic resource pyramid from Bachu et al. (2007)	90

Figures

Figure 1. Graphical representation of the categories of storage capacity by application of technical and economic constraints, after Bradshaw et al. (2007), indicating increasing certainty of storage potential with potentially decreasing storage capacity from left to right. .7	.7
Figure 2. Graphical representation of the classification of storage capacity by application of the concepts of reserves and resources, after Bachu et al. (2007), indicating increasing certainty of storage potential with potentially decreasing storage capacity from left to right. .8	.8
Figure 3. Graphical representation of the storage resource categories (Gorecki et al., 2009) indicating increasing certainty of storage potential from left to right.9	.9
Figure 4. Graphical representation of the SRMS (SPE-SRMS, 2017) storage resource classification system indicating increasing certainty of storage potential from left to right. ..11	.11
Figure 5: Equivalence of the Storage Readiness Levels with the Storage Resources Management System project maturity classes and subclasses (SPE-SRMS, 2017) from Akhurst et al. (2021).14	.14
Figure 6. Time-lapse difference data for 2001, 2004, 2006, 2008 and 2010 surveys showing a N-S seismic line through the axial part of the plume. The nine layers identified within the CO ₂ plume are labelled, where visible, in the two latest vintages. The top layer is seen to grow with time whilst the imaging of the lower layers degrades, a consequence of seismic wave interference and time delays causing attenuation of the reflectivity, from White, J C et al. (2018b).....31	.31
Figure 7. The Layers of the Sleipner Plume in plan view showing the growth of the accumulation through 4D time-lapse imaging, and the ellipses describing the horizontal extent of the whole plume.....32	.32
Figure 8. Seismic lines from the first baseline (2003) and the second baseline (2009) surveys highlighting the geological structure at Snøhvit (top). Difference data shows changes between 2003 and 2009, and subsequently to 2009 (bottom). Green lines delineate the intersection between the N-S and E-W lines. Black boxes show the location of the difference panels. Arrows point to the Stø anomaly, to differentiate from the deeper time shifted Tubåen reflectivity. From White et al., 2015.....33	.33
Figure 9. Upper panels: thickness of CO ₂ accumulation at Snøhvit in 2011 (left) and 2012 (right) calculated from seismic data. Lower panels: Spatial extent of the plume and fitted ellipse. Inline and Xline spacing for the 3D surveys was 12.5 m.34	.34
Figure 10. The growth of the Ketzin CO ₂ accumulation in plan view, showing the growth of the anomaly through 4D time-lapse imaging in 2009 and 2012.35	.35
Figure 11. Horizontal permeability of the static model. Vertical exaggeration is 5 times. WELL_C is used for CO ₂ injection/water production from the crest, and WELL_F is used for CO ₂ injection/water production from the flank. Values correspond to P50 Deltaic environment of (Gorecki et al., 2009) and are directly linked to porosity. Bottom inset is a cross section through WELL_C, zoomed in with the scale shown.....39	.39
Figure 12. Cross-section view of the gas saturation after 100 years of simulation (run #2, see Table 11 for details).40	.40
Figure 13. (a) Dipping aquifer model used in the flow simulations. The porosity distribution was generated in PETREL using a Gaussian random function simulation algorithm, with parameters published by IEAGHG (2009). (b) Log-linear porosity-permeability transform used to compute the permeability field from (a). The endpoints of the fit were again taken from IEAGHG (2009).42	.42
Figure 14. (a) Brookes-Corey relative permeability curves using the average parameter values given in Table 9. (b) Brookes-Corey relative permeability curves using the average parameter values given in Table 1, upscaled to an irreducible water saturation of 0.3. Key:	

$S_{g_{MAX}}$ = maximum gas saturation; $S_{gt_{MAX}}$ = maximum trapped gas saturation; S_{gc} = cell gas saturation; S_{gt} = trapped gas saturation.....	46
Figure 15. Plot of trapped gas saturation vs. initial gas saturation for a wide range of sandstone reservoir rocks. Data from Burnside and Naylor (2014), Weatherford Laboratories (2015) and Reynolds et al. (2018). The data can be fit by a Land trapping model with a trapping coefficient, C , of 1.37. The mean trapped gas saturation is 0.31 and the median 0.29.....	47
Figure 16. Compilation of CO ₂ -brine capillary pressure data from Wu et al., 2018. Best-fit Brooks-Corey (solid blue line) capillary pressure model used in the simulations.	48
Figure 17. Examples of ellipse fitted to CO ₂ footprint to calculate storage coefficient: (a) when CO ₂ is injected into the flank (WELL_F), and (b) is CO ₂ injected into the crest of the dome (WELL_C). Blue shows the lateral area where CO ₂ is present in any of the layers in the model. Grey depicts areas without CO ₂	51
Figure 18. Evolution of the storage coefficient for CO ₂ injected into the dome (blue, case #1) and the flank (red, case #2) of the dome model. For case details see Tables 11 and 12.	52
Figure 19. Horizontal permeability of the model populated with properties from the shallow-shelf environment of IEAGHG (2009) as used in the dipping aquifer model.	53
Figure 20. Comparison of results using properties from the Deltaic environment (DOME_BASE and DOME_FLANK) and from the shallow shelf environment (DOME_BASE_SS and DOME_FLANK_SS).	54
Figure 21. Storage coefficient calculated for cases with high and low injection rates. For case details see Tables 11 and 12.	54
Figure 22. Influence of water production on storage coefficient when CO ₂ is injected into a structural dome. For case details see Tables 11 and 12.	55
Figure 23. The impact of water production from WELL_C on storage coefficient of a plume injected through WELL_F. For case details see Tables 11 and 12.	56
Figure 24. A cross-sectional view of the gas saturation after 100 years of simulation. (a) with no water production (b) with a water production ratio 2:1, i.e. cases 2 and 8 in Table 11. For case details see Tables 11 and 12.	57
Figure 25. The impact of hysteresis on the storage coefficient for the base cases of injection into the crest and the flank of the dome. For case details see Tables 11 and 12. Note that results for DOME_BASE and DOME_BASE_NH are identical.....	57
Figure 26. Variation in storage coefficient over time for high, medium and low injection rates, both with and without hysteresis. For case details see Tables 11 and 12.	58
Figure 27. Cross-sectional view of the gas saturation after 100 years of simulation (a) with hysteresis and (b) without hysteresis, corresponding to case #2 and #10 respectively.	58
Figure 28. Comparison of all cases with injection into the crest of the dome, with and without hysteresis and water production. For case details see Tables 11 and 12.	59
Figure 29. Breakdown of the trapping states of CO ₂ for case 1 (injection into crest).	60
Figure 30. Breakdown of CO ₂ trapping states of CO ₂ for case 2 (injection into flank).....	60
Figure 31. Proportion of CO ₂ in each trapping state for case 2 (injection into flank).....	61
Figure 32. Proportion of CO ₂ in each trapping state for case 10 (no hysteresis modelled).....	61
Figure 33. (a) Elliptical fit to the CO ₂ plume developed 100 years after the onset of injection for Case 1 in Tables 14 and 15. The minimum bounding ellipse used to define the reservoir area swept by the CO ₂ plume is shown as an orange polygon. The blue polygon denotes the boundaries of the gas plume. (b) Minimum bounding rectangle (orange polygon) enclosing the CO ₂ plume developed 100 years after the onset of injection for Case 1 in Tables 14 and 15: the blue polygon denotes the boundaries of the gas plume.	65

Figure 34. Storage efficiency evolution with time calculated by fitting an ellipse (a, c, e) and a minimum bounding rectangle (b, d, f) to the growing CO₂ plume. All based on the dipping aquifer model.66

Figure 35. Variations in efficiency coefficient with grid size. Numbers in the legend correspond to the lateral size of cells in the grid (in metres)– 285 is the coarsest and 160 is the finest. 67

Figure 36. Impact of grid size on the efficiency coefficient for cases of different injection rates. 67

Figure 37. Diagram of a CO₂ plume spreading under a flat caprock. The plume is axisymmetric about the z-axis and extends horizontally a radial distance, r_N70

Figure 38. Diagram of a buoyant CO₂ plume spreading under a dipping caprock. Note that injection is modelled as a point source directly beneath the caprock.73

Figure 39. Comparison of analytical storage efficiency values with a caprock of no dip (blue) and a dip angle of 4.5 degrees (corresponding to the dome model in Section 5). A constant injection rate of 1 Mt/yr is assumed.74

Figure 40. Influence of the angle of dip on the value of the storage coefficient calculated from Equation 9.....74

Tables

Table 1. Storage resource schemas, benchmarked against Bachu et al. (2007) and compared with industry resource management systems.....	6
Table 2. US DOE Efficiency factor terms, taken from IEAGHG (2009).....	21
Table 3. The key parameters drawn from the literature review and the impact of each on CO ₂ storage resources estimation.....	26
Table 4. Determination of time-lapse storage efficiency for the Sleipner CO ₂ injection.	36
Table 5. Determination of time-lapse storage efficiency for the Snøhvit CO ₂ injection in the Stø formation.....	36
Table 6. Determination of time-lapse storage efficiency for the Ketzin CO ₂ injection using the full reservoir interval.	37
Table 7. Determination of time-lapse storage efficiency for the Ketzin CO ₂ injection using the high-quality reservoir interval.	37
Table 8. Details of the simulation grid used in this study.	39
Table 9. Modified Brookes-Corey relative permeability parameters for a CO ₂ /brine system derived from a series of rock samples from western Canada. Data reproduced from Bachu (2013).	44
Table 10. Summary statistics showing the relationship between maximum measured gas saturation and the trapped gas saturation for the CO ₂ /brine system in sandstones - data summarised from literature (Burnside and Naylor, 2014; Reynolds et al., 2018; Weatherford Laboratories, 2015). The data are plotted in Figure 15.	47
Table 11: Summary table of model runs using the dome model. Water production ratio is the ratio of reservoir volume of water produced to reservoir volume of CO ₂ injected.....	49
Table 12. Table showing the value of the storage coefficient at given time steps for each simulated case.....	51
Table 13. Storage efficiencies calculated by fitting an ellipse to the modelled CO ₂ plume extents (see text for an explanation). All cases used the dipping aquifer model.....	63
Table 14. Storage efficiencies calculated by fitting a rectangle to the modelled CO ₂ plume extents (see text for an explanation). All cases used the dipping aquifer model.	63
Table 15. Parameters used to calculate the analytical approximation of the storage efficiency for the base case using the dome model. Brine density is taken as 1055 kg/m ³	72
Table 16. Comparison of storage coefficients measured from operational data and analytical approximation for three case studies: Sleipner, Snøhvit and Ketzin. The difference between 2009 and 2012 analytical estimations at Ketzin is the density of the CO ₂ . Parameters used for analytically derived solutions at Sleipner and Snøhvit are not time dependent.....	72

Summary

IEAGHG commissioned the British Geological Survey (BGS) to undertake a study to assess the development of classification schemes for CO₂ storage resources and the use and development of storage efficiency coefficients. A review of published storage assessment classifications showed the initial development of two main methodologies: one developed by the Carbon Sequestration Leadership Forum (CSLF) and the second by the United States Department of Energy (US DOE). Over time these, and other, classification methodologies have developed towards the current Storage Resources Management System (SRMS, developed by the Society of Petroleum Engineers) - which may become the industry standard over time. The project-based SRMS approach is aligned to industry needs and links geological risks to economic, regulatory and operational uncertainties associated with the development of CO₂ storage projects.

Storage resource calculation techniques were reviewed, including volumetric and dynamic estimates appropriate at different stages of project development. Their use in various commonly utilised national and international databases was discussed, highlighting the differing data volumes assessed and the variability in complexity of the storage assessment calculations. This is the main context for use of high-level storage efficiency coefficients but sites do not progress onto the SRMS classifications until a specific project is established. As a project is developed, more detailed resource assessment through the use of dynamic numerical modelling becomes the primary method for estimating storage resources. The extension of a storage resource classification scheme, similar to SRMS, to areas with potential future projects would aid in comparison of sites worldwide. This should be a key focus as more nations look to maximise their geological carbon storage potential and explore areas for potential new projects.

A review of storage resource calculations was also carried out. This explored the different definitions of storage efficiency coefficients in both depleted fields and saline aquifers and dynamic factors which can also be incorporated. The definition chosen in this study primarily focus on the volumetric displacement efficiency. The storage efficiency coefficient is defined as the ratio between the volume of CO₂ stored in the reservoir and the pore volume contained within an elliptical cylinder defined by the lateral extent of the CO₂ plume and the thickness of the reservoir. The uses of storage efficiency coefficients was also reviewed with national/regional databases as an example.

The key subsurface parameters that influence the storage efficiency of a region or site under investigation were identified as geological geometry, depth, temperature, permeability, relative permeability, boundary conditions, number of wells/injection rate, heterogeneity, and pressure limitations. This review was linked to existing modelling studies using generic reservoirs and enabled opportunities for further modelling to be identified.

Data from real-world operational sites were used to calculate storage efficiency coefficients observed in the field and assess their evolution over operational time scales. Three case studies were used, the offshore projects at Sleipner and Snøhvit, and the onshore Ketzin storage research project. Storage coefficients were calculated from time-lapse seismic data and published plume outlines. This is a first step in the verification of modelled storage coefficients. Further work was identified to extend this to other operational sites as more data makes its way into the public domain.

A key component of this study was a modelling exercise, carried out to assess CO₂ migration and trapping over timescales that influence discussions regarding storage appraisal and efficiency. The modelling focuses on parameters identified from previous published studies: the structural setting, the role of water production and the consequences for storage security. Storage coefficients were evaluated for every case. The greatest storage coefficients were found in cases

where CO₂ was injected into a structural trap, with values approaching around 12%. This structural case limited the lateral spreading of the plume and resulted in a relatively thick (about 50 m, determined by the topography) layer of CO₂ under the caprock. A dipping aquifer model was used which may represent an open aquifer with migration-assisted trapping, or a fetch trap (where there is an ultimate closure after a potentially long migration distance). In this case, the storage coefficient increased during the injection phase, reached a peak after 20-30 years of injection and gradually reduced in the post-injection phase as CO₂ continued to migrate. The values calculated are representative of the parameterisation employed in the models, but the results have wider implications for long term behaviour in the subsurface where free CO₂ can continue to migrate. In the modelling conducted for this study, a storage efficiency value of around 6% was determined after 100 years of simulation and CO₂ migration. Longer simulation times were also used to determine the ultimate storage coefficient.

It was found that higher injection rates lead to higher storage coefficients. The impact of water production on the storage coefficient was considered. The primary effect of water production is to reduce the reservoir pressure and therefore reduce the likelihood of the system reaching pressure limitations such as the fracture pressure and provide operational, safety and security benefits. This may also increase the committable storage volumes if the pressure limit is reached prior to unacceptable plume migration. The impact of water production on the actual position of the CO₂ plume was limited however, even when large volumes of brine were produced. This meant that the impact of water production on a storage efficiency coefficient based on the lateral extent of the CO₂ plume was minimal.

Analytical modelling work was applied in a novel context, calculating storage coefficients across a wide parameter space. Analytical expressions for the storage coefficient were derived for simple models of CO₂ injection for cases of both a flat and a dipping caprock. They clearly show the influence of each parameter considered and are most useful for assessing and screening sites at low Storage Readiness Levels (SRLs) where large amounts of site-specific data are not yet available.

From this report, the wider Carbon Capture and Storage (CCS) stakeholder community can better understand the role of storage coefficients in CO₂ storage resource classifications and assessments. Storage efficiency coefficients are mostly only applicable at low SRLs where detailed information about a site is not available. This is primarily for screening purposes. As soon as possible, dynamic numerical modelling with as much site-specific parameter data as possible is the preferred means to estimate the storage resources of a site. As further data becomes available it is also incorporated into the modelling to give a more informed result. More mature sites can be used to provide realistic calculations of storage efficiency coefficients from operational/numerical data. This may be seen as analogous to recovery factors for hydrocarbon projects. The task of verifying storage coefficients with operational data from real sites has been started, and as the uptake of CCS increases around the world, it is anticipated that more data will be available for the verification process.

Storage coefficients are only a part of the site appraisal process and must be considered in conjunction with other factors, such as injectivity and reservoir pressure. Security of CO₂ storage is also an important factor which is not considered by storage coefficients. Residual, dissolution and mineral trapping may not have a drastic impact on storage efficiency intuitively but can greatly decrease the amount of free, mobile, buoyant CO₂ within a reservoir. This may lead to a greater final capacity of a site by limiting the migration of CO₂ towards any spill points/boundaries/vulnerable features such as historical wellbores.

1 Introduction

1.1 OBJECTIVES OF THIS REPORT

This report reviews the methods for evaluation of storage resources alongside approaches to calculate storage efficiency coefficients. The review is undertaken in the context of classification of total storage resources for the geological storage of CO₂. The commonly adopted classification systems are highlighted, and the strengths, weaknesses, similarities and differences between the approaches are discussed. This approach demonstrates how classification schemes are used to provide assurance of storage resource and convey the uncertainty associated with storage resource estimates. A set of national and international CO₂ storage atlases are used to provide examples of resource estimation at a range of scales and complexity.

There is a requirement to evaluate and classify the potential of the subsurface for CO₂ storage as the injected fluids cannot utilise the entire volume of a storage site or region. The injected CO₂ must be confined to the storage reservoir interval and safely contained within a site boundary. In addition, only the pore space between the rock matrix is available for a fluid to reside and a significant proportion of the available pore space is not accessible due to a range of factors discussed throughout this report. An evaluation of storage efficiency estimation schemes is provided to highlight the key parameters required to generate estimates of storage resources. These findings are linked to existing modelling studies that have attempted to derive ranges of total storage resources and storage coefficients from technically realistic development schemes in a range of geological formations using flow simulations. In addition, data from operational and defunct CO₂ storage projects are used to address the evolution of storage efficiency over the lifetime of operation to enable a discussion on the trade-off between storage security and storage efficiency.

Following this review, an assessment on the applicability of these existing studies is presented and outstanding knowledge gaps are highlighted. A modelling study then that evaluates the influence of geological variability and structural setting, and investigates the role of trapping mechanisms injection rate, water production and hysteresis in the calculation of storage efficiency. Subsequently, analytical approximations of storage coefficients that capture the physics, geology, and geometry of the system are derived. Analytical expressions highlight the dependence of storage efficiency on certain parameters. These expressions can be utilised quickly, especially when the characterisation of the storage resource is limited. Results are compared with the outputs from the modelling study and the review of operational data.

1.2 SCOPE OF THIS REPORT

This IEAGHG report opens with a literature review highlighting the common classification systems for storage resource estimation, and highlights how they have evolved. The report seek to assess how storage coefficients are calculated and used, as well as how the outcomes of modelling can be used to produce realistic estimates of storage efficiency in a range of geological settings and injection scenarios. This approach allows for the identification of gaps in the existing work. The current study defines the storage efficiency E as defined by Oldenburg (2021), the ratio of the volume of CO₂ injected to the pore volume of a cylinder encompassing the plume.

Following the literature review, modelling to inform the discussion on storage efficiency factors and maturity of storage project resource assessments is conducted. The current study defines the storage efficiency E as defined by Oldenburg (2021), the ratio of the volume of CO₂ injected to the pore volume of a cylinder encompassing the plume. A modelling study to evaluate storage coefficients for a range of geological scenarios and injection programmes for saline aquifers under realistic reservoir conditions, based on the outcomes of the literature review, is devised and presented. It assesses a limited parameter space within a realistic range of sensitivities for key variables. Further discussion on the role of trapping mechanisms in understanding calculated storage efficiency and the links to long-term storage security followed. These assessments allow for the derivation of analytical solutions for storage efficiency which are compared with data from operational and modelled storage complexes.

1.3 REPORT STRUCTURE

This IEAGHG report presents its findings on storage resource and storage coefficient research over the following chapters. **Chapter 2** summarises the storage resource classification systems and highlights the role they play in providing assurance of storage resources. Within the review, care is taken to align equivalent stages of alternative classification schemes to enable direct comparison of the methodologies. A discussion on the relative merits of dynamic and static storage assessment methods follows with the key factors that determine the levels of uncertainty in estimates of storage resource and reserve identified.

Chapter 3 starts with a review of storage resource calculation techniques and a set of commonly utilised storage databases are discussed, highlighting the data volumes assessed to generate the parameterisation and the complexity of the storage assessment calculations contained within. This leads to a review of the methods used within the CO₂ storage community for dynamic estimation of storage resource and coefficients, and a critical assessment of the limitations of specific techniques. Finally, a review of the key parameters in the literature highlights opportunities for further modelling.

Chapter 4 uses real data from operational and pilot sites to assess the evolution of storage resources over a project lifetime. Storage coefficient calculation methods are applied to three case studies: Sleipner, Snøhvit and Ketzin storage projects. This provides an understanding of the evolution of storage efficiency and the limitations of real data in establishing accurate assessments.

Chapters 5 contains the bulk of the new research, presenting a new modelling study assessing CO₂ migration and trapping over timescales that influence discussions regarding storage appraisal and efficiency. The modelling focuses on the structural setting, the role of water production and the consequences for storage security.

Chapter 6 presents the mathematical construction of analytical expressions to assess efficiency and uses the results from the modelling exercise and the case study to assess the accuracy of the new findings.

Finally, **Chapter 7** discusses the key learning and knowledge gaps, with **Chapter 8** presenting the main conclusions.

2 Published storage resource assessments

2.1 BACKGROUND

A literature review was conducted to inform an understanding of the established and common practises used to assess CO₂ storage resources alongside the technical modelling and analytical approximation research that exists to support observations from field examples. The examination of published storage resource assessments in the following text sections distinguishes review of publications on: total storage resources estimation methodologies; classification of storage resources; non-technical indices and readiness levels.

The storage resource assessments reviewed variously describe categories, classifications, levels and frameworks. Where these are all collectively referred to in the subsequent text the term 'scheme' is used.

2.2 STORAGE RESOURCE ESTIMATION METHODOLOGIES

Developing an understanding of geological CO₂ storage potential is a necessary and ongoing challenge during the development of decarbonisation policy making and planning. Research groups worldwide have considered methods to address the challenge of a unified method to estimate comparable potential storage volumes.

Storage resource assessment methodologies have been proposed and applied by organisations, research groups and projects since 2007. Methodologies were developed and subsequently extended by the Carbon Sequestration Leadership Forum (CSLF) Task Force (Bachu et al., 2007a; Bachu et al., 2007b; Bradshaw et al., 2007), and the United States Department of Energy (US DOE) Subgroup in 2007 on CO₂ Storage Capacity Estimation (Goodman et al., 2011; Gorecki et al., 2009; IEAGHG, 2009; NACAP, 2012; NETL, 2012).

A comparison of the estimation methodologies by Bachu (2008a) concluded both groups present broadly identical methodologies for storage resources estimation with only minor differences in computational formulation. This methodology is presented in Section 3.1. However, the comparison highlighted several analogies and minor differences in the estimation of storage resources within deep saline aquifers:

- 1) Only volumetric (static) storage of CO₂ in free phase is considered and discussed by the US DOE Capacity and Fairways Subgroup with no CO₂ in solution;
- 2) On the other hand, unlike the CSLF Task Force, the US DOE Capacity and Fairways Subgroup does not limit the volumetric trapping in deep saline aquifers only to stratigraphic and structural traps; rather the entire aquifer is considered;
- 3) The effect of irreducible water saturation is not taken into account explicitly in the calculation proposed by the US DOE Capacity and Fairways Subgroup, but is included in the efficiency factor (E) through the pore-scale displacement efficiency;
- 4) The two methodologies are computationally equivalent if the storage efficiency factor is equal to the capacity coefficient multiplied by a reciprocal of the irreducible water saturation and if an average CO₂ density at in-situ conditions is used in relation rather than minimum and maximum values.

Bachu (2008) also noted the US DOE Capacity and Fairways Subgroup explicitly recommends considering only saline aquifers (Total Dissolved Solids greater than 10,000 ppm) deeper than 800 metres or the necessary depth to ensure that CO₂ is in dense liquid or supercritical phase. The aquifers should also be confined by aquitards or aquicludes (cap rock) which include shale, anhydrite and evaporite. The CSLF Task Force did not make any specific recommendations in this regard, these screening criteria being implicit on the basis of the Intergovernmental Panel on Climate Change (IPCC) Special Report on CO₂ Capture and Storage (IPCC, 2005). A further discussion on the requirements for suitable CO₂ storage sites is included in Appendix A.

Building on these methodologies, the techniques were applied by multiple stakeholders to better understand local storage potential. The list below provides some examples with references for further reading:

- **ACST**; Australian Carbon Storage Task Force (Carbon Storage Task Force, 2009);
- **BGR**; Federal Institute for Geosciences and Natural Resources (BGR), Germany – Recalculation of Potential Capacities for CO₂ Storage in Deep Aquifers (Knopf et al., 2010);
- **BPM**; Best Practice Manual for the storage of CO₂ in saline aquifers (SACS and CO₂STORE projects, Chadwick et al., 2008);
- **CO₂SCREEN**; NETL CO₂ Storage prospective Resource Estimation Excel aNalysis (Sanguinito et al., 2020)
- **CO₂STOP** – a project mapping both reserves and resources for CO₂ storage in Europe (Poulsen, 2012; Poulsen et al., 2015)
- **NPD**; CO₂ Storage Atlas: Norwegian Sea (Norwegian Petroleum Directorate, 2014; Vangkilde-Pedersen, 2009);
- **Ogawa**; Saline-aquifer CO₂ Sequestration in Japan (Ogawa et al., 2011);
- **Silva**; A study of methodologies for CO₂ storage capacity estimation of coal (Silva et al., 2012);
- **TNO**; Geological Survey of the Netherlands (TNO) – Independent Storage Assessment of Offshore CO₂ Storage Options for Rotterdam (Neele et al., 2011a, b; 2012; EBN Gasunie, 2017);
- **UKSAP**; United Kingdom CO₂ Storage Appraisal Project (Gammer et al., 2011; Bentham et al. 2014);
- **USGS**; United States Geological Survey (USGS) (Brennan et al., 2010; Blondes et al., 2013).

2.3 CO₂ STORAGE RESOURCE ASSESSMENT METHODOLOGIES

In 2011, the International Energy Agency (IEA) convened workshops to review CO₂ storage assessment methodologies to harmonise estimates worldwide (Heidug, 2013). The workshops were attended by six national geological survey organisations and ten CO₂ storage assessments were compared for the UK, USA, Australia, Japan, Germany and Norway. The assessments compared at the workshops are included in the examples listed above in Section 2.2 and comparisons are tabulated in Heidung (2013, Annex 1). Output from the workshops identified best practise in the form of steps for the assessment of storage resource throughout the world, distinguishing whether management of subsurface pressure was required (Heidung, 2013). To further support harmonisation, it was recognised that enhanced international co-

operation between organisations that have completed assessments and those looking to begin assessment would be beneficial to all parties (Heidung, 2013).

In a study to support the work of the CSLF, potential barriers to national geological storage assessment were evaluated. Vincent et al. (2017) concluded that methodologies to estimate storage resource vary widely although there is continuous development in terms of technique. They also suggested that researchers and developers are unlikely to be persuaded to use only one methodology as the process of CO₂ storage appraisal was continually evolving and improving. Therefore, the population and publication of databases containing the parameters required to calculate storage resources was essential. The tabulated parameters should include input data needed for the calculation of storage resources (e.g., depth, porosity, formation thickness, net sandstone to gross thickness, areal coverage, volume of hydrocarbons removed, formation compartmentalisation, pressure, and temperature values) and the source of the data should be identified. As methodologies advance new calculations can then be re-applied to the underlying data and allow researchers to compare results from different methodologies. A summary of the analysis is given by Vincent et al. (2017).

2.4 STORAGE RESOURCE CLASSIFICATIONS

Common appraisal schemes to estimate CO₂ storage resources were reviewed and are summarised and compared in Table 1. The categories of storage resource are benchmarked against the storage characterisation activities of Bachu et al. (2007). In Table 1 the first-published works (Bachu et al., 2007; Bradshaw et al., 2007) consider classification of storage resource. The later-published schemes integrate the concepts of resource and reserve used by the petroleum industry at the time of publication (IEAGHG, 2009). A comparison of the storage resource classification systems is made with the Petroleum Resources Management System (PRMS) update published in 2011 (Etherington and Ritter, 2008) and its application to CO₂ storage project development in the Storage Resource Management System (SRMS) (SPE-SRMS, 2017). The benchmarking and comparison in Table 1 informed an assessment of maturity of data appraisal and understanding for the UK national CO₂ storage database (www.co2stored.co.uk). Users of the UK database sought an indication of the level of understanding for each of the more than 500 storage units as a component of a future CO₂ storage project. These classifications convey the level of understanding of the total storage resource, whereas the resource management system categories convey the thresholds achieved leading to the commercial development of a CO₂ storage project.

The published storage resource classifications considered in Table 1 were output from two parallel appraisal groups. The two groups considered here are:

- The Carbon Storage Leadership Forum (CSLF);
- The United States Department of Energy (US DOE) and International Energy Agency Greenhouse Gas Research and Development Programme (IEAGHG).

Table 1. Storage resource schemas, benchmarked against Bachu et al. (2007) and compared with industry resource management systems.

Storage characterisation activities of Bachu et al. (2007)	Comparison of published storage capacity schemas benchmarked against Bachu et al. (2007)				Comparison of storage resource schemas with the Petroleum and Storage Resource Management Systems (PRMS and SRMS)							
	Bradshaw et al. (2007) CSLF	Bachu et al. (2007)	(Gorecki et al., 2009; IEAGHG, 2009)		PRMS (2011) project maturity			SRMS (SPE-SRMS 2017)			Storage project maturity classes and sub-classes	
					Range of uncertainty			Range of uncertainty				
					Proved P10	Probable P50	Possible P90	Proved P10	Probable P50	Possible P90		
Matching of CO ₂ sources and sites; storage resources, injectivity, rates of supply	Viable capacity	Matched capacity	Practical storage capacity (viable under current economic conditions)	Proved capacity (practically and commercially feasible under current economic, technical and regulatory conditions)	Saleable reserves			Storage capacity				Discovered commercial
Probable capacity (anticipated economic conditions within a reasonable time-frame)				1P	2P	3P	1P	2P	3P	Approved for development		
Possible capacity (future economic condition)		Contingent Resource			Contingent storage resource			Discovered sub-	Justified for development			
Contingent storage resource (consider for future economic conditions)		1C	2C	3C	Low 1C	Best 2C	High 3C		Development pending Project activities ongoing			
Geological and engineering constraints applied	Realistic capacity	Effective capacity	Effective storage resource		Undiscovered prospective resources			Prospective storage resource			Undiscovered	Prospect project sufficiently defined to be a viable drilling target
					Low	Best	High	Low 1U	Best 2U	High 3U		Lead project poorly define and need further data and/or evaluation
					Uncharacterised storage resource							Play requires data and evaluation
Calculation of the physical limit that the geological system can accept	Theoretical capacity	Theoretical capacity	Theoretical storage resource	Characterised storage resource, takes account of porosity and water saturation	Useable storage resource							Total storage resource
				Uncharacterised storage resource	Unusable storage resource							

2.4.1 Evolution of capacity and resource assessment

The evolution in the classification of storage resources is summarised in Table 1 and described in the following numbered points, illustrated in Figure 1 to Figure 4. Moving through the classification systems is facilitated as data and understanding of a site/region is developed. This process reduces the uncertainty in storage resources and results in the justification and subsequent utilisation of the storage resource, the concept is illustrated in the simple schematic figure below.

1. Bradshaw et al. (2007) define three categories by application of technical and economic constraints as shown in Figure 1. The *theoretical capacity* defines the physical limit that the geological system can accept, the *realistic capacity* is determined by application of geological and engineering limits to the theoretical capacity; the *viable capacity* is further restricted by economic, legal and regulatory constraints. At each stage the certainty of storage potential increases with a concomitant potential decrease in storage capacity.

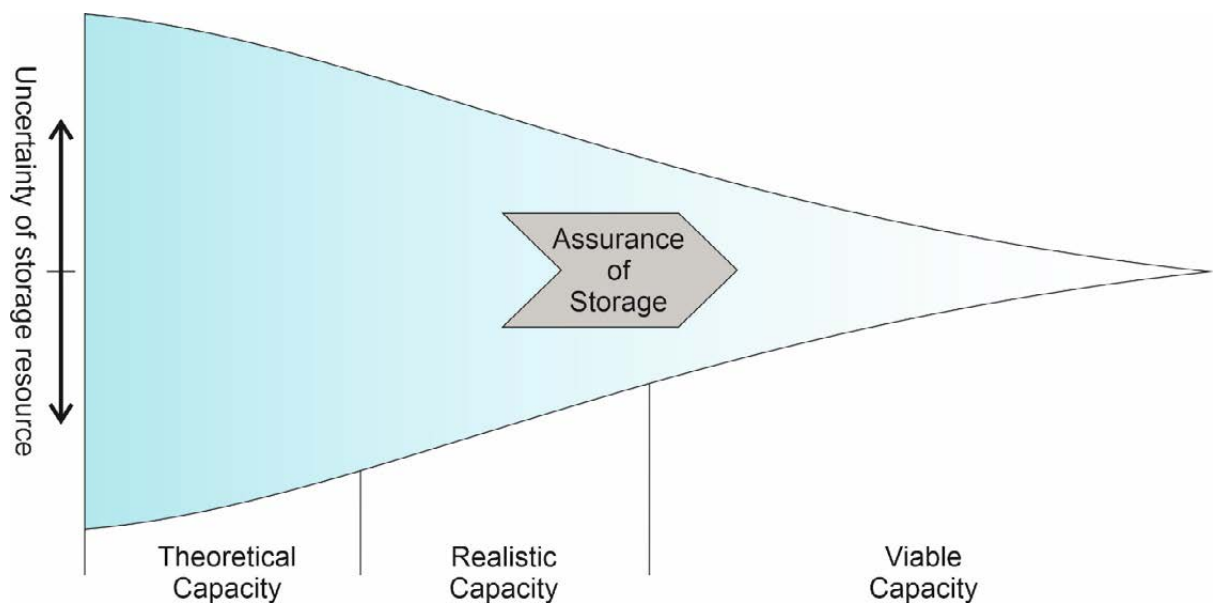


Figure 1. Graphical representation of the categories of storage capacity by application of technical and economic constraints, after Bradshaw et al. (2007), indicating increasing certainty of storage potential with potentially decreasing storage capacity from left to right.

2. Bachu et al. (2007) equate the development of understanding of CO₂ storage capacity to the concepts of resources, quantities of a commodity that are estimated at a given time, and reserves, commercially recoverable quantities of a known commodity, as followed for other energy and mineral commodities (Figure 2). The previous realistic capacity is re-termed as *effective capacity*, the former viable capacity is re-termed as 'practical capacity' and an additional category of *matched capacity* is included.

Matched capacity equates to a *marketable reserve* by the mining industry, in which the capacity, injectivity and supply rate correspond to a matched CO₂ source. Bachu et al. (2007) present their classification as levels of increasing certainty of estimation within a resource pyramid based on: availability of data; time and resources spent to interpret available data; necessary skills to undertake storage capacity estimates. The techno-economic resource-reserve pyramid and levels of Bachu et al. (2007) are illustrated and described in Appendix B.

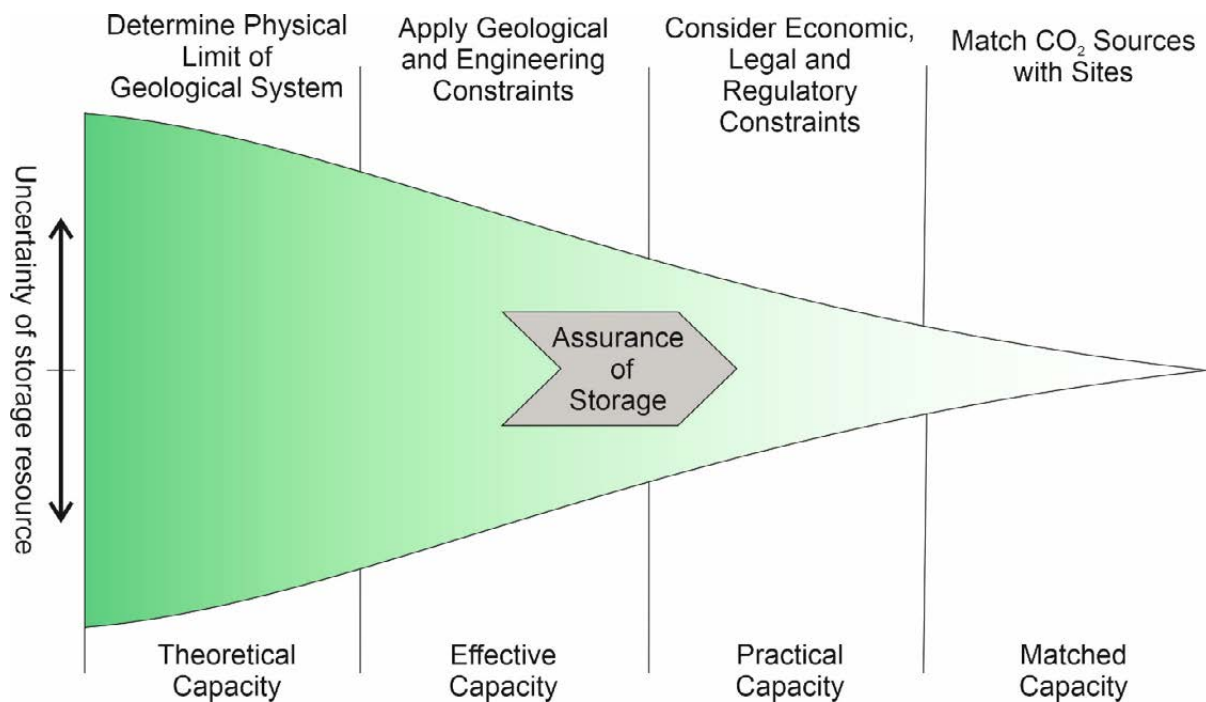


Figure 2. Graphical representation of the classification of storage capacity by application of the concepts of reserves and resources, after Bachu et al. (2007), indicating increasing certainty of storage potential with potentially decreasing storage capacity from left to right.

- IEAGHG (2009) classify storage capacity assessment by incorporating the techno-economic categories of Bradshaw et al. (2007) with resource appraisal to define and apply categories of resource and capacity specific to CO₂ storage (Figure 3). The scheme of IEAGHG (2009) is based on previously published techno-economic resource classifications and definitions (Bachu et al., 2007b; DOE, 2008). Comparison of the storage capacity estimation methodologies of the CSLF and US DOE/IEAGHG groups by Bachu (2008b) concluded the underlying methodologies are the same with only minor computational differences (for details see Section 3.1). *Resource* is defined by IEAGHG (2009) as the approximate available pore volume that is accessible for CO₂ storage. *Capacity* is the volume of CO₂ that can be stored after technical and economic constraints have been applied and the physical limit that a geological system can accept is termed the *theoretical storage resource* (IEAGHG, 2009); and equivalent to the theoretical capacity of Bradshaw et al. (2007) and Bachu et al. (2007). The theoretical storage resource category is sub-divided (Gorecki et al., 2009) into *characterised* pore volume, taking account of spatial variability of porosity and irreducible water saturation, and that which is

uncharacterised. Technical characterisation investigations may reveal pore volume that is available and *usable* for injection of CO₂ given current technical conditions) and distinguished from a theoretical storage resource that is *unusable* for CO₂ storage (IEAGHG 2009). The realistic/effective capacity of Bradshaw et al., (2007) and Bachu et al. (2007) is termed the *effective storage resource* by IEAGHG (2009) and termed the total accessible storage resource category by Heidug et al. (2013). The methods described in points 2 and 3 are a clear improvement on the work of Bradshaw et al. (2007) due to the clear alignment with subsurface project development.

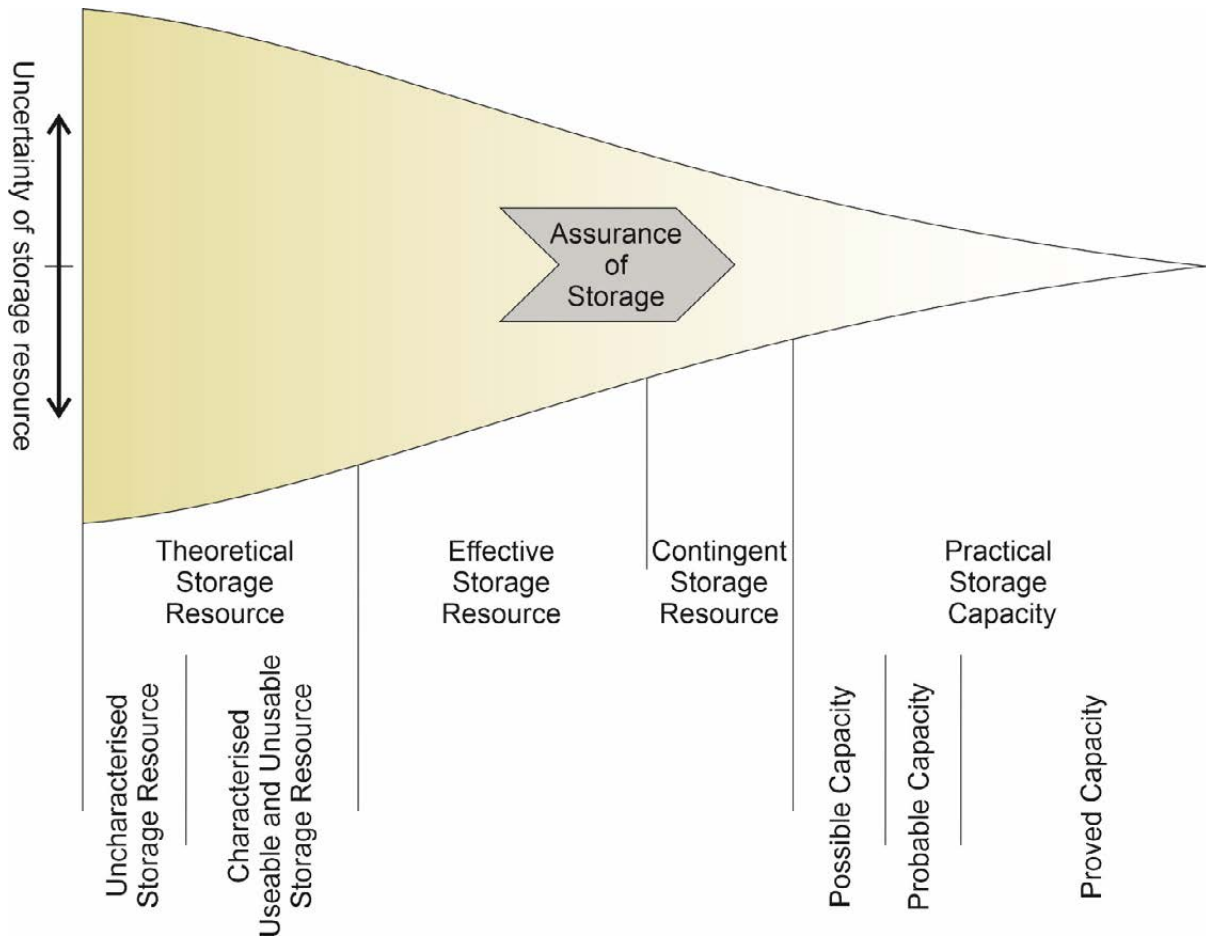


Figure 3. Graphical representation of the storage resource categories (Gorecki et al., 2009) indicating increasing certainty of storage potential from left to right.

- Application of economic constraints to the pore volume of effective storage resource by Gorecki et al. (2009) informs the step from a resource to a capacity (Figure 4). Where injection of CO₂ within a storage unit is viable under current economic conditions this is termed a *practical storage capacity*. Where an effective storage capacity is considered viable under future economic conditions it is termed a *contingent storage resource*. The assessment of *practical storage capacity* is further subdivided by readiness for, and timing of, storage into *proved, probable* and *possible storage capacity* (IEAGHG 2009). If a pore

volume is commercially feasible after geoscientific and engineering analysis, under current economic conditions, operating methods and government regulations it is termed *proved storage capacity* by IEAGHG (2009) and equivalent to the matched capacity of Bachu et al. (2007). In the category of *probable storage capacity* of IEAGHG (2009) it is expected to be economically viable to store CO₂ within a 'reasonable time frame' and the category of *possible storage capacity* anticipates readiness for storage viability under future economic conditions.

5. IEAGHG (2009) applied the categories of possible, probable and proved capacity published in the Petroleum Resource Management System (PRMS, 2007). In an update published in 2011 (PRMS, 2011) the increasing degree of understanding within the probable and possible capacity categories is based on indication of the range of certainty reflecting low (1P), best (2P), and high (3P) case outcomes for a hydrocarbon project, i.e., the likelihood of saleable reserves for a field. The low or highly likely estimate of *proved capacity* (P₉₀), the best or most likely estimate of *probable capacity* (P₅₀) and the high or less likely estimate is *possible capacity* (P₁₀). The three 'case' categories are applied to Contingent Resources (1C, 2C and 3C) and suggests that in future considerations be applied to Undiscovered Prospective Resources (Table 1).
6. An adaptation of the PRMS, the SRMS (SRMS-SPE, 2017) applies the resource management approach to CO₂ storage resources. Storage capacity is defined as only the pore volume that meets technical and commercial factors for an operational, approved or justified for development CO₂ storage project or 'discovered resource' (Table 1, Figure 4). Cumulative uncertainty categories of proved, probable, and possible storage capacity are defined by probabilistic measures. Pore volume that is potentially accessible but is not yet a commercial prospect is termed contingent storage resources. The probabilistic uncertainty categories might also be applied to contingent storage resources if criteria for project discovery and development apply. The key step is from an undiscovered prospective resource to a discovered contingent resource. Direct evidence (for example from wells drilled within or close to storage site) of storage resource potential is required for a discovery, i.e., the presence of the storage formation, and ability to receive and contain injected CO₂. Otherwise, the general cumulative terms of low, best and high estimates should be used for both contingent and prospective (undiscovered) storage resources, termed 1U, 2U and 3U (Table 1). Sub-classes of project development are applied to the accessible storage resource associated with increasing chance of commerciality, as used for petroleum resources (PRMS, 2011). Prospective (undiscovered) storage resources may be considered as plays, leads or prospect storage projects with increasing appraisal, confidence in understanding and chance of commerciality. The developmental assessment of projects with sub-commercial, contingent storage resources may be considered as unclarified, not viable, on hold, or pending development associated with increasing commercial feasibility (SPE-SRMS, 2017). The commercial development subclasses are defined, and guidelines given for their usage by the SRMS (SPE-SRMS, 2017). The SRMS uses a two-axis system to allow for technical uncertainty to be expressed on the x-axis and is becoming the internationally standard scheme. Total storage resource is geologically linked and is development scheme codependent. It is the total quantity of CO₂ that can be stored in a 3D volume for millenia and is the sum of the structurally trapped, residually trapped, dissolution trapped and mineralised trapped CO₂ in a rock volume and every pore is connected.

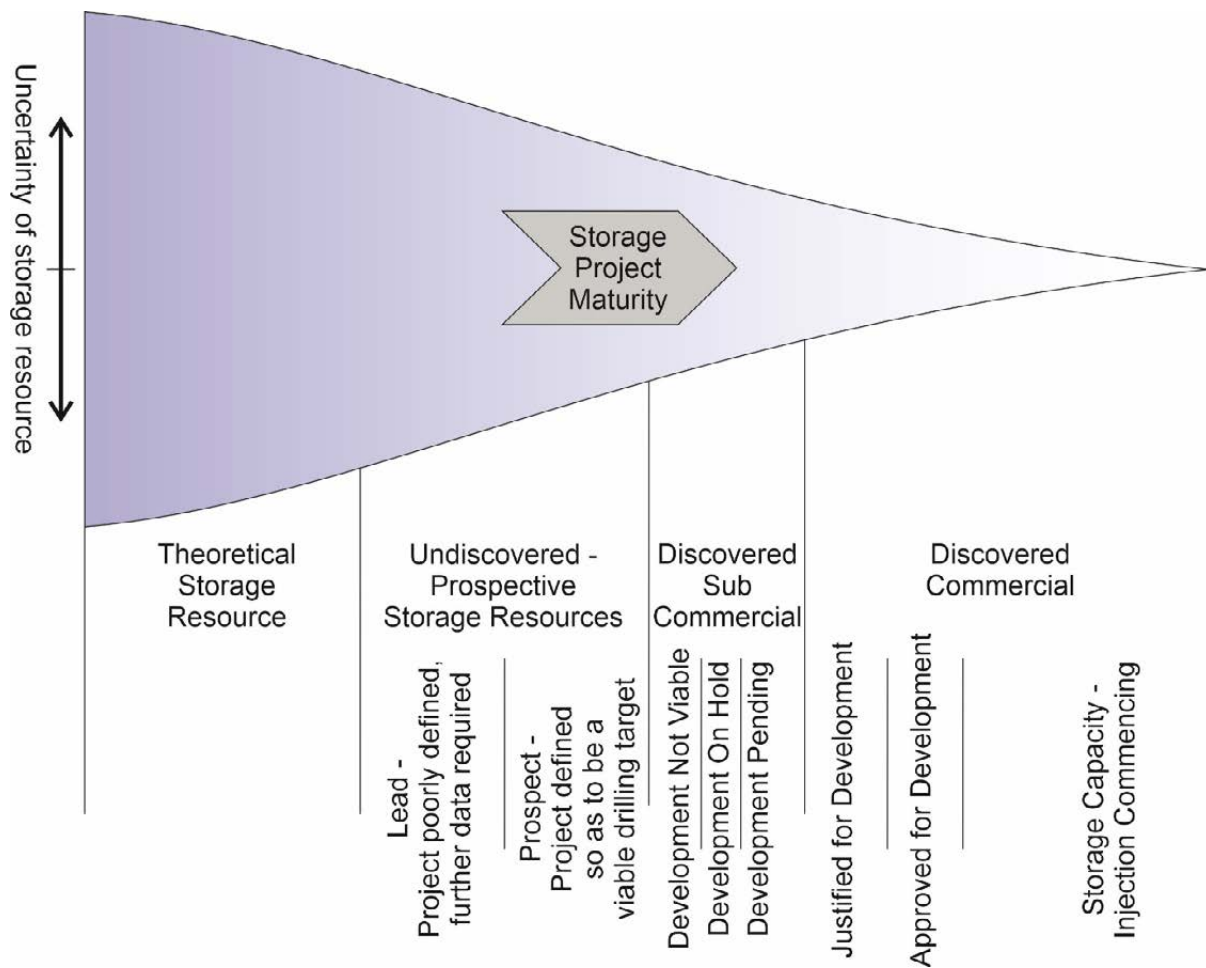


Figure 4. Graphical representation of the SRMS (SPE-SRMS, 2017) storage resource classification system indicating increasing certainty of storage potential from left to right.

An alternative classification system to the SRMS is developed by the United Nations Economic Commission for Europe (2020). The United Nations Framework Classification for Resources (UNFC) is a three-axis system. The axes are: environmental-socio-economic viability, technical feasibility, and degree of confidence. It is not specific to CO₂ storage like the SRMS and is not included in detail in this study.

2.5 CO₂ STORAGE MATURITY OF UNDERSTANDING, READINESS INDICES AND LEVELS

Assessments of maturity of understanding, and indices and levels of readiness for CO₂ storage have also been published. These assessments consider factors in addition to storage resource assessment that are relevant to the development of CO₂ storage sites.

Maturity of understanding and levels of appraisal, as well as quality of available data, have been considered in the compilation of CO₂ storage atlases around the globe. The high-level mappings found in these atlases are usually focused on identifying sedimentary basins where exploration

for storage resources for a region or country's potentially captured CO₂ is likely to be successful. For example, the CO₂ atlas for the Norwegian continental shelf (Norwegian Petroleum Directorate, 2011) applies the storage resource classification of Bradshaw et al. (2007, Section 2.4.1 and Appendix C).

The Global CCS Institute's CCS (carbon capture and storage) readiness index (Consoli et al., 2017) (Consoli et al. 2017, and subsequent annual updates) is a high-level analysis applied country by country to rank major barriers and enablers for CCS deployment. A country's position within the CCS readiness index is based on the final score across four indicators:

- National interest – set of criteria based on global shares of fossil fuel production and consumption.
- Policy – criteria based on an extensive range of policy measures that governments at all levels can use and are critical to CCS. This includes direct support for CCS as well as broader implicit support through measures such as carbon pricing and research funding for example.
- Legal and regulatory frameworks – criteria used offer a detailed examination and assessment of a country's national legal and regulatory frameworks, which are critical to the regulation of CCS. These may include environmental assessments, public consultation and long-term-liability.
- Maturity of storage resource assessment on a national level – using criteria that consider all geological and technical aspects that could impact an injection and storage project within the borders of a country, including the geology, the maturity of storage assessments, site characterisation development and technical ability to store CO₂.

The maturity of storage resource indicator grades the assessment of potential storage resource classification. It follows the methodologies summarised in Section 2.4.1. The grade is converted to a score that is weighted, converted to a total out of 100 and allocated to one of five status levels from 'prepared for wide-scale storage' to 'yet to make a start or very low potential' (Consoli et al., 2015). Application of a standardised approach to storage resource classification has benefitted the ranking of a country's CCS development and deployment. Consoli et al. (2017) acknowledge that a country's score within the indicators may change dramatically particularly in the policy and regulation, rather than storage resource assessment indicator.

Application of the SRMS (SPE-SRMS, 2017) to the national CO₂ storage portfolios in the UK and the Netherlands by Akhurst et al. (2021) placed the vast majority of the storage units within a single category. More than 550 UK and 100 Netherlands sites are classified as undiscovered storage resource despite the differing levels of understanding from research investigations of feasible CO₂ storage project concepts by industry and academia (Akhurst et al., 2021). Akhurst et al. (2021) note that the SRMS classification does not reflect the range of maturity of understanding and assurance of resource and containment of the storage units classified as 'undiscovered' storage resource. This is because the SRMS is project-based, and therefore not applicable to the lowest storage readiness levels. Sites in a regional atlas would require the setup of individual projects and specific data acquisition to climb to the SRMS maturation scheme. In their assessment of availability of CO₂ storage resources, the Oil and Gas Climate Initiative (OGCI, 2017) conclude that 97% of the global storage resource is prospective in nature. Cavanagh et al. (2020) also recommended that application of the SRMS should not be the principal method to assess maturity of understanding for CO₂ storage in promising regions as the requirements for 'discovered' status was too high a standard to meet. They recommend a tiered approach to quantitative capacity estimation based on the classification of Bachu et al. (2007, Section 2.4.1) and a Boston square analysis to represent a broader assessment for data quality and suitability of attributes (Cavanagh et al., 2020).

Akhurst et al. (2021) also note that the storage resources and SRMS classifications do not consider all factors that influence feasibility of a prospective site for an operational CO₂ storage project. Non-technical factors will also determine the feasibility of a site, including ownership, regulatory regime, available CO₂ for storage, and prior planning and permitting, as the storage component of a CCS project (Akhurst et al., 2021). The SRMS classification and the maturity appraisals of CO₂ storage databases/atlasses do not also convey what has been achieved and what remains to be undertaken to CO₂ storage stakeholders unfamiliar with CO₂ storage permitting and CCS project planning, although it is noted that these may not be the main target audience of the SRMS. Akhurst et al. (2021) present a framework of CO₂ Storage Readiness Levels (SRLs) to communicate technical understanding, progress toward regulatory requirements for CO₂ storage and injection, and planning of a site as a component of a commercial CO₂ storage project. The objective is to convey a common understanding to technical and non-technical stakeholders alike of the technical appraisal of a site, achievement of permits, and planning for a CO₂ storage project. The SRL framework is designed to complement and exist alongside the industry SRMS classification, building on hydrocarbon industry knowledge and practice, since such expertise and assets are anticipated for commercial implementation of CCS (Figure 5).

Storage Readiness Level (SRL)	Storage Resources Management System Storage project maturity classes and subclasses (SPE-SRMS, 2017)		
SRL 9 – Storage site on injection	Discovered storage resources	Commercial (capacity)	On injection
SRL 8 – Commissioning of the storage site and test injection in an operational environment			Approved for development
SRL 7 – Storage site is permit ready or permitted			Justified for development
SRL 6 – Storage site integrated into a feasible CCS project concept or a portfolio of sites (contingent storage resource)		Sub-commercial (contingent storage resources)	Development pending – Project activities ongoing
			Development on hold or unclarified
			Development not viable
SRL 5 – Storage site validated by detailed analyses, then a relevant 'real world' setting	Undiscovered storage resources	Prospect – Project sufficiently well-defined to be viable drilling target	
SRL 4 – Storage site validated by desktop studies and storage project concept updated		Lead – Project poorly defined and needs data and/or evaluation	
SRL 3 – Screening study to identify an individual storage site and an initial project concept		Play – Requires more data and/or evaluation	
SRL 2 – Site identified as theoretical capacity in a storage atlas			
SRL 1 – First-pass assessment of storage capacity at country-wide or basin scales			

Figure 5: Equivalence of the Storage Readiness Levels with the Storage Resources Management System project maturity classes and subclasses (SPE-SRMS, 2017) from Akhurst et al. (2021).

3 Storage resource calculation

CO₂ storage cannot utilise the entire volume of a storage site/region and must be confined to the pre-determined storage reservoir both laterally and vertically. In addition, within the reservoir the entire available pore space is not accessible. This is a consequence of a number of factors, including immiscible displacement physics, irreducible water saturation, segregation from CO₂ buoyancy/gravity forces, geological heterogeneity, reservoir compartmentalization, limits to permissible pressurisation, distance from injection wells, and the presence of resident fluids. To make meaningful estimates of storage resources, the concept of storage coefficients, also termed storage efficiency coefficients, efficiency coefficients, or storage efficiency, is used as defined by the proportion of a given pore volume accessible to or occupied by injected CO₂.

The literature review above identified differing storage assessment techniques. The methods often build upon the experience of the hydrocarbon and mineral industries (Bachu et al., 2007b; Brennan et al., 2010). The methods vary in their classification definitions and are applicable to saline aquifer and depleted field storage. The approaches are linked in the determination of a storage coefficient to provide robust estimation of the storage potential at a scale appropriate to the geological domain under consideration. An increase in certainty of storage is achieved as more characterisation/operational data are acquired.

Capacity coefficients as defined by the CSLF (Bachu et al., 2007) and storage efficiency factors as defined by the EERC (IEAGHG, 2009) are storage coefficients, which are multipliers that approximate the percentage of a region/site's total pore volume that will contribute to CO₂ storage. Techniques vary with how they quantify trapping mechanisms but generally they start with simple volumetric calculations, leading to complex mathematical approaches that simulate the flow of fluid in the subsurface. The different methods and studies assess varying storage options (aquifer, depleted field, enhanced hydrocarbon recovery, enhanced coal bed methane, etc).

The schemes adopted tend to include factors for:

1. Pore space estimation. Accounting for factors such as: heterogeneity, injectivity etc.
2. Understanding of reservoir dynamics. Moving towards a dynamic estimate from a static volumetric approach and accounting for response of storage unit and fluids to physical process linked to injection e.g., pressure

Storage resource evaluation schemes require that the reservoir be adequately positioned in the stratigraphy and dependent upon a suitable overlying sealing unit. The assessment of Brennan et al. (2010) describes this pair of reservoir rock underlying a suitable sealing unit as a Storage Assessment Unit. Appendix A describes the requirements for a suitable storage complex. The rock parameters are also sometimes classified as 'unsuitable for storage' and minimum porosity, permeability or injectivity values are set in the USGS, UKSAP, BPM and TNO methodologies.

Storage appraisals, for example as used in the databases described below in greater details, often require storage below a cut-off depth of approximately 800 m to ensure dense phase storage, which gives greater volumetric efficiency. In addition, some calculation schemes also specify a maximum depth (e.g., Brennan et al., 2010) due to high pressures, consequences for injectivity and reservoir quality.

3.1 VOLUMETRIC STORAGE RESOURCE CALCULATION

Estimation of CO₂ storage resources begins with evaluating the total pore volume of the target reservoir/formation. Additional processes will act to reduce the available storage resources. A

simple open aquifer may be modelled with a simple volume balance, replacing water with CO₂. This is described by the following:

$$V_{CO_2} = V \phi (1 - S_{wir}) \quad (1)$$

Where V_{CO_2} is the volume of stored CO₂, V the total bulk volume of the storage site (defined laterally by a given extent where CO₂ must be contained within and vertically by the reservoir interval), ϕ the effective porosity (including net-to-gross), and S_{wir} is the irreducible water saturation.

These volumetric calculations do not consider additional, important factors such as the physics of immiscible displacement when injecting CO₂ into a brine saturated formation, injectivity, permeability, heterogeneity, dissolution and residual trapping, and migration of CO₂ out of the storage site. Dynamic factors can drastically reduce the storage resources of a site and can be estimated by using efficiency coefficients, as discussed later. These coefficients are very site specific, most helpfully estimated using detailed numerical simulations. They represent a correction factor between reality and the ideally available pore space. Volumetric estimates are generally significantly higher than dynamic values of storage coefficients, they require much less data input and therefore can be applied to sites with very low SRLs, and require minimal computational effort.

3.1.1 Saline aquifers

Saline aquifers provide the greatest potential for CO₂ storage globally. For example, in the UK 80% of the available pore space is likely to be found in saline aquifers (www.co2stored.co.uk). The ability to characterise the potential efficiency of a storage system varies with domain size, as estimates may be required from site to basin scale, and the results may not be transferable from one size to another. This lack of transferability is often a consequence of the wider reservoir compartmentalisation, or heterogeneity in the geological system and/or trapping mechanism.

Compartmentalisation plays a key role in the calculation of storage efficiency in saline aquifers. Where boundary conditions constrain the assessment, acting to restrict the lateral flow of fluids from the appraisal volume, it is necessary to consider the domain as a closed system and calculate the storage efficiency accordingly.

The storage resources of a closed aquifer is described by the total change in volume experienced with a consistent pressure increase to the pore and fluid system. This is the sum of the water and pore volume changes, and is based on the compressibility of the water and pore space:

$$V_{CO_2} = V \phi (c_w + c_p) \Delta p \quad (2)$$

Where in this case V_{CO_2} is the volume of CO₂, V is the bulk volume, ϕ the effective porosity, c_w and c_p are the compressibility of the water and rock, respectively, and Δp is the allowable increase in pressure within the geomechanically defined limits of the reservoir and caprock.

In the end member case of an open system, where the injection takes place in a regional system and formation brine can migrate away from the injection point, and there is no significant pressure build up in the reservoir, a simple substitution can be applied as above. Most real cases have some level of pressure increase.

3.1.2 Depleted fields

The role of depleted oil and gas reservoirs in CO₂ storage projects is likely to be significant since the reservoirs have a proven history of long-term secure storage of subsurface fluids. In addition, the history of exploration and production will accumulate important information informing site characterisation, baselining and dynamic reservoir performance.

Depleted fields are reservoirs where production of hydrocarbons have declined to the point where it is no longer economically viable to continue extraction. The knowledge and data gained through the hydrocarbon extraction process can progress the characterisation from uncharacterised to characterised storage resources.

The standard methods for estimation of storage resource in depleted fields have been offered from several research groups and are often very similar to those of saline aquifers. The most common methods for calculating storage resource in depleted fields are based two simple methods. Firstly, a material balance assumes that the reservoir volume of extracted hydrocarbons is equal to the reservoir volume available for CO₂ storage. This is similar to that of Equation 1. Secondly, the compressibility of all present fluids (i.e. brine plus oil/gas) can be used together with the allowable pressure increase in a format analogous to Equation 2. The volume and compressibility of each of the components must be included.

Depleted fields can either be open or closed systems. Some use the term semi-closed to refer to closed systems allowing for some level on migration into the over- and/or under-burden (Zhou, Q. et al., 2008). In a confined aquifer, behaving like a closed system, it is expected that the pressure will remain low after depletion until CO₂ injection acts to raise it up towards pre-extraction hydrostatic levels. In an open system, however, as the hydrocarbons are produced from the reservoir and the pressure decreases, pore fluids from the surrounding aquifer will migrate into the site, recharging the pressure. In this case, injection of CO₂ will then need to once again displace the resident brine in a drainage process more typical of a saline aquifer.

The US DOE approach is constructed as a volumetric framework and states:

$$G_{CO_2} = A * h_n * \varphi_c * (1 - S_w) * \rho_{CO_2} * E$$

Where G_{CO_2} is the effective mass estimate of the CO₂ resource, A is the area of assessment for the storage calculation, h_n is the oil and gas column height of the formation. (This a simple approach, and where possible the actual volume is used based on 3D models.) φ_c is the average porosity of the formation within the net thickness, S_w is the average water saturation within the volume defined by the area and height, ρ_{CO_2} is the density of CO₂ at formation conditions, and E is the storage efficiency factor, which also includes the recovery factor. This can also be used for saline aquifers, is very similar to Equation 1 and introduces the storage coefficient.

The CSLF provides a very similar volumetric tool to assess storage capacity:

$$M_{CO_2E} = C_c * \rho_{CO_2r} * [R_f * A * h * \varphi * (1 - S_w) - V_{iw} + V_{pw}]$$

Where M_{CO_2E} is the effective, characterised mass of the resource, C_c is the capacity coefficient, ρ_{CO_2r} is the density of CO₂ at reservoir conditions, R_f is the recovery factor of the formation defines a capacity coefficient, C_c , which is broken down into a number of factors which describe the consequences of subsurface process and reservoir behaviour that act to reduce the total storage resources such that:

$$C_c = C_m * C_b * C_h * C_w * C_a$$

Where the subscripts m , b , h , w and a denote mobility, buoyancy, heterogeneity, water saturation and reservoir strength respectively. For further details see Bachu (2008a).

The two methods are comparable, initially aiming to express the volume of the storage trap and then calculating the mass of CO₂, at reservoir conditions, that can be stored within the volume. However, the CSLF utilise a recovery factor, R_f , to describe the hydrocarbon volume and terms accounting for the pore space that has been saturated, V_{iw} , or made available, V_{pw} , through water injection or production activities.

The volumetric approach for depleted field storage resource estimation is a suitable scheme when dealing with open or large semi-open reservoirs. In these scenarios the storage resources are strongly influenced by the efficiency of CO₂ to displace existing pore fluids.

Where the reservoir is closed to outside pressure influences the total storage resources are more strongly influenced by the volume of produced hydrocarbons and the compressibility of the formation and fluids to the associated pressure increase. In these scenarios it is better to use a mass balance calculation that determines the available pore space through an evaluation of the storage volume created by production. CSLF report equations for gas and oil reservoirs:

$$M_{CO_2T} = \rho_{CO_2r} * R_f * (1 - F_{IG}) * OGIP * \frac{P_s * Z_r * T_r}{P_r * Z_s * T_s}$$

GAS

$$M_{CO_2T} = \rho_{CO_2r} * [R_f * OOIP - V_{iw} + V_{pw}]$$

OIL

Where F_{IG} is the fraction of injected gas; the original gas in place is $OGIP$, and P , Z , and T are the pressure, compressibility factors, and temperature, respectively, at the reservoir, r , and surface conditions, s . The original oil in place is $OOIP$ and is represented in stock tank volume. These equations are not suitable for the more complicated cases of reservoirs with both oil and gas.

The rest of this study, including case studies and modelling work, is focussed on saline aquifers.

3.2 DYNAMIC STORAGE EFFICIENCY COEFFICIENTS

Dynamic storage coefficients include additional factors that cannot be captured using simple analytical volumetric methods. The usual method of calculating the storage efficiency coefficient is to use numerical modelling. This can incorporate both static and dynamic processes to estimate the proportion of pore volume that can be utilised by CO₂ storage. Factors such as gravity effects and heterogeneity, can have a complicated influence on the storage efficiency which is not appropriate for static, volumetric methods. Also, the dynamic response of a reservoir, such as injectivity, pressure increase and connectivity can strongly influence the amount of CO₂ that can be stored economically. Numerical models only provide an estimate of the storage coefficient of a site. They are limited by the effects included in the model and based on the parameters provided. These parameters are each associated with uncertainty, and some can be very difficult to predict. Accurate estimates of CO₂ storage volumes and corresponding storage efficiency factors are best achieved using dynamic flow simulations and detailed 3D geological models. In a similar way to the storage resource pyramid, the more site-specific information available, the smaller the uncertainty in the storage coefficient. For early-stage estimates, high accuracy is not needed (and perhaps not possible due to differences between sites) but a ballpark estimate and more analytical methods provide a cost-effective estimate.

The US DOE (Goodman et al., 2011) use a volumetric scheme to determine the total storage resources of saline formations:

$$G_{CO_2} = A * h * \varphi * \rho_{CO_2} * E$$

Where G_{CO_2} is the effective mass estimate of the CO₂ resource, A is the area of assessment for the storage calculation, h is the thickness of the formation, φ_e is the average porosity of the formation, ρ_{CO_2} is the density of CO₂ at formation conditions, and E is the storage efficiency coefficient.

E is determined through assessment of variables that reduce the capability to fill the entire pore space and incorporates dynamic factors. The US DOE variables that form seven multiplicative terms can be split into two groups. The first group relates to the heterogeneity of the formation and defines the reachable volume of pore space with terms accounting for area, A_n/A_t the fraction of region under assessment where suitable formation exists, thickness, h_n/h_g the fraction of the formation where suitable porosity and permeability for injection and storage exist, and porosity, $\varphi_{eff}/\varphi_{tot}$ the fraction of effective, interconnected porosity that exists. The second group consider the volume of reservoir rock close to the injection well and relate to the effectiveness and efficiency of displacing pore fluids. E_A defines the fraction of area that can be contacted by CO₂, E_I defines the fraction of the vertical thickness within the region that can be contacted by CO₂, E_g defines the fraction of the net thickness that, as a consequence of the density difference between brine and CO₂, can be contacted by CO₂ and E_d defines the fraction of the CO₂ contacted volume where brine can be replaced by CO₂.

$$E = A_n/A_t * h_n/h_g * \varphi_{eff}/\varphi_{tot} * E_A * E_I * E_g * E_d$$

This US DOE method was introduced at a similar time to an equivalent approach from the CSLF. The two methods are similar, but differences do exist, and in 2008, CSLF released a document which compared the two methods (CSLF, 2008). The two schemes are discussed at length by IEAGHG (2009) where the major differences highlighted show that the CSLF method only considers storage in traps while the US DOE method considers storage across entire saline formations at the regional scale. They conclude that ‘differences are basically the arrangement of the equations, which in the end makes the methods virtually equivalent’.

IEAGHG (2009) worked extensively on how to best estimate storage efficiency and ran a series of numerical studies under a range of structural settings to consider the key parameters on storage efficiency and storage resources across a set of geological realisations. The outcome of this work is summarised by IEAGHG (2009) as:

- The identification and refinement of equations for estimating CO₂ storage resources in saline formations
- The development of coefficient values for such systems, representing a wide variety of geological features at scales ranging from small to very large
- An approach for utilizing those equations and coefficients toward the development of technically defensible and consistent storage resource estimates.

IEAGHG (2009) considered a large parameter space in the modelling. They used key variable ranges derived from an “Average Global Database” (AGD) and fluid and geological properties for over 20,000 hydrocarbon reservoirs representing a wide variety of reservoir types from all over the world. The approach developed a series of generic 3D models that were representative of different lithologies, depositional environments, and structures and all models used probabilistic P10, P50, and P90 geological and fluid property values derived from the AGD for selected structures and depositional environments. Their study ran numerical simulations and calculated storage coefficients (termed C_e in their work) from the models.

The modelling approach resulted in a storage coefficient calculated at the end of injection following injection of 1 million tons of CO₂ over 1 year. This isn’t a very realistic scenario as injection of only 1 Mt is not economically viable and doesn’t utilise much of the pore space. The modelling was constrained by a bottom-hole pressure limit set at 0.6 of the lithostatic pressure

gradient. Due to the timescales involved they considered residual and solution gas trapping and did not include mineral trapping. The simulation grid used extended 3.22 km by 3.22 km split into 69, 69, 43 cells (I, J, K) – the minimum model size to contain all the injected CO₂. Following injection, the free-phase CO₂ saturation (all mobile and residually trapped CO₂) was used to define the boundaries of the plume.

The calculation of storage coefficients was undertaken with values assigned for net-to-gross area (assigned from the US DOE Atlas), net-to-gross thickness (calculated from AGD at the site-specific level) and effective-to-total porosity (calculated from the AGD). This enabled IEAGHG (2009) to calculate the four displacement efficiency terms based on their numerical simulations. The terms that were considered most likely to influence the storage coefficient and considered in the following text sections (and their influence on storage efficiency) were:

- **Depth** - higher efficiency at greater depths
- **Temperature** - higher efficiency at higher temperatures
- **Vertical to horizontal permeability ratio (k_v/k_h)** - higher efficiency at lower values of k_v/k_h
- **Injection rate/fluid velocity** - higher efficiency at higher injection rates
- **Relative permeability/irreducible water saturation** - variable complex relationships. Irreducible water saturation is counted separately in some definitions of efficiency
- **Structure** - efficiency increases significantly with structural trapping

3.2.1 Definitions of storage coefficients

The storage coefficient is an estimate of the proportion of pore volume of a reservoir that is utilised by injected CO₂. The contacted reservoir volume is generally based on the extent of the free and (residually) trapped CO₂ plume. IEAGHG (2009) consider four concepts to define the plume area: maximum radius; minimum area circle (diameter is maximum length of the plume); convex hull (polygon based on the outermost points of all lobes of the plume); and minimum area rectangle (based on maximum width of the plume and maximum extent perpendicular to maximum width). Okwen et al. (2010) and Ringrose (2020a) define the storage coefficient based on a cylinder with radius corresponding to maximum extent of the CO₂ plume. Also there is the vertical extent to consider, in this study we include the whole reservoir thickness in the calculation of efficiency. A different definition may use the spill point of a trap as the maximum depth, but this would give a much higher storage coefficient whilst the deeper pore space was not utilised.

As the CO₂ spreads and travels (post-injection) the areal footprint is increased, and the storage coefficient, based on the extent of the plume (or sweep), is reduced. Gravity effects dictate that buoyant CO₂ rises towards the top of the reservoir. Depending on the relative properties of the water and CO₂, the permeability ratio (k_v/k_h) and any heterogeneities (e.g., low permeability shale layers) can lead to a large pore volume beneath a thin plume that is not utilised by CO₂ and therefore a low storage coefficient. Horizontal baffles, such as shale layers, work to increase the storage coefficient by utilising more of the thickness of the reservoir for CO₂ storage. Plumes with multiple layers, as seen at the Sleipner operation (Norway), may allow for a much higher storage coefficient than a single layer.

The definition of storage efficiency coefficients is not widely agreed upon and can give a wide variety of values and meanings. IEAGHG (2018) base the denominator of their storage efficiency coefficient on the total pore volume of the model. The model areas used were arbitrary rectangles. Although this allowed analysis of the maximum simulated CO₂ injection in a given area, account was not taken of the area outside of the arbitrary boundaries. IEAGHG (2018) study the “dynamic efficiency”, defined as the effect that increased pressure caused by fluid injection has on the storage resources of a formation. Their focus was on the maximum amount of CO₂ that could be

injected into particular models (i.e. a given pore volume), given the pressure limitations of boundary conditions and caprock.

These two very different definitions of what a storage coefficient is, based on two different values in the denominator result in different factors being considered important. When conducting a CO₂ storage project all factors have to be taken into consideration, not just storage coefficient alone with either definition used.

The storage coefficient may be separated into a number of different factors, such as the ones listed in Table 2. Geological factors such as net-to-gross and porosity can be applied independently. Other factors, such as gravity are more often grouped together and estimated with numerical simulations. For structural traps, there is a strong dependence on structural amplitude (trap height over spill point depth) vs reservoir thickness, this can be very site specific and is usually incorporated in numerical modelling.

In this study we focus on the volumetric displacement efficiency. This is defined as the ratio between the reservoir volume of injected CO₂ and the accessible pore volume of a reservoir defined by the propagating CO₂ plume (the area swept by the CO₂ plume and its trail).

Table 2. US DOE Efficiency factor terms, taken from IEAGHG (2009).

Term	Symbol (range)	Description
Terms Used to Define the Entire Basin/Region Pore Volume		
Net to Total Area	A_n/A_t (0.2–0.8)	Fraction of total basin/region area that has a suitable formation present.
Net to Gross Thickness	h_n/h_g (0.25–0.75)	Fraction of total geologic unit that meets minimum porosity and permeability requirements for injection.
Effective to Total Porosity Ratio	$\phi_{\text{eff}}/\phi_{\text{tot}}$ (0.6–0.95)	Fraction of total porosity that is effective, i.e., interconnected.
Terms Used to Define the Pore Volume Immediately Surrounding a Single-Well CO₂ Injector		
Areal Displacement Efficiency	E_A (0.5–0.8)	Fraction of immediate area surrounding an injection well that can be contacted by CO ₂ ; most likely influenced by areal geologic heterogeneity, such as faults or permeability anisotropy.
Vertical Displacement Efficiency	E_I (0.6–0.9)	Fraction of vertical cross section with the volume defined by the area (A) that can be contacted by the CO ₂ plume from a single well; most likely influenced by variations in porosity and permeability between sublayers in the same geologic unit. If one zone has higher permeability than others, the CO ₂ will fill this zone quickly and leave the other zones with less CO ₂ or no CO ₂ in them.
Gravity	E_g (0.2–0.6)	Fraction of net thickness that is contacted by CO ₂ as a consequence of the density difference between CO ₂ and in situ brine.
Microscopic Displacement Efficiency	E_d (0.5–0.8)	Portion of the CO ₂ contacted, brine-filled pore volume that can be replaced by CO ₂ .

3.2.2 Trapping mechanisms

The security of CO₂ storage is dependent on both the structure of the CO₂ storage site and the various mechanisms in which the CO₂ is trapped. Following injection, the CO₂ will migrate through the storage unit and displace in situ pore fluids, leaving at least the residual water saturation in place. Initial trapping relies upon physical processes as discussed in this section.

CO₂ is contained beneath a low permeability sealing unit overlying the reservoir and preventing further upward migration of CO₂. During this process the CO₂ partly displaces the native pore fluids. Stratigraphic or structural trap occurs when the topography of the sealing unit (caprock) is such that further lateral migration is not possible due to buoyancy forces. Anticlinal structures act to contain CO₂ within a lateral area, within a spill point. An open, dipping aquifer allows for continual lateral migration of CO₂ as it travels up-dip. This may be towards some eventual point of closure (fetch-trap) or until other trapping mechanisms (such as residual and dissolution trapping) prevent further migration.

During the migration process residual trapping occurs as some CO₂ remains attached to the surfaces of the grains of rock due to capillary forces. Through this process, CO₂ is left in the path of the migrating CO₂ distribution.

Carbon dioxide can dissolve into the pore fluid and so become trapped in solution (formation water with dissolved CO₂ is denser than native formation water and so will have negative buoyancy). These trapping mechanisms are dependent on the salinity of the pore fluid and the temperature and pressure in the reservoir. Once dissolved the denser pore fluid sinks to the base of the storage unit enabling unsaturated water to encounter the migrating CO₂. The rate that mixing occurs influences the amount of dissolution trapping, and in order to dissolve a significant mass of CO₂ long time periods may be necessary.

The reactions between the CO₂, the rock matrix and the native pore fluids results in chemical trapping of the CO₂. The mechanism is dependent on the mineralogy of the reservoir rock, the composition and chemistry of the pore fluid and the amount of migration experienced by the CO₂ plume. The timescale for mineral trapping is long, even millennia, but the security of storage is the key benefit to finding a suitable reservoir.

3.2.3 Methods and limitations of published works

The efficiency coefficient depends on time. IEAGHG (2009) calculate the efficiency coefficient at the end of the injection phase (1 year) but the value will change throughout the injection and post-injection phases. Bachu (2015) show a rapid increase in the efficiency coefficient during early injection and a levelling off as the total resource estimate of the reservoir is reached. (Wang et al., 2013) also show that the efficiency factor increases with injection time. This is a result investigated also by Gorecki et al. (2014). Simulations continuing for hundreds of years can achieve high storage efficiency factors which may not be realistically achieved over an operational timescale, or where there is significant CO₂ migration, very low values of storage coefficients. Storage efficiency factors calculated after only a single month or year of injection may not represent a fully developed CO₂ plume.

Kopp et al. (2009a) go through defining coefficients and then use a database of US gas fields (U.S. National Petroleum Council public database). They compile data from 1250 fields and assume that properties of saline aquifers are similar, taking forward the extremes (5th and 95th percentiles). Numerical simulations are performed in 1D, no gravity (one cell high), axisymmetric.

The number of wells can be used to optimise the storage resources of a storage site and also the efficiency factor (Wang et al., 2013). Kopp et al. (2009b) consider additional injection wells. They inject CO₂ until a given pressure limit is reached, wait for a number of years, e.g. 5/20 years, then

recommence injection, however this technique was shown to have a limited effect on a scenario of 40 kt/yr, and is not economically realistic. The authors also consider permeability (homogeneous and heterogeneous) and compressibility of both the aquifer and seal/caprock. Increasing the porosity does not increase the storage coefficient because it is applied as a separate factor. They show that there is a definite optimum number of injection wells – more wells increase the storage efficiency only up to a point. This is because it is modelled as a closed system and therefore there is limited pressure space in the reservoir, based on a limit defined by the fracture pressure. The plume only occupies a small amount of the available space as resident brine is unable to leave the site.

Kopp et al. (2009) consider temperature, depth, relative permeability, capillary entry pressure, injection rate and permeability. They found that deep reservoirs with lower geothermal gradients and low permeability gave the highest coefficients. Relative permeability had a significant influence too and was studied by Haeri et al. (2022).

To incorporate water production, a simple material balance may be used – the reservoir volume of water produced is equivalent to the volume of additional CO₂ which can be stored. This, like all the volumetric calculations, represents an upper limit and is reduced by other factors. Water production and its impact on storage coefficients was considered dynamically by Gorecki et al. (2015). It was noted that water production had the greatest impact in closed systems, increasing the storage coefficient (as defined by those authors) by more than 450%. In an open system case study, the coefficient was increased by approximately 100%. In this case the storage coefficient was defined based on a given pore volume and would increase as CO₂ was injected up to a pressure limit. In the current study the storage coefficient is based on the extent of the plume and how the pore space is utilised within the area of the plume.

Okwen et al. (2010) derive an analytical solution for the efficiency coefficient based on the shape of the plume given by Nordbotten et al. (2005a). The authors define efficiency as the ratio between volume of injected CO₂ and the pore volume of a cylinder with radius defined by the distance between the injection well and the CO₂ front (which increases with time). This is based on the permeability and viscosity of the water and CO₂, and the residual water saturation; and represents a very large open aquifer. Okwen et al. (2010) use dimensional analysis to assess the relative importance of buoyancy effects (and therefore the region between the leading edge of the CO₂ plume and where the plume fills the whole thickness of the reservoir, i.e., they try to estimate the efficiency in a reservoir of non-negligible thickness. Key parameters are identified as mobility - depending on (relative) permeability and viscosity. Haeri et al. (2022) also identify relative permeability as a key parameter but do not show dependency of the efficiency factor on it. Decreasing the mobility of the CO₂ (i.e., increase viscosity and reduce relative permeability) acts to increase the storage coefficient. Reduced CO₂ mobility also acts to limit the injectivity, a factor which is very important for any CO₂ storage operation, but not directly related to the efficiency factor. A review of analytical approaches is given by Ringrose (2020b).

Oldenburg (2021) introduce the idea of “local flow controls”. These aim to adapt the injection flow rate and/or pressure locally along the injection interval to the effective transmissivity of each reservoir layer.

3.3 CASE STUDIES: DATABASES

There is an interest in cataloguing national resources and different countries have a different level of characterisation, resources and understanding to undertake this work. They used different aspects of the classification schema as described previously to provide interested stakeholders with a broad perspective of total storage resource potential. We briefly summarise some of these national databases below.

3.3.1 United Kingdom

The **United Kingdom** national database of CO₂ storage information was first populated in 2011 by the UK Storage Appraisal Project (Gammer et al., 2011) supported by £3.9M public-private funding.

The CO₂Stored database provides access to overview data for over 500 potential CO₂ storage sites around offshore UK. This database was generated by a BGS-led consortium and is now managed by BGS. The database identifies all potential storage formations for the UK continental shelf (UKCS). The potential storage sites are classified within the database as storage units (individual geology-based units of assessment) and daughter units (mapped individual water-bearing or hydrocarbon bearing traps). A number of total storage resource estimations are provided for the storage units. P10, P50 and P90 capacities are reported.

Structurally simple, homogeneous flow simulation models were constructed to investigate generic effects of sensitivity of various key parameters (such as depth, thickness, horizontal and vertical permeability, dip etc) on storage in open aquifers, closed systems and structural traps. For these units a storage efficiency factor provided by representative numerical models of the storage unit was used in the storage resources estimate calculation (Bentham et al., 2014).

3.3.2 Europe

CO₂StoP¹ was initiated by the European Commission in 2012-2013. A total of 27 European countries were included in the database though only a few of these provided updates based on research funded at national level, otherwise publicly available data from the GeoCapacity project were used. CO₂StoP used an improved methodology for storage potential assessment, and a pan-European database has been produced. The database is hosted by the EC Joint Research Centre in Petten, the Netherlands, and was made public via the EDGI platform in 2020. Project results include the database, GIS and a calculation engine capable of providing probabilistic estimates of CO₂ storage resources. A Data Analysis/Interrogation Tool is also available, which can perform calculations of storage resource estimates, injection rates and their stochastic analyses.

The CO₂StoP methodology complies with the CSLF recommendations. The methods and calculations for determining the fractions of the resource, used in the CO₂Stop project, also align with the IEA proposals for harmonising total storage resource estimation methodologies (Heidug, 2013). The CO₂StoP calculation engine can calculate the Technically Accessible CO₂ Storage Resource (TASR) or theoretical storage resource as used by the USGS (Brennan et al. 2010). This method should only be used for extra-European international resource comparisons because it is certain that the TASR is several times larger than the practical CO₂ storage resources. The CO₂StoP estimate differs in one main respect from the TASR estimated by the USGS method: It adds the storage resources of hydrocarbon fields to that of the saline aquifer formation which it resides within. The pore volume of hydrocarbon fields is not provided in the database, and therefore cannot be subtracted from the pore volume of the storage units before their total storage resources are estimated.

The CO₂StoP database allows the user to enter the storage efficiency factor defined as the ratio of used space. Storage capacities are estimated using the Blondes et al. (2013) methodology. Storage efficiency factors of 2% and 1% were applied to the storage units in the database. These values have been used for both storage and daughter units. The storage efficiency described by Bachu et al. (2007) is trap/site specific and not usually applied to a regional aquifer formation. A bulk volume resource estimate of a regional aquifer is by nature theoretical. Theoretical storage

¹ <https://ec.europa.eu/energy/en/studies/assessment-co2-storage-potential-europe-co2stop>

resource estimates are only an initial step and may include unrealistic and uneconomic volumes based on assumptions that we know are invalid. For bulk volume calculation of regional aquifer formations, a storage efficiency factor of 2% is suggested, based on work by the US DOE. Frailey (2007) used Monte Carlo simulations to calculate P50 storage efficiencies between 1.8 and 2.2% of the bulk volume of a regional aquifer (with low and high values of 1% and 4%, respectively).

Bachu et al. (2007) also include the net to gross ratio (NG) in both the theoretical and the effective capacity estimates. This is a site-specific parameter and is dependent on local geological variations. This parameter may not be available within saline formations without hydrocarbon exploration activity. In this instance a default value of 0.25 is suggested.

The methodology used for hydrocarbon fields yield theoretical storage capacity according to the methodology described by the Carbon Sequestration Leadership Forum (CSLF). To reach effective storage capacity CSLF introduce a number of capacity coefficients representing mobility, buoyancy, heterogeneity, water saturation and aquifer strength, respectively and all reducing the storage capacity. However, there are very few studies and methodologies for estimating the values of these capacity coefficients and hence theoretical and effective storage capacity for hydrocarbon fields is not distinguished.

3.3.3 Norway

The Norwegian CO₂ storage atlas was first published in 2011 for the whole Norwegian continental shelf, in three separate books for the North Sea, the Norwegian Sea and the Barents Sea areas. The storage atlas is based on a stepwise methodology to arrive at the total storage resources and includes all the potential aquifers and hydrocarbon fields. The storage resources for hydrocarbon fields is calculated based on a fluid/gas replacement methodology. Resource estimation calculations for both hydrocarbon fields and saline aquifers mainly relied on regional pore pressure distributions and data from leak-off tests combined with observations of natural gas seeps.

Storage efficiencies used in closed systems are generally less than 1% and more than this in open or partially open systems where up to 20% is used. The storage efficiency used has been determined by detailed reservoir simulation.

The digital version of the books and shapefiles for the relevant data are in development (2019) to be published at NPDs website, free to download, no user account is required.

3.3.4 Spain

The Spanish CO₂ storage atlas was published as the result of the work between 2009 and 2010 by Geological Survey of Spain (IGME). The study focuses on the identification of onshore deep saline aquifers with high potential for the CO₂ storage and estimation of storage resources. The map of the selected structures is completed and includes description of the regional and local geology, stratigraphic and structural conditions, and seal-storage formation system. There is a free online version available. Later updates, including a few offshore structures, have been provided to the CO₂STOP database.

3.3.5 Brazil

The Brazilian CO₂ Storage Atlas contains storage capacities estimated at basin scale using a semi-quantitative approach following the methodology proposed by the Carbon Sequestration Leadership Forum (Ketzner et al., 2015).

3.3.6 CO₂SCREEN

The CO₂SCREEN tool is developed by the US Department of Energy National Energy (US DOE) Technology Laboratory for estimating prospective storage resources (Sanguinito et al., 2017) (<https://edx.netl.doe.gov/dataset/co2-screen>). The tool applies US DOE methods and equations for estimating prospective CO₂ storage resources for saline formations. This provides a dependable method for calculating prospective CO₂ storage resources allowing for consistent comparison of results between different research efforts. CO₂-SCREEN consists of an Excel spreadsheet containing geological inputs and outputs, linked to a GoldSim Player model that calculates prospective CO₂ storage resources via Monte Carlo simulation.

Each of the above case studies have different levels of storage appraisal, methods of cataloguing and level of government investment to characterise CO₂ storage. The available literature enables improved estimates of storage potential around the world and at all levels of the classification schema. Section 3.4 highlights the variables which have the most significant influence on storage resources estimation.

3.4 KEY PARAMETERS IDENTIFIED FROM THE LITERATURE

Summarising the literature review, Table 3 shows the most influential parameters in the estimation of CO₂ storage resources and consequences of variability/uncertainty for each one.

Table 3. The key parameters drawn from the literature review and the impact of each on CO₂ storage resources estimation.

Parameter	Studies with numerical modelling	Results
Geological structure – flat, dipping, dome	(IEAGHG, 2009)	Efficiency increases with curvature of structure
Depth	(IEAGHG, 2009; Kopp (2009)	Increases with depth (higher CO ₂ density)
Relative permeability	(IEAGHG, 2009; Heari et al., 2022; Okwen et al., 2014)	Complex, no clear relationship between S_{wirr} and E, no strong effect.
Permeability anisotropy (k_v/k_h)	(IEAGHG, 2009)	Low values give higher E
Temperature	(IEAGHG, 2009)	Not huge dependence, high temperature gives slightly higher E at shallow depths near critical point.
Injection rate	(IEAGHG, 2009; Kopp, 2009)	Higher injection rate gives higher E as deeper pore space is utilised before gravity effects dominate

Lithology type	(Gorecki et al., 2014; Gorecki et al., 2009; Haeri et al., 2022; Okwen et al., 2014)	Can have a large effect on porosity/permeability and therefore efficiency
Boundary conditions – open or closed	(Bachu, 2015; Gorecki et al., 2009; Zhou, Q. et al., 2008)	Higher E in a more closed system (Zhou, Quanlin et al., 2008)
Number of injection wells	(Gorecki et al., 2014; Wang et al., 2013)	More wells mean higher E (subject to a maximum)
Heterogeneity – permeability distribution	(Tian et al., 2016; Wang et al., 2013)	E decreases with both λ (correlation length) and σ (log permeability standard deviation) of the heterogeneity (Tian et al., 2016)
Pauses in injection once BHP limit reached	(Wang et al., 2013)	Little added benefit
Porosity	(Wang et al., 2013)	No significant results
Time dependency of storage coefficients	(Bachu, 2015; Gorecki et al., 2014; Okwen et al., 2014)	E increases with time up to a plateau. Can take long time period to approach volumetric values.
Water production	(Gorecki et al., 2014; IEAGHG, 2018)	Water production greatly increases E in closed systems, increases E a bit in open systems
Net-to-Gross	(Kopp et al., 2009b)	Not a good measure
S_{wirr}	(Haeri et al., 2022)	Irreducible water saturation determines the microscopic displacement efficiency.

3.5 LIMITATIONS OF STORAGE COEFFICIENTS

In this section the limitations of storage coefficients are considered and some of the reasons why they need to be used as part of a comprehensive plan. Accurate estimates of CO₂ storage volumes and corresponding storage efficiency factors are best done using dynamic flow simulations and detailed 3D geological models. However, analytical modelling approaches are useful in early phase/screening to produce a quick estimate of likely storage resources.

Storage coefficients can be very useful for estimating the total storage resources for cases at low storage readiness levels where there is not a large amount of site-specific data available. They are generally used as a high-level method of resource estimation when more detailed data such as 3D geological models populated using well/seismic data with dynamic numerical simulations are not available. This report later emphasises that storage coefficients can be calculated at more

mature sites with operational/numerical data and used to inform the estimation of storage coefficients at other/similar sites.

Efficiency coefficients, as defined in this report, are based on ratio between the volume of CO₂ stored (numerator) and the pore volume swept by a plume of CO₂ (denominator). This requires an estimate of the lateral area and thickness of reservoir. For a given mass of CO₂, the more compact the plume then the higher the efficiency. This is based on the volumetric displacement efficiency. Other studies define efficiency based on the total pore volume of a storage site. This can be used to incorporate pressure effects but is more dependent on the injection regime and site boundaries. Both have value in different ways and focus on different factors which all must be considered when planning a CO₂ storage operation.

It is not unusual for geological units to decrease in quality with increasing depth, shales and other facies with limited porosity and permeability can become more prevalent towards the base (or top) of a reservoir interval. One example of this is at the site of the Ketzin project, Germany. The storage coefficient calculated based on the whole reservoir interval is significantly lower than that based on the thickness of only good-quality reservoir.

Another issue with defining the lateral extent of a CO₂ plume is that it tends to spread as a thin (potentially less than a few metres) layer underneath an impermeable horizon. This could include a thin nose that is below the detectability limit of monitoring such as seismic data. In this case, even real-world field data can suggest values of storage coefficients that are not realistic. Also, there is no internationally agreed way to measure the lateral extent of a plume – IEAGHG (2009) quote four methods of shape fitting and in this study an ellipse is fitted. As detailed further in Section 5.3.6 this can impact the value of the storage coefficient.

One of the most significant factors not included in the storage coefficient as defined in this report is pressure. In closed systems and particularly depleted fields, the storage coefficient can be calculated almost solely on available pressure space. This may also be useful for open/regional systems as an end member case. However, in open systems pressure is generally considered at the stage of dynamic simulations when an appropriate geological model of specific site is attainable with realistic pressure limitations. On a site-specific basis, storage volumes may be determined by plume migration to spill points and/or the pressure response. In fact, high values of storage efficiency can arise from overly high pressures. Excessive pressure in a reservoir can lead to fracturing and damage to the reservoir and caprock. Storage coefficients are valuable only as part of a comprehensive plan for CO₂ storage and not if used in isolation.

Other factors which must be considered together with storage coefficients include injectivity. Simulations of sites with low injectivity might yield high storage coefficients because the mobility of CO₂ is limited. It is important to then consider the area over which the storage coefficient is applied, if used to produce an estimate of the total storage resources. Some of the pore space may not be able to be utilised due to the lack of mobility of the CO₂. In cases such as this, additional injection wells might be an option to increase the storage efficiency coefficient and utilisation of a site, if economically worthwhile with the limited injectivity.

The accuracy of storage coefficients increases as the site is developed through the storage readiness levels and the amount of available data increases. As the site progresses towards becoming operational, a realistic and very site-specific estimate of the total storage resources is required. This is achieved through geological models of the site and numerical flow simulations rather than general storage efficiency factors. Once this is available, earlier estimates of the storage coefficient may become redundant. This will include known factors such as any geological channels (high permeability pathways) which reduce the value in applying the derived storage coefficient to other sites.

Likewise for geological structural traps, the storage coefficient of the site will be very dependent on the topography of the seal. The amount of CO₂ that can be stored in the site will depend on the pore volume available within the structural trap(s). Certain factors within the storage coefficient (such as irreducible water saturation), which are useful for when the pore space is saturated with CO₂, might be applied in conjunction with a CO₂-water contact to give a better estimate of the total storage resources of the site, rather than a traditional storage coefficient applied to the entire pore space.

3.6 OPPORTUNITIES FOR FURTHER MODELLING

Following a review of the recent literature on storage coefficients, several areas are highlighted for possible further development. Although IEAGHG (2009) ran a comprehensive suite of simulations, most of which only were for a single year of injection. In the current study, the storage coefficient will be calculated at a number of time steps throughout both an injection and a post-injection period.

A range of geological geometries will be considered: a flat caprock, a dipping aquifer and a structural dome. Injection rate has been identified as a key parameter, and its influence on storage coefficients will be assessed in this study.

Water production is a topic of current interest for CO₂ storage. The removal of resident brine from a reservoir allows for storage of increased volumes of CO₂ as well as alleviating issues of high pressure. The relationship between water production and storage coefficients has not been explored, therefore this study aims to study how these two are related. According to Vosper et al. (2018) the lateral location of a CO₂ plume is difficult to influence through water production, so it is expected that water production is not strongly linked to storage efficiency as defined in this report, but it does greatly impact the pressure limitations.

Hysteresis and residual trapping increase the security of CO₂ storage and a migrating plume of CO₂ can leave a trail of a high proportion of its volume. The impact and importance of this when assessing storage coefficients will also be investigated in this report.

There is also only a limited amount of data linking the concept of storage coefficients to real-world CO₂ storage operations. In this study three projects with available seismic data are taken, and the storage coefficient calculated at time steps with available data.

4 Cases studies: operational data

Large scale CO₂ storage projects have been running across the globe for sufficient time to be able to assess the storage efficiency through plume sweep monitoring. European CO₂ storage demonstration has been pioneered by Norway with the Sleipner and Snøhvit projects capturing and storing over 25 Mt of CO₂ in offshore saline aquifers. Ringrose et al. (2018) highlighted the observed performance of the storage sites and compared the findings with projections from gravity dominated fluid dynamic process modelling. The results showed broad agreement with the observed data. In addition, the Ketzin project in Germany injected gaseous phase CO₂ for a research project coordinated by the German Research Centre for Geosciences (GFZ). Widespread seismic imaging enabled the plume growth to be tracked and allowed for an estimate of storage efficiency in the reservoir.

In all these examples the geophysical data were acquired in a time-lapse manner meaning the storage efficiency estimates can be compared through the project lifetime. This provides a real-world estimate of the calculated storage efficiency and demonstrates how the values may evolve based on the CO₂ distribution, the rate of plume growth, the location and size of the injection perforation, geological heterogeneity, reservoir compartmentalisation, layering within the CO₂ anomaly and the quality of geophysical imaging under realistic signal-to-noise levels.

In the following sections we recalculate the storage efficiencies, highlight their variability with time and look at the reasons for the differences between the observed values at the three sites.

4.1 SLEIPNER

The CO₂ storage demonstration project at Sleipner commenced in 1996 and had successfully stored nearly 19 Mt by 2020 (Williams and Chadwick, 2021). The injection and storage are within the unconsolidated, high porosity, high permeability Utsira Sand under the Norwegian North Sea at depths approaching 1,000 m below sea level. The pressure and temperature regime at this depth ensures dense phase storage of CO₂. The CO₂ supply is from separation of natural gas produced by Equinor (formerly Statoil) from the underlying Sleipner gas field.

The Utsira sand in the Sleipner area is approximately 200 m thick (Arts et al., 2004; Chadwick et al., 2004). The reservoir contains a number of thin horizontal mudstone baffles that control the evolution of the CO₂ anomaly partially trapping buoyant CO₂ to generate a multi-tiered plume (Figure 6).

Due to the long lifetime of the Sleipner CO₂ storage operation and the availability of geophysical data and models, the CO₂ accumulation has been studied extensively (Bergmann and Chadwick, 2015; Boait et al., 2012; Chadwick and Noy, 2010; Cowton et al., 2016; Falcon-Suarez et al., 2018; Zhang et al., 2017). The operators and partners have focused on tracking the evolution of the CO₂ accumulation in the reservoir, and actively monitoring the overburden for signs of leakage with 4D seismic data. Published work has focused on quantitative seismic analysis (Chadwick et al., 2019; Furre et al., 2015; White, J C et al., 2018b) to determine plume migration and assess layer thickness, and fluid flow simulation (Cavanagh and Haszeldine, 2014; Williams and Chadwick, 2017, 2021; Zhang et al., 2017; Zhang et al., 2014; Zhu et al., 2015) to model the spread of the buoyant CO₂ beneath the topographic relief of the caprock. The data have ensured the growth of the plume is well constrained and conditioned for appraisal of storage efficiency. At Sleipner, the constrained structural trapping beneath the top seal is the key stabilisation process. The significant spatial extent of the accumulation, and the multiple layers of CO₂ in the plume give rise to dissolution of free CO₂ into the reservoir porewater.

Gravimetric surveys provide a complementary dataset to the seismic data, giving an independent measurement of density in the reservoir. Alnes et al. (2011) utilised time-lapse gravity monitoring to give an upper bound on CO₂ dissolving in brine and estimated that the actual CO₂ dissolution rate is between 0.5% and 1% per annum,

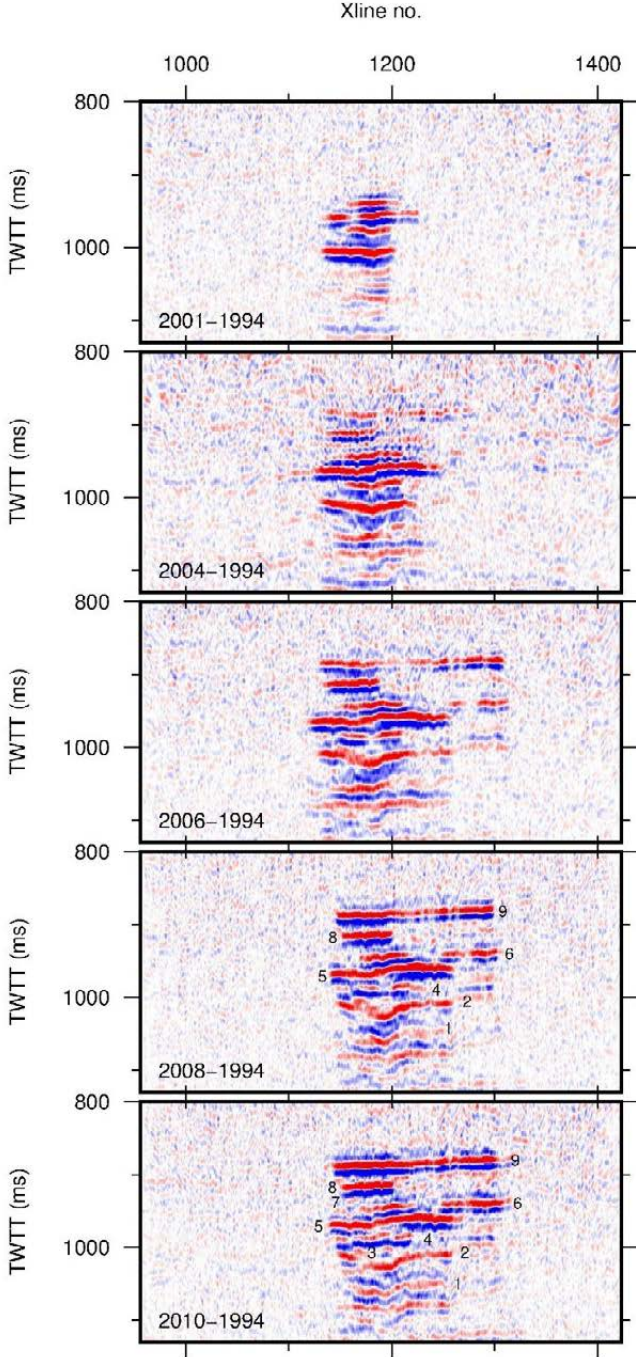


Figure 6. Time-lapse difference data for 2001, 2004, 2006, 2008 and 2010 surveys showing a N-S seismic line through the axial part of the plume. The nine layers identified within the CO₂ plume are labelled, where visible, in the two latest vintages. The top layer is seen to grow with time whilst the imaging of the lower layers degrades, a consequence of seismic wave interference and time delays causing attenuation of the reflectivity, from White, J C et al. (2018b).

To assess the plume growth, individual layers were mapped on the seismic data and plotted in Figure 7. It is clear that the thin mudstones counteract the effects of buoyancy and give rise to a stacked accumulation (Figure 6). This prohibits the rapid rise of injected CO₂ to the reservoir-top seal boundary and results in growth of the plume across the layers. The spatial extent of the plume is seen to increase between each time-lapse vintage and a single ellipse is fitted covering the overall extent of the anomaly in each instance. This ellipse is used to calculate the storage efficiency of the reservoir.

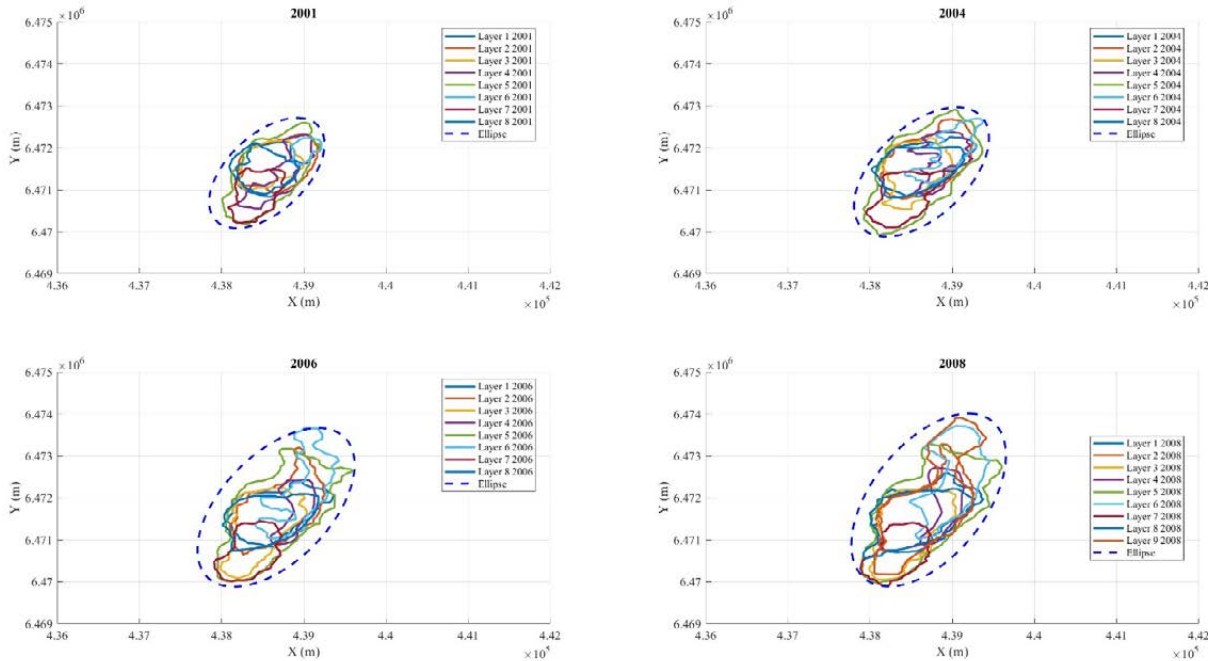


Figure 7. The Layers of the Sleipner Plume in plan view showing the growth of the accumulation through 4D time-lapse imaging, and the ellipses describing the horizontal extent of the whole plume.

Table 4 shows the evolution of storage efficiency at Sleipner. The values calculated are reasonably consistent, at around 2%, and reflect the growth of the plume into layers migrating beneath partially sealing units. This suggests limited pressure response to injection and dominated by lateral growth at a range of structural levels. The calculated values are lower than the values published by Ringrose (2018), where details of the input values are not provided, but fall within the limits of the theoretical fluid dynamic framework study from the same publication, which predicts a range of 1-6% efficiency.

4.2 SNØHVIT

Snøhvít is a commercial CO₂ storage project located near Hammerfest, offshore Norway, and operated by Equinor and partners. The project commenced in 2008, injecting an average of 0.7 Mt CO₂/year (6.5 Mt by end 2019) (Hansen et al., 2013) using CO₂ separated onshore with amine scrubbers, then piped back to the storage site and reinjected into a saline aquifer reservoir. Two

distinct periods of injection have taken place (Hansen et al., 2013; Osdal et al., 2013; Osdal et al., 2014).

Injection initially took place into the Tubåen Formation at a top reservoir depth of 2600 m with just over one million tonnes of CO₂ stored by the time injection ceased in early-2011. Injection Phase 1 was terminated because of a steady increase in downhole pressure (Grude et al., 2014a; Grude et al., 2013; Grude et al., 2014b; Hansen et al., 2013; White et al., 2015), a consequence of lower than anticipated connectivity in the reservoir and compartmentalisation. Injection Phase 2, into the overlying Stø Formation at 2400 m depth, is performing as expected, with no significant increase in downhole pressure (Osdal et al., 2013; Osdal et al., 2014). Figure 8 shows examples from the time-lapse seismic vintages and highlights the imaging quality at Snøhvit.

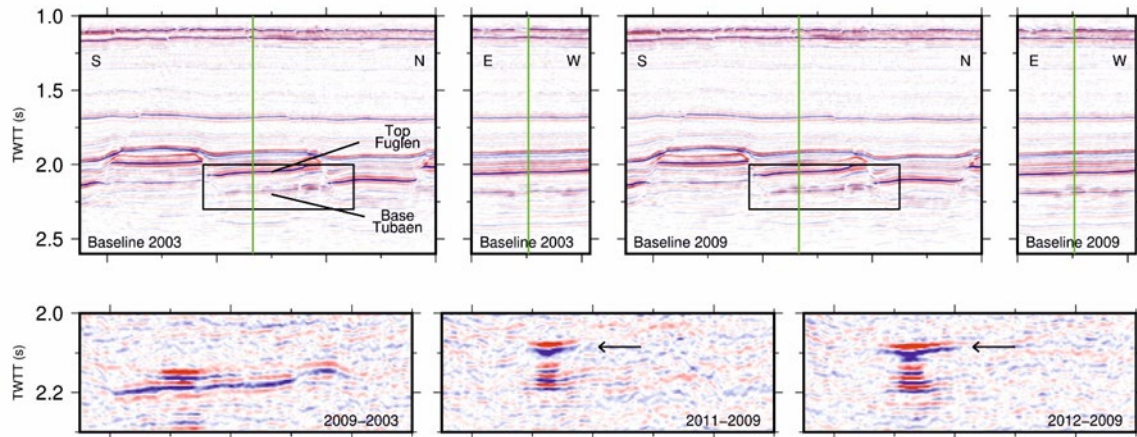


Figure 8. Seismic lines from the first baseline (2003) and the second baseline (2009) surveys highlighting the geological structure at Snøhvit (top). Difference data shows changes between 2003 and 2009, and subsequently to 2009 (bottom). Green lines delineate the intersection between the N-S and E-W lines. Black boxes show the location of the difference panels. Arrows point to the Stø anomaly, to differentiate from the deeper time shifted Tubåen reflectivity. From White et al., 2015.

The same compartmentalisation was not observed during Phase 2 of injection (White, J C et al., 2018a) and analysis of the geophysical data shows a radial distribution of CO₂. Figure 9 shows the plume growth, following injection into the Stø Formation, from time-lapse analysis of seismic data using spectral decomposition techniques (White, J C et al., 2018a). Fitting an ellipse to the plume growth, the storage efficiency can be calculated and is documented in Table 5.

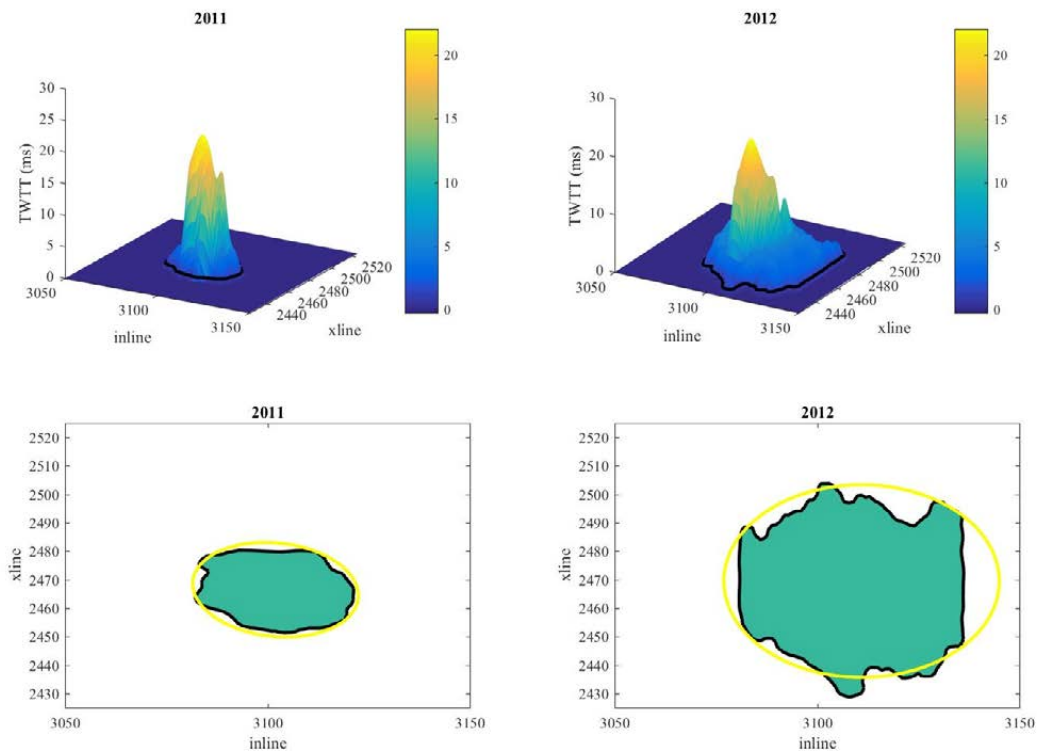


Figure 9. Upper panels: thickness of CO₂ accumulation at Snøhvit in 2011 (left) and 2012 (right) calculated from seismic data. Lower panels: Spatial extent of the plume and fitted ellipse. Inline and Xline spacing for the 3D surveys was 12.5 m.

The results of the storage efficiency assessment give rise to higher storage efficiency values for the Stø Formation at Snøhvit, between 7.8% and 10.2%, than those calculated at Sleipner. This is likely a consequence of the lower permeability at Snøhvit, with growth of the plume across a greater proportion of the vertical extent of the reservoir.

4.3 KETZIN

The Ketzin CO₂ storage project was an onshore research facility coordinated by the German Research Centre for Geosciences (GFZ) that ran between 2008 and 2013. The project injected 67 kt of CO₂ into a sandstone interval within the Triassic Stuttgart Formation. The 70 m thick reservoir is divided into high quality sandstone and lower porosity/permeability units at a ratio of ~50:50. Norden and Frykman (2013) showed that the higher quality units, with higher effective porosity, were spatially mixed across the thickness of the Stuttgart Formation. Two repeat seismic data sets were acquired in 2009 and 2012 and formed the basis of the geophysical monitoring scheme (Huang et al., 2016; Luth et al., 2012; Wipki et al., 2016). The project research team observed ‘reasonable conformance between the observed and simulated plume behaviour’ (Luth et al., 2015) and were able to demonstrate an understanding of site performance and satisfy regulators of the long-term safety of the storage site.

Figure 10 shows the plume growth from time-lapse analysis of seismic data (Huang et al., 2016; Luth et al., 2012; Wipki et al., 2016). Using an ellipse fitted to the plume growth, the storage efficiency is calculated and documented in Table 6 and Table 7 using both the full reservoir interval and the thickness of storage reservoir quality sandstone.

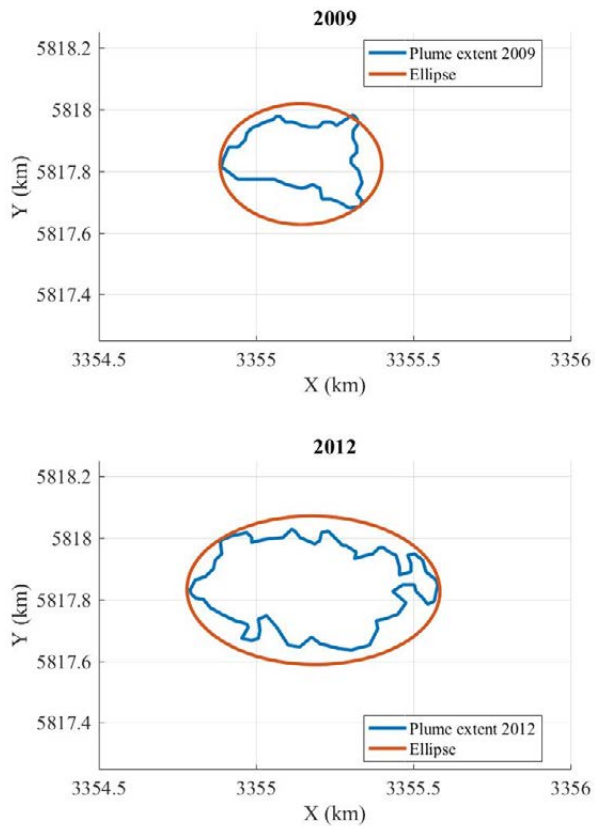


Figure 10. The growth of the Ketzin CO₂ accumulation in plan view, showing the growth of the anomaly through 4D time-lapse imaging in 2009 and 2012.

The choice of reservoir thickness has clear implications for the calculated storage efficiency. This highlights the clear requirement to adequately document the methodology when calculating storage efficiency values. The approach adopted here defines the area of the ellipse as the potential storage volume. The Ketzin results provide an estimate of the evolution of time-lapse storage efficiency in gaseous phase CO₂ injection, into medium quality reservoir units.

Table 4. Determination of time-lapse storage efficiency for the Sleipner CO₂ injection.

Year	CO ₂			Ellipse				Storage efficiency	
	Injected mass (T)	Density (kg m ⁻³)	Volume (m ³)	Area (m ²)	Thickness (m)	Total volume (m ³)	Porosity		Available volume (m ³)
2001	4,200,000	720	5,833,000	4,358,000	200	871,640,000	0.37	322,507,000	1.8%
2004	7,000,000	720	9,722,000	6,161,000	200	1,232,201,000	0.37	455,914,000	2.1%
2006	8,700,000	720	12,083,000	8,602,000	200	1,720,316,000	0.37	636,517,000	1.9%
2008	10,500,000	720	14,583,000	10,694,000	200	2,138,811,000	0.37	791,360,000	1.8%

Table 5. Determination of time-lapse storage efficiency for the Snøhvit CO₂ injection in the Stø formation.

Year	CO ₂			Ellipse				Storage efficiency	
	Injected mass (T)	Density (kg m ⁻³)	Volume (m ³)	Area (m ²)	Thickness (m)	Total volume (m ³)	Porosity		Available volume (m ³)
2011	130,000	712	183,000	167,000	80	13,341,000	0.175	2,335,000	7.8%
2012	550,000	712	772,000	544,000	80	43,482,000	0.175	7,609,000	10.2%

Table 6. Determination of time-lapse storage efficiency for the Ketzin CO₂ injection using the full reservoir interval.

Year	CO ₂			Ellipse				Storage efficiency	
	Injected mass (T)	Density (kg m ⁻³)	Volume (m ³)	Area (m ²)	Thickness (m)	Total volume (m ³)	Porosity		Available volume (m ³)
2009	23,500	260	88,300	159,000	70	11,186,000	0.2	2,335,000	3.9%
2012	61,000	215	284,000	307,000	70	21,477,000	0.2	7,609,000	6.6%

Table 7. Determination of time-lapse storage efficiency for the Ketzin CO₂ injection using the high-quality reservoir interval.

Year	CO ₂			Ellipse				Storage efficiency	
	Injected mass (T)	Density (kg m ⁻³)	Volume (m ³)	Area (m ²)	Thickness (m)	Total volume (m ³)	Porosity		Available volume (m ³)
2009	23,500	260	88,300	159,000	37	11,186,000	0.2	1,182,000	7.4%
2012	61,000	215	284,000	307,000	37	21,477,000	0.2	2,270,000	12.5%

5 Numerical flow modelling to estimate storage coefficients

In this section, numerical flow models are used to simulate a number of cases of CO₂ injection in saline aquifers and calculate the corresponding value of the storage coefficient. A static model of a structural dome is built and populated with relevant parameters. Injection into the crest of the dome is used to simulate CO₂ storage in a structural trap, and injection into the flank of the dome is used to simulate flow in a dipping aquifer (fetch trap). A further model of a simple dipping aquifer is also built and used to verify results. The modelling work aims to follow on from existing literature identified in Section 3 and extend it in line with the opportunities identified in Section 3.6 to further study the evolution of storage coefficients over time, throughout injection and post-injection periods. The role of water production and its effect on storage efficiency is investigated, together with the impact of increased/decreased injection rates and the influence of hysteresis. Storage coefficients are calculated for all modelled cases.

5.1 STATIC MODELS

5.1.1 Structural dome

The model represents a generic example of a regional anticline with four-way dip closure, similar to the Triassic Bunter Sandstone salt cored domes of the United Kingdom Southern North Sea (UKSNS). These dome-like structures represent important target sites for a number of proposed commercial-scale CCS projects in the UK (ETI, 2016a, b; Furnival et al., 2017; Furnival et al., 2014; National Grid, 2016; Noy et al., 2012). Similar regional anticlinal closures have been targeted by existing demonstration projects at Citronelle and Cranfield in the United States (Freifeld et al., 2013; Koperna et al., 2017), Tomakomai in Japan (Sawada et al., 2018; Tanaka et al., 2014; Tanase et al., 2013), Ketzin in Germany (Norden et al., 2010; Wiese et al., 2010) and In Salah in Algeria (Rutqvist et al., 2010).

The apex of the dome is located at a depth of 1300 m below Mean Sea Level (MSL) in the model, and the reservoir thickness is 200 m. The simulation grid covers an area of 20x20 km with 80 250 m grid cells in the X and Y directions and 80 2.5 m grid cells along the vertical axis of the model. Section 5.4 investigates the sensitivity of the results to the size of the grid. Open boundary conditions have been applied to all sides of the model domain, using large pore volume multipliers. The reservoir formation is assumed to be saturated with brine containing 100,000 ppm NaCl prior to CO₂ injection. Details of the simulation grid are given in Table 8.

A single static model is used in this section, and different regions are utilised to represent flow in distinct topographical case studies. Injection into the apex of the dome represents an end-member case of flow in a structural trap. But for a real project, this provides a poor utilization of the subsurface pore volume because it does not utilize residual phase trapping (and dissolution) of pore volume underneath the trap's spill point depth. However, in the context of storage coefficients there is value in modelling the end member scenario where CO₂ does not need to travel any distance before pooling under an impermeable caprock in a simple structural trap. This eliminates the possibility of additional residual trapping and is likely to give the minimum sweep and maximise the storage coefficient as defined in this study.

Table 8. Details of the simulation grid used in this study.

Model	Model extent (km)	Number cells	Average cell size (m) (near plume)	Depth to reservoir top (m)	Reservoir thickness (m)	Boundary conditions	Wetting pore fluid
Dome	X = 20 Y = 20 Z = 0.2	NX = 80 NY = 80 NZ = 80	X = 250 Y = 250 Z = 2.5	Min = 1300 Max = 2000	200	Open	100,000 ppm NaCl brine
Dipping aquifer	X = 100 Y = 40 Z = 0.2	NX = 160 NY = 40 NZ = 80	X = 250 Y = 250 Z = 10	Min = 1000 Max = 4500	200	Open	100,000 ppm NaCl brine

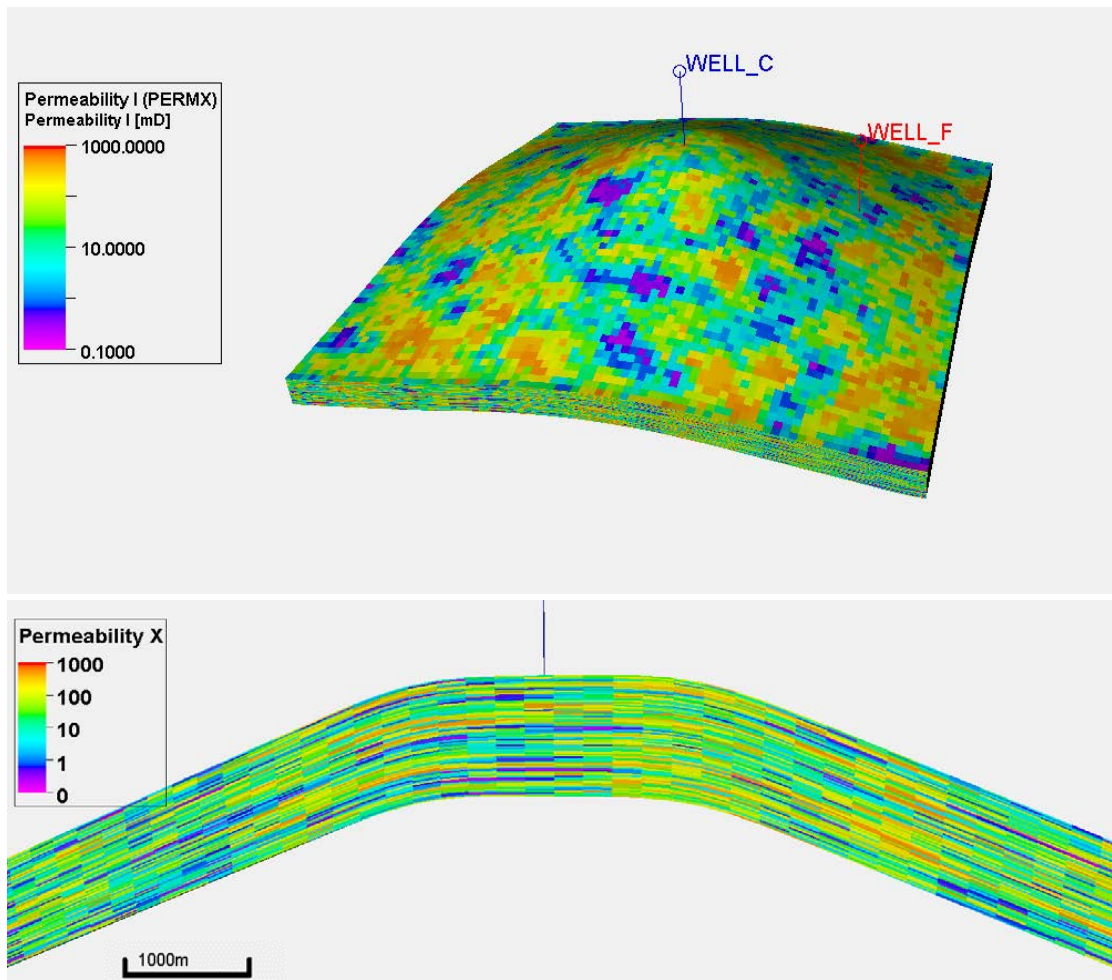


Figure 11. Horizontal permeability of the static model. Vertical exaggeration is 5 times. WELL_C is used for CO₂ injection/water production from the crest, and WELL_F is used for CO₂ injection/water production from the flank. Values correspond to P50 Deltaic environment of (Gorecki et al., 2009) and are directly linked to porosity. Bottom inset is a cross section through WELL_C, zoomed in with the scale shown.

The region on the flanks of the dome is used to represent a structurally open dipping saline aquifer. Injected CO₂ is expected to migrate buoyantly towards the crest of the dome, as the CO₂ has a significantly lower density than the surrounding brine, leaving behind a trail of residually trapped and dissolved CO₂. In this model the CO₂ typically reaches the top (6 km away from the injection well) after 100 years of simulation and begins to pool by 200 years. The final fate of the CO₂ is to pool in the structural trap, but a steady state is not reached within operational timescales. A further static model, dedicated to the study of flow in a dipping, open aquifer is given in Section 5.1.2. This is a particularly relevant scenario with the current interest in fetch traps (Bump and Hovorka, 2023). Although in this scenario the CO₂ eventually reaches a structural trap, first it must pass through a stage of migration assisted storage.

Porosity and permeability data is taken following Gorecki et al. (2009) who collate data from a wide range of reservoirs applicable to CO₂ storage. A heterogeneous reservoir porosity distribution was used in all the model runs. The distribution was created using a Gaussian random function simulation algorithm in Schlumberger’s PETREL modelling platform. A spherical variogram was used with an anisotropy range of 1504 m in the major and minor directions and 5 m in the vertical direction. A normal porosity distribution, with a mean of 0.15 and a standard deviation of 0.0625, was distributed throughout the grid. The variogram was based on P50 figures published by Gorecki et al. (2009) for a deltaic sandstone facies: The values were computed from a database containing fluid and geological properties from over 20,000 hydrocarbon reservoirs.

In this study, the P50 values for porosity and permeability from the deltaic environment are used as that is most applicable to the anticlinal geometry of the static model. The mean porosity is 0.15, mean permeability 230 mD and permeability range 0.13-522 mD (Figure 11). A random distribution of porosity was created, with permeability linked directly to porosity.

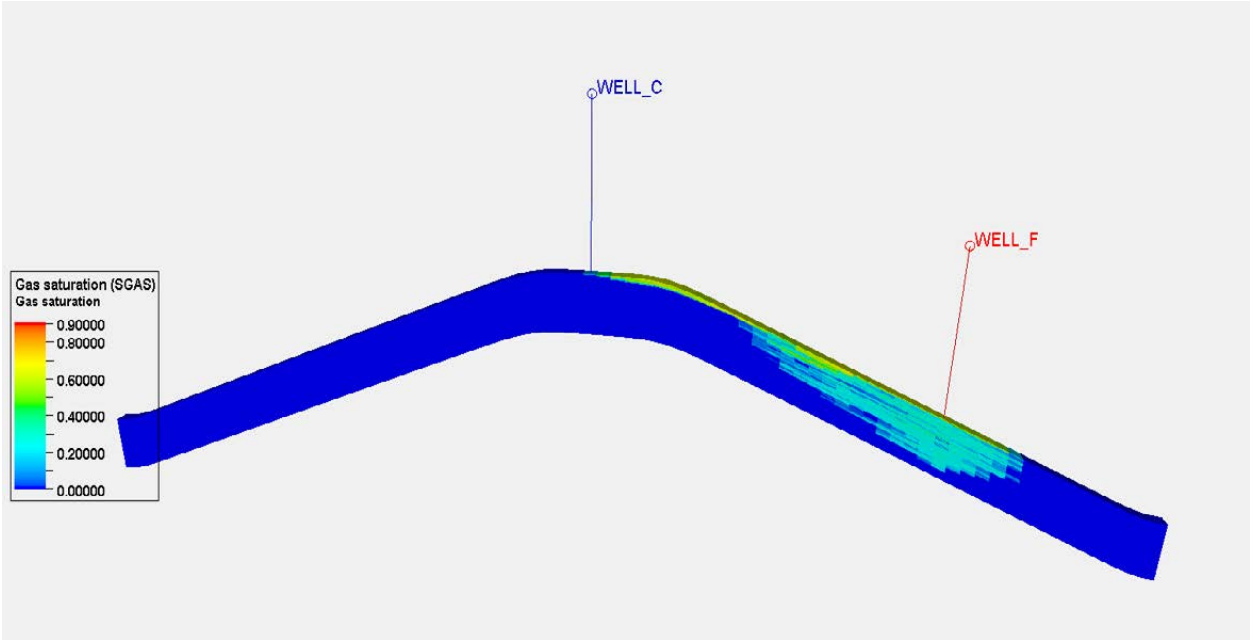


Figure 12. Cross-section view of the gas saturation after 100 years of simulation (run #2, see Table 11 for details).

5.1.2 Dipping aquifer

The dipping aquifer model (Figure 13a) represents a structurally open saline aquifer with a dip of 2°, spanning a depth range from 2400 m to 1000 m below sea level. The model domain is 100 km long in the X direction, 40 km in the Y direction and the reservoir is 200 m thick. A tartan gridding scheme has been used to provide adequate grid resolution in the vicinity of the plume, whilst allowing for a large model extent to accommodate a long post-injection period of plume migration. The simulation grid comprises 160, 40 and 80 cells in the X, Y and Z directions respectively, with a cell size of 250 m x 250 m x 10 m in the vicinity of the plume. Porosity and permeability data are discussed below

Open boundary conditions have been applied to all sides of the model domain, using large pore volume multipliers. The CO₂ is injected through a single well located towards the down-dip boundary of the simulation grid, with the top perforations located at a depth of c. 4200 m below MSL. A production well has been included in some of the model runs, this is located c. 6500 m away from the injector, in an up-dip direction. In real sites it would almost always be located down-dip, to reduce the risk for re-production of injected CO₂. The reservoir formation is assumed to be saturated with brine containing 100,000 ppm NaCl prior to CO₂ injection.

Both the simulation grids have been designed so that the CO₂ remains supercritical throughout the whole reservoir. At these temperature and pressure conditions, the CO₂ has a density of c. 650 kg/m³ and a viscosity of c. 0.06 cP. The geothermal gradient for both models was set at 32.5 °C/km, with a surface temperature of 12 °C. The gas is expected to migrate rapidly up-dip, driven by buoyancy forces, as the CO₂ will have a significantly lower density than the formation brine at reservoir temperatures and pressures. Consequently, residual trapping and dissolution of CO₂ into the formation pore waters will be very important processes in these simulations.

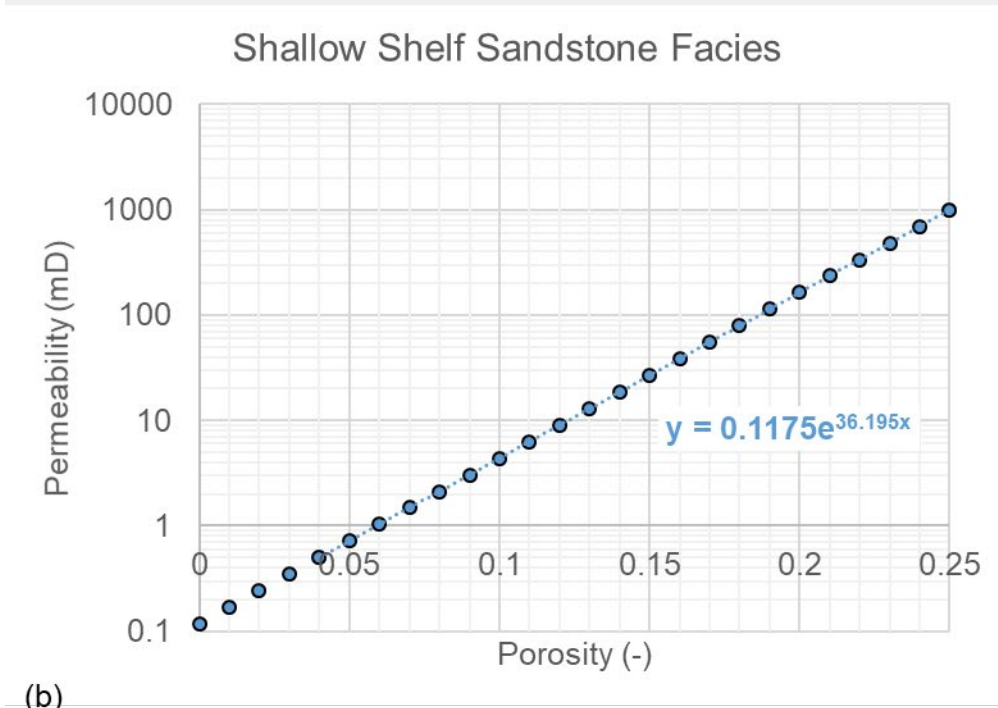
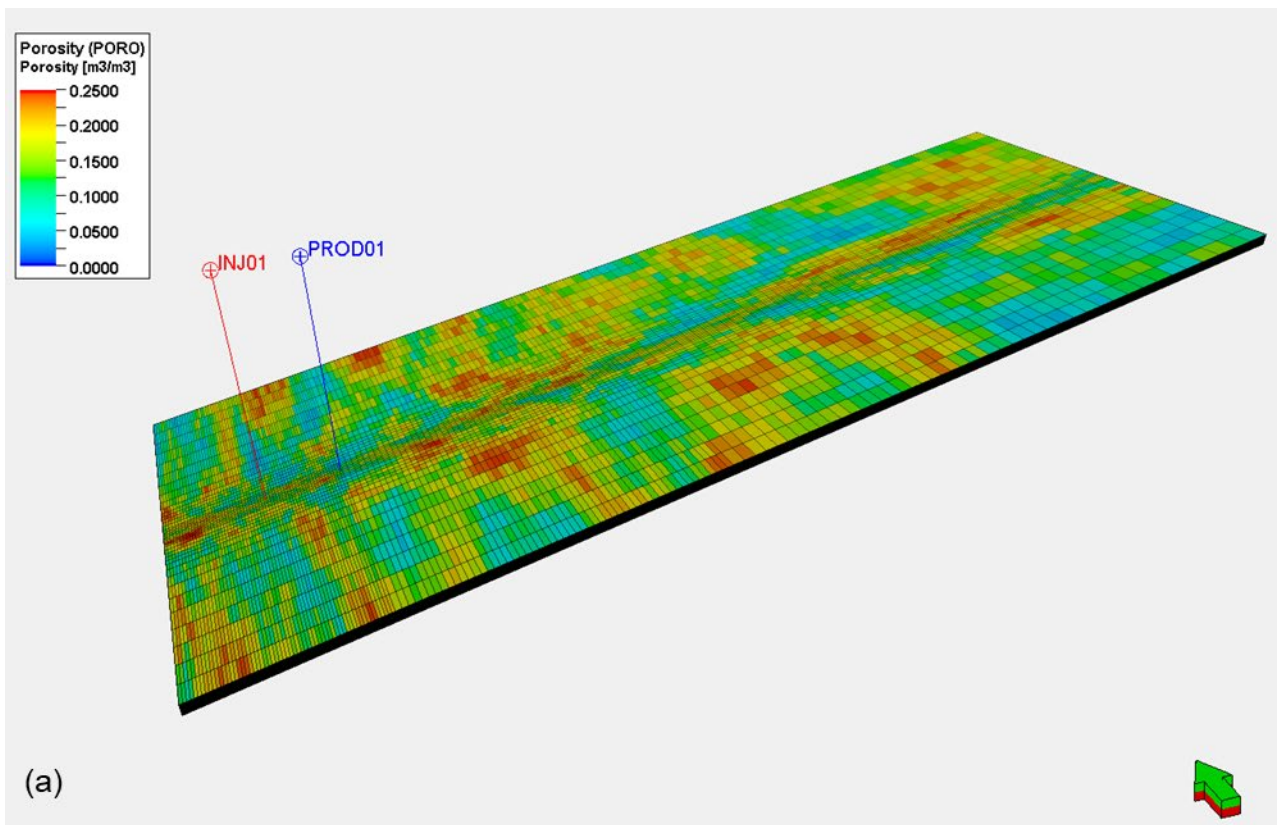


Figure 13. (a) Dipping aquifer model used in the flow simulations. The porosity distribution was generated in PETREL using a Gaussian random function simulation algorithm, with parameters published by IEAGHG (2009). (b) Log-linear porosity-permeability transform used to compute the permeability field from (a). The endpoints of the fit were again taken from IEAGHG (2009).

A heterogeneous reservoir porosity distribution (Figure 13a) was used in all the model runs. The distribution was created using a Gaussian random function simulation algorithm in Schlumberger's PETREL modelling platform. A spherical variogram was used with an anisotropy range of 6792 m in the major and minor directions and 5 m in the vertical direction. A normal

porosity distribution, with a mean of 0.15 and a standard deviation of 0.0625, was distributed throughout the grid. The variogram was based on P50 figures published by Goreki et al. (2009) for a shallow shelf sandstone facies: Goreki computed these values from a database containing fluid and geological properties from over 20,000 hydrocarbon reservoirs. Due to the nature of the grid, with smaller cells at the centre (where the CO₂ plume is expected to travel) and at the deeper end, the correlation length varies throughout the grid. The effect of this anisotropy is expected to slightly channel the flow up-dip rather than towards the sides of the model.

5.2 RESERVOIR FLOW PROPERTIES

5.2.1 Relative permeability curves

The relative permeability curves used in the models are based on a compilation of measurements for sandstone formations in western Canada published by Bachu (2013)): the data are summarised in Table 9. The relative permeability curves shown in Figure 14a were calculated using a Modified Brooks-Corey model and the average values for the parameters in Table 9.

Most laboratory studies of the relative permeability of CO₂ and brine in sandstones suggest that the end-point relative permeability of the rock to CO₂ is low (<0.5) and the irreducible water saturation relatively high (>0.3). However, it has been suggested that experimental limitations might be the cause of this behaviour. For example, Jeong et al. (2021), investigated the effect of flow rate on the relative permeability curve in the CO₂-brine system. They concluded that as flow rate increases, CO₂ endpoint relative permeability increases and the corresponding residual water saturation decreases, allowing for higher CO₂ saturations. Thus, high CO₂ flow rates during a commercial-scale CCS operation are likely to result in a higher displacement efficiency.

Given the inherent uncertainty in upscaling laboratory measurements to field conditions, the models described in this contribution use the upscaled relative permeability curves shown in Figure 14b. The shape of the curves is based on the average values in Table 9 (see Bachu (2013)), but the data have been upscaled to an irreducible water saturation of 0.3. These curves are likely to be more representative of flow conditions during a commercial-scale CCS operation.

Some of the simulation runs incorporated the effects of relative permeability hysteresis and capillary trapping. Other simulation runs did not include relative permeability hysteresis effects, in order to quantify the effect of hysteresis. Burnside & Naylor (2014) published a summary review of laboratory-based measurements of residual trapping available in the literature. Summary statistics for all the data published by Burnside & Naylor are shown in Table 10: the mean trapped gas saturation is 0.31 and the median 0.29.

The reservoir simulator used in this study implements Carlson's relative permeability hysteresis model for a water-wet brine-gas system (Carlson, 1981). Carlson's model does not compute the maximum trapped gas saturation using a trapping curve, rather one specifies a primary drainage relative permeability curve for the non-wetting phase (dashed curve in Figure 14b) and a bounding imbibition curve (solid curve in Figure 14b). Carlson's method is essentially a geometric construction that generates a series of 'scanning curves' to describe different saturation paths in the model (dotted curve in Figure 14b).

This study follows Snippe and Tucker (2014) in defining the trapped gas saturation (S_{gt}) as the horizontal interval between the drainage and scanning curves at the non-wetting phase relative permeability, for the current gas saturation (S_{gc}) in the model cell (Figure 14b). Thus, S_{gt} takes a value between 0 at the point of maximum gas saturation in a model cell (S_{gMAX}) and the maximum trapped gas saturation (S_{gtMAX}) when the gas-phase relative permeability is zero.

Consequently, the trapped gas saturation is zero during a primary drainage process. This represents the case where all the gas in the pores is connected. The maximum achievable trapped gas saturation ($S_{gt_{MAX}}$ in Figure 14b) can only be achieved in a model cell at the end of the imbibition process and if the cell has previously reached the maximum achievable gas saturation. If imbibition is reversed at any point during the model run, only an intermediate fraction of gas will be trapped. In this study we have used a maximum trapped gas saturation of 0.3 in all the model runs, close to the mean and median values of measured laboratory data published by Burnside and Naylor, 2014 (see Table 10).

Table 9. Modified Brookes-Corey relative permeability parameters for a CO₂/brine system derived from a series of rock samples from western Canada. Data reproduced from Bachu (2013).

<i>Drainage</i>							
Rock Sample	K_w (mD)	KR_G S_{WIR}	@	S_{WIR}	Corey (w)	m	Corey n (g)
Viking Fm. #3	1558.65	0.10		0.60	1.33		4.34
Clearwater Fm.	0.02	0.49		0.34	1.24		1.60
Ellerslie Fm. #2	3812.36	0.57		0.38	1.18		4.79
Rock Creek Fm.	65.03	0.04		0.48	2.19		1.90
Halfway Fm.	54.23	0.27		0.47	3.12		3.48
Belloy Fm.	536.60	0.08		0.65	1.67		5.22
Graminia Fm.	133.90	0.15		0.44	1.42		4.98
Gilwood Fm.	0.75	0.55		0.57	1.75		3.73
Basal Cambrian Ss #2	0.01	0.21		0.57	1.45		3.89
Basal Cambrian Ss #3	252.50	0.16		0.49	1.63		1.35
Basal Cambrian Ss #4	157.80	0.21		0.65	4.54		3.74
Basal Cambrian Ss #5	0.03	0.33		0.28	1.21		5.48
Deadwood Fm. #1	103.66	0.11		0.49	1.80		7.00
Deadwood Fm. #2	69.11	0.09		0.60	1.50		4.00
Deadwood Fm. #3	137.90	0.26		0.65	1.20		6.57
Granite Wash	70.13	0.41		0.58	1.15		1.81
Average	434.50	0.30		0.50	1.80		4.00
<i>Imbibition</i>							
Rock Sample	KR_w S_{GT}	@	S_{GT}	S_{WIR}	Corey (w)	m	Corey n (g)

Viking Fm. #3	0.52	0.22	0.60	1.27	2.53
Clearwater Fm.	0.77	0.15	0.34	1.15	2.25
Ellerslie Fm. #2	0.24	0.42	0.38	1.01	2.67
Rock Creek Fm.	0.03	0.48	0.48	1.35	3.09
Halfway Fm.	0.03	0.46	0.47	1.01	1.94
Belloy Fm.	0.07	0.28	0.65	2.55	3.90
Graminia Fm.	0.09	0.38	0.44	2.11	1.67
Gilwood Fm.	0.07	0.36	0.57	2.03	1.15
Basal Cambrian Ss #2	0.33	0.23	0.57	1.25	3.01
Basal Cambrian Ss #3	0.15	0.40	0.49	1.38	1.29
Basal Cambrian Ss #4	0.25	0.27	0.65	1.45	1.41
Basal Cambrian Ss #5	0.18	0.52	0.28	1.71	2.11
Deadwood Fm. #1	0.40	0.38	0.49	3.00	2.50
Deadwood Fm. #2	0.37	0.29	0.60	4.00	1.78
Deadwood Fm. #3	0.24	0.24	0.65	2.12	1.20
Granite Wash	0.17	0.23	0.58	1.05	1.45
Average	0.20	0.30	0.50	1.80	2.10

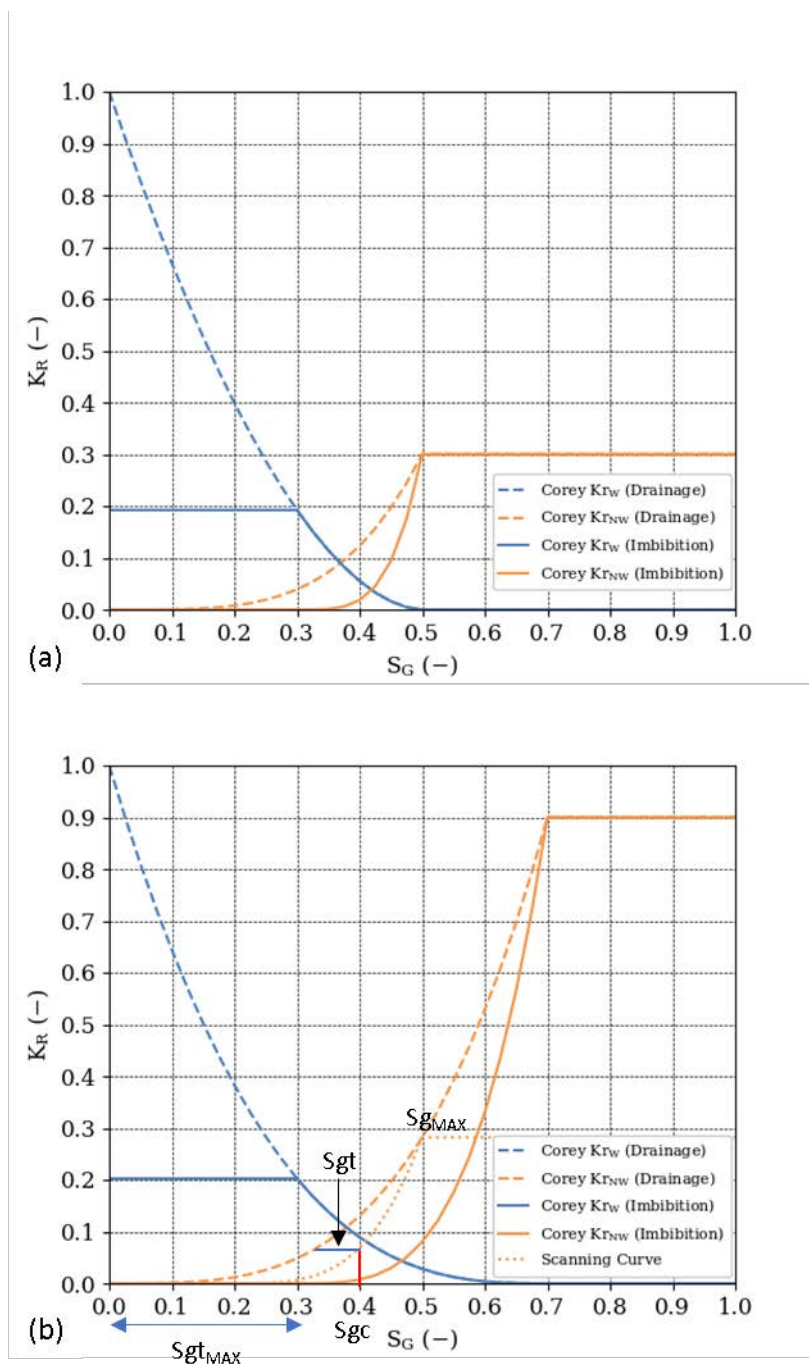


Figure 14. (a) Brookes-Corey relative permeability curves using the average parameter values given in Table 9. (b) Brookes-Corey relative permeability curves using the average parameter values given in Table 1, upscaled to an irreducible water saturation of 0.3. Key: $S_{g_{MAX}}$ = maximum gas saturation; $S_{gt_{MAX}}$ = maximum trapped gas saturation; S_{gc} = cell gas saturation; S_{gt} = trapped gas saturation.

5.2.2 Relative permeability hysteresis and residual trapping

It is clear that residual trapping is expected to play a very important role in immobilising CO_2 in the reservoir. Burnside and Naylor (2014) published a summary review of laboratory-based measurements of residual trapping available in the literature. These values are plotted in Figure 15, together with residual trapping measurements for the Triassic Sherwood (Bunter) Sandstone, which is a key potential storage formation for CCS in the United Kingdom (Reynolds et al., 2018;

Weatherford Laboratories, 2015). The data have been fitted with a Land trapping model (shown as a black dashed line in Figure 15). The Land trapping coefficient, C, is around 1.4 and the curve predicts a maximum trapped gas saturation of approximately 0.35 at a residual water saturation of 0.3. Summary statistics for all the data plotted in Figure 15 are shown in Table 10: the mean trapped gas saturation is 0.31 and the median 0.29.

	$S_{g_{MAX}}$	S_{GT}
Minimum	0.31	0.10
Maximum	0.85	0.52
Mean	0.53	0.31
P ₁₀	0.35	0.21
P ₅₀	0.53	0.29
P ₉₀	0.70	0.42

Table 10. Summary statistics showing the relationship between maximum measured gas saturation and the trapped gas saturation for the CO₂/brine system in sandstones - data summarised from literature (Burnside and Naylor, 2014; Reynolds et al., 2018; Weatherford Laboratories, 2015). The data are plotted in Figure 15.

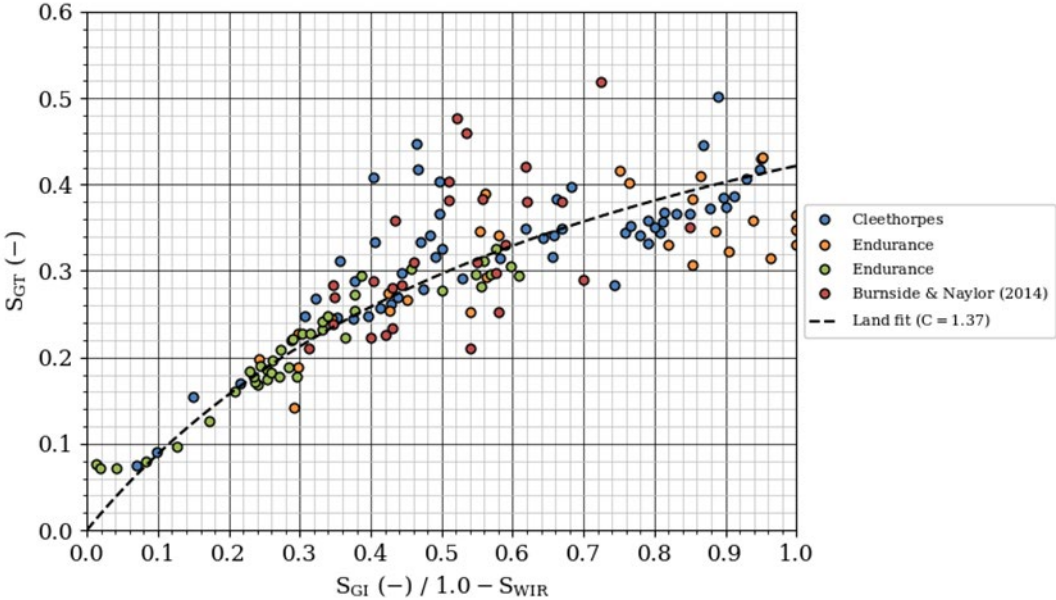


Figure 15. Plot of trapped gas saturation vs. initial gas saturation for a wide range of sandstone reservoir rocks. Data from Burnside and Naylor (2014), Weatherford Laboratories (2015) and Reynolds et al. (2018). The data can be fit by a Land trapping model with a trapping coefficient, C, of 1.37. The mean trapped gas saturation is 0.31 and the median 0.29.

5.2.3 Capillary pressure curves

Figure 16 plots a compilation of CO₂-brine capillary pressure measurements summarised in Wu et al. (2018). The solid curve represents the best fit Brooks-Corey (1964) capillary pressure model. The curve has a pore size distribution index (λ) of 0.55 and a capillary entry pressure of 0.162 bar.

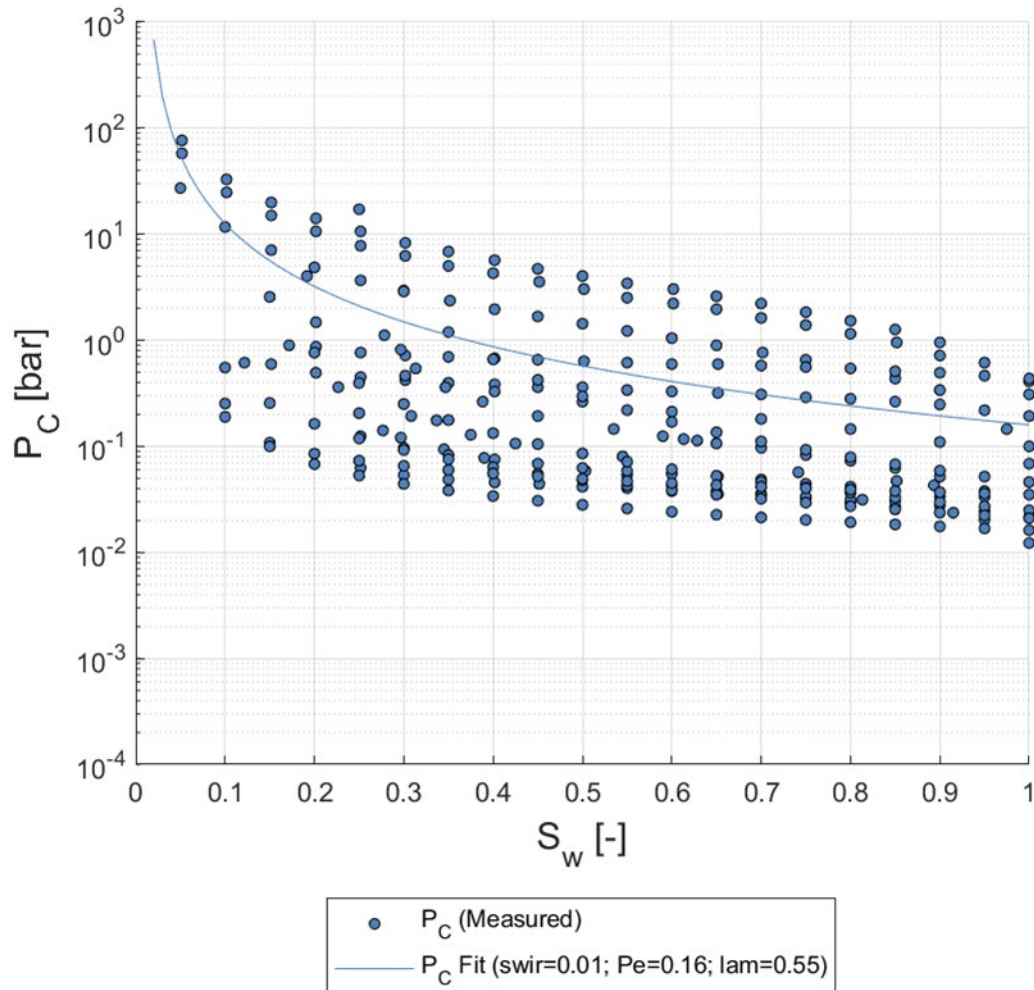


Figure 16. Compilation of CO₂-brine capillary pressure data from Wu et al., 2018. Best-fit Brooks-Corey (solid blue line) capillary pressure model used in the simulations.

5.2.4 Injection and production schedule

The injection timescale was chosen to be realistic and simple. A single well injects 1 Mt/yr for a 30-year injection period, a total of 30 Mt CO₂. This injection rate also corresponds to the P50 value used in (IEAGHG, 2009). All wells are perforated over the middle half of the reservoir interval. To test the effect of water production on CO₂ storage efficiency, an equivalent (density-corrected) pore volume of formation brine was produced from the production well in Figure 11. An additional set of simulations investigated the effect of extracting a larger volume (equivalent to twice the reservoir volume of stored CO₂) of pore water. Simulations continued for a further 70 years post-injection, that is a total of 100 years of simulation. Selected simulations were continued

for 1000 years to ensure the system behaves as expected in the longer term. Simulation runs 3 and 11 (see Table 11 simulate a high injection rate: 2 Mt/yr (a total of 60 Mt) and simulation runs 4 and 12 represent a low injection rate, 0.5 Mt/yr (a total of 15 Mt).

5.2.5 Simulations

The parameterisation of each model run is summarised in Table 11. All simulations were run using the PFLOTTRAN-OGS reservoir simulator (<https://opengosim.com/>). PFLOTTRAN-OGS has a built in two-phase (gas and water) model specifically adapted for CO₂ storage. This model allows the aqueous phase to contain dissolved gas, and the gas phase to contain vaporised water. Thermo-physical properties of the CO₂ phase are computed internally within the simulator, using the equation of state developed by Span and Wagner (1996). The density, viscosity, internal energy, and enthalpy of pure water are taken from the IFC steam tables (IFC, 2010). The water density and viscosity are then corrected to account for salinity using the correlations of Batzle and Wang (1992), whilst the density correction necessary to account for a dissolved CO₂ component uses the formulation proposed by (Duan et al., 2008). The amount of CO₂ dissolved in the formation brine is calculated using the empirical formulations developed by (Duan and Sun, 2003).

Table 11: Summary table of model runs using the dome model. Water production ratio is the ratio of reservoir volume of water produced to reservoir volume of CO₂ injected.

Sim #	Title	Injection rate [Mt/yr]	Injection well	Water production ratio	Water production well	Hysteresis included
1	Inject into crest of dome	1	WELL_C	None	N/A	Yes
2	Inject into flank of dome	1	WELL_F	None	N/A	Yes
3	High injection rate	2	WELL_F	None	N/A	Yes
4	Low injection rate	0.5	WELL_F	None	N/A	Yes
5	Produce down dip	1	WELL_C	1:1	WELL_F	Yes
6	Produce up dip	1	WELL_F	1:1	WELL_C	Yes
7	Produce double down dip	1	WELL_C	2:1	WELL_F	Yes
8	Produce double up dip	1	WELL_F	2:1	WELL_C	Yes
9	Inject crest, no hysteresis	1	WELL_C	None	N/A	No
10	Inject flank, no hysteresis	1	WELL_F	None	N/A	No
11	High injection rate, no hysteresis	2	WELL_F	None	N/A	No

12	Low injection rate, no hysteresis	0.5	WELL_F	None	N/A	No
13	Produce down dip, no hysteresis	1	WELL_C	1:1	WELL_F	No
14	Produce up dip, no hysteresis	1	WELL_F	1:1	WELL_C	No
15	Produce double down dip, no hysteresis	1	WELL_C	2:1	WELL_F	No
16	Produce double up dip, no hysteresis	1	WELL_F	2:1	WELL_C	No

5.3 RESULTS

The simulations detailed in Table 11 were all performed using PFLOTTRAN and the results inspected for quality, including injection/production rates and pressure values. Maps of the entire extent of CO₂ saturation were output after 1, 10, 20, 30 and 100 years for every case.

5.3.1 Calculating storage efficiency

The calculation of storage coefficients was discussed in Section 3 and Section 4 where storage coefficients were calculated for a range of operational sites and time-steps. The same methodology is carried forward here to the data from numerical modelling. The storage efficiency is calculated based on the volume of injected CO₂ at reservoir conditions and the volume of reservoir based (laterally) on an ellipse containing the plume (see Figure 17) and (vertically) the total thickness of the reservoir:

$$E = \frac{Qt}{\phi(\pi ab)H}$$

Where Qt is the injected volume (at reservoir conditions) of CO₂ (i.e., injection rate, Q multiplied by time, t), ϕ the porosity, πab the area of an ellipse with a [m] and b [m] representing the major and minor axes respectively, and H is the thickness of the reservoir. The value of the storage efficiency for each case is given in Table 12, and the impact of each of the parameters is discussed in the following sections.

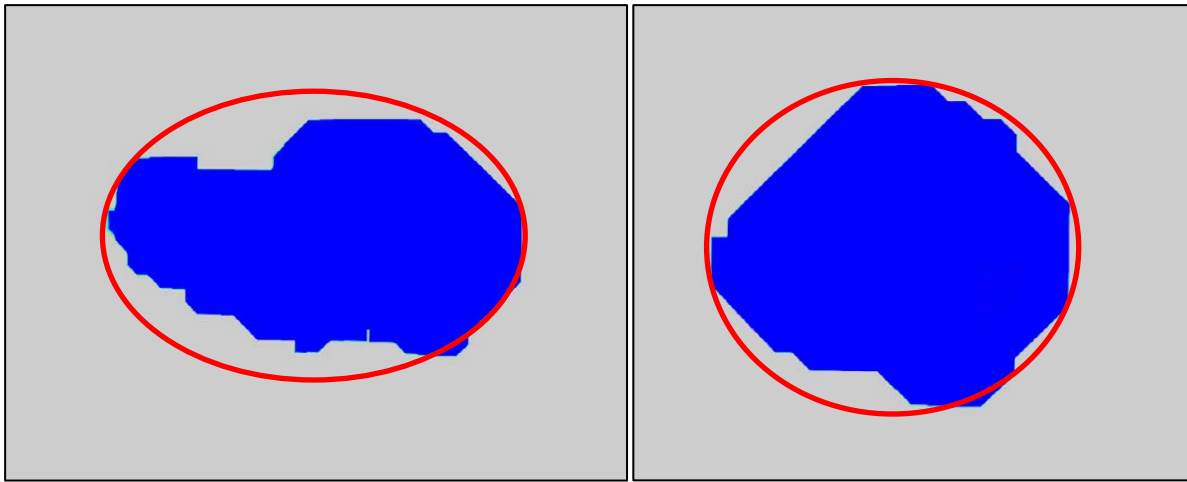


Figure 17. Examples of ellipse fitted to CO₂ footprint to calculate storage coefficient: (a) when CO₂ is injected into the flank (WELL_F), and (b) is CO₂ injected into the crest of the dome (WELL_C). Blue shows the lateral area where CO₂ is present in any of the layers in the model. Grey depicts areas without CO₂.

Table 12. Table showing the value of the storage coefficient at given time steps for each simulated case.

Sim #	Title	Storage coefficient at time [years]				
		1	10	20	30	100
1	Case					
1	DOME_BASE	1.99%	6.82%	9.66%	11.96%	11.74%
2	DOME_FLANK	2.26%	7.78%	9.32%	9.14%	6.02%
3	HIGH_INJ_RATE	3.18%	9.69%	11.65%	13.18%	8.48%
4	LOW_INJ_RATE	1.32%	5.59%	7.24%	7.31%	4.59%
5	DOWN_DIP_PROD	1.84%	7.13%	9.54%	12.09%	11.88%
6	UP_DIP_PROD	2.29%	7.65%	9.32%	9.17%	5.90%
7	DOWN_DIP_PROD2	1.82%	7.12%	9.79%	12.16%	11.94%
8	UP_DIP_PROD2	2.31%	7.61%	9.34%	9.95%	6.13%
9	DOME_BASE_NH	2.04%	6.99%	9.89%	11.96%	11.74%
10	DOME_FLANK_NH	2.36%	7.78%	9.32%	9.14%	5.52%
11	HIGH_INJ_RATE_NH	3.26%	9.75%	11.65%	12.76%	7.89%
12	LOW_INJ_RATE_NH	1.33%	5.67%	7.20%	7.31%	4.35%
13	DOWN_DIP_PROD_NH	1.88%	7.16%	9.88%	12.40%	11.99%
14	UP_DIP_PROD_NH	2.33%	7.93%	9.09%	9.96%	5.65%
15	DOWN_DIP_PROD2_NH	1.83%	7.22%	9.82%	11.97%	11.50%
16	UP_DIP_PROD2_NH	2.36%	7.80%	9.09%	10.60%	5.81%

Injection of CO₂ is modelled over the middle half of the reservoir interval, i.e. not into the shallowest 25% or deepest 25% of the reservoir. Initially CO₂ spreads radially from the injection well along the entire perforation interval. As injection continues, CO₂ rises buoyantly towards the top of the reservoir, entering fresh pore space above the perforation interval. This increases the efficiency coefficient because whilst more CO₂ is entering the reservoir and finding new pore space, it is primarily moving vertically instead of spreading laterally (which the efficiency is based upon). As the CO₂ reaches the top of the reservoir it begins to spread laterally under the caprock, and the storage efficiency reaches a peak. When injection ceases the volume of CO₂ in the reservoir remains constant but the lateral area continues to increase as all the mobile CO₂ rises to form a thin layer under the caprock which spreads laterally according to the topography of the impermeable seal.

5.3.2 Structural geometry

Structural geometry has a great impact on the lateral behaviour of a CO₂ plume. Injection into a structural trap allows CO₂ to accumulate in an increasingly thick layer, lowering the CO₂-water contact whilst spreading laterally at a reduced rate according to the topography. As a result, CO₂ injection into a structural trap gives a higher value of the storage coefficient because there is a thicker accumulation of CO₂. Throughout the injection period the storage coefficient increases because the thickness of the CO₂ plume is increasing faster than the lateral extent, which the storage coefficient is based upon.

Since the CO₂ is injected to the very crest of the dome, the CO₂ is almost in a steady state as soon as injection ceases, and therefore the storage coefficient is constant throughout the post-injection phase, as shown in Figure 18.

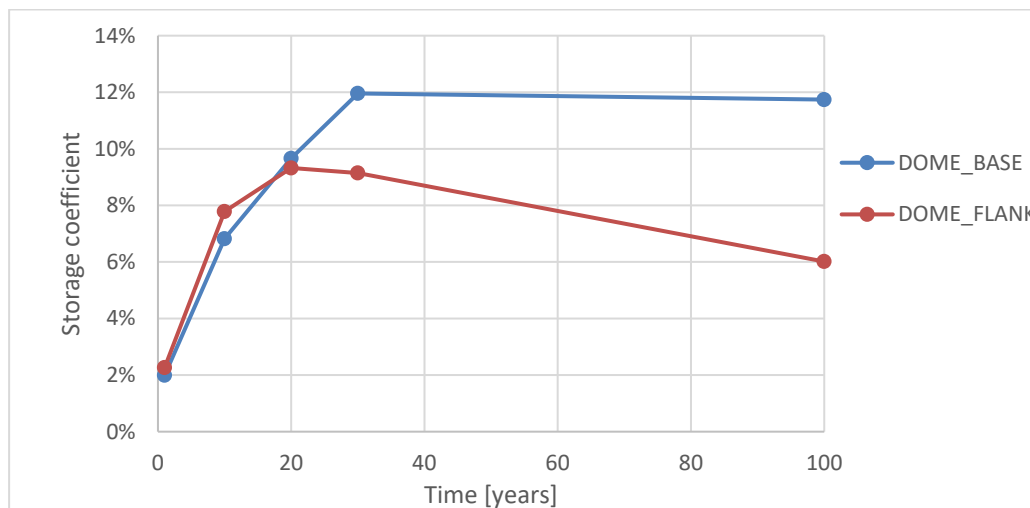


Figure 18. Evolution of the storage coefficient for CO₂ injected into the dome (blue, case #1) and the flank (red, case #2) of the dome model. For case details see Tables 11 and 12.

When CO₂ is injected into the flank of the dome, gravity forces drive the buoyant plume up towards the crest. During the post-injection phase CO₂ continues to migrate up-dip, leaving behind a trail consisting of free (both migrating and trapped in heterogeneity) and residually trapped gas. This causes the storage efficiency to decrease – the lateral area of the plume is increasing but the volume of stored CO₂ remains a constant. This effect is displayed in Figure 18 (red) and is consistent with Bachu (2015). Over the very long term (1000s of years) the plume is stable. After

5000 years of simulation the storage coefficient was 12.9% for injection into the crest and 5.91% for injection into the flank.

5.3.3 Geological heterogeneity

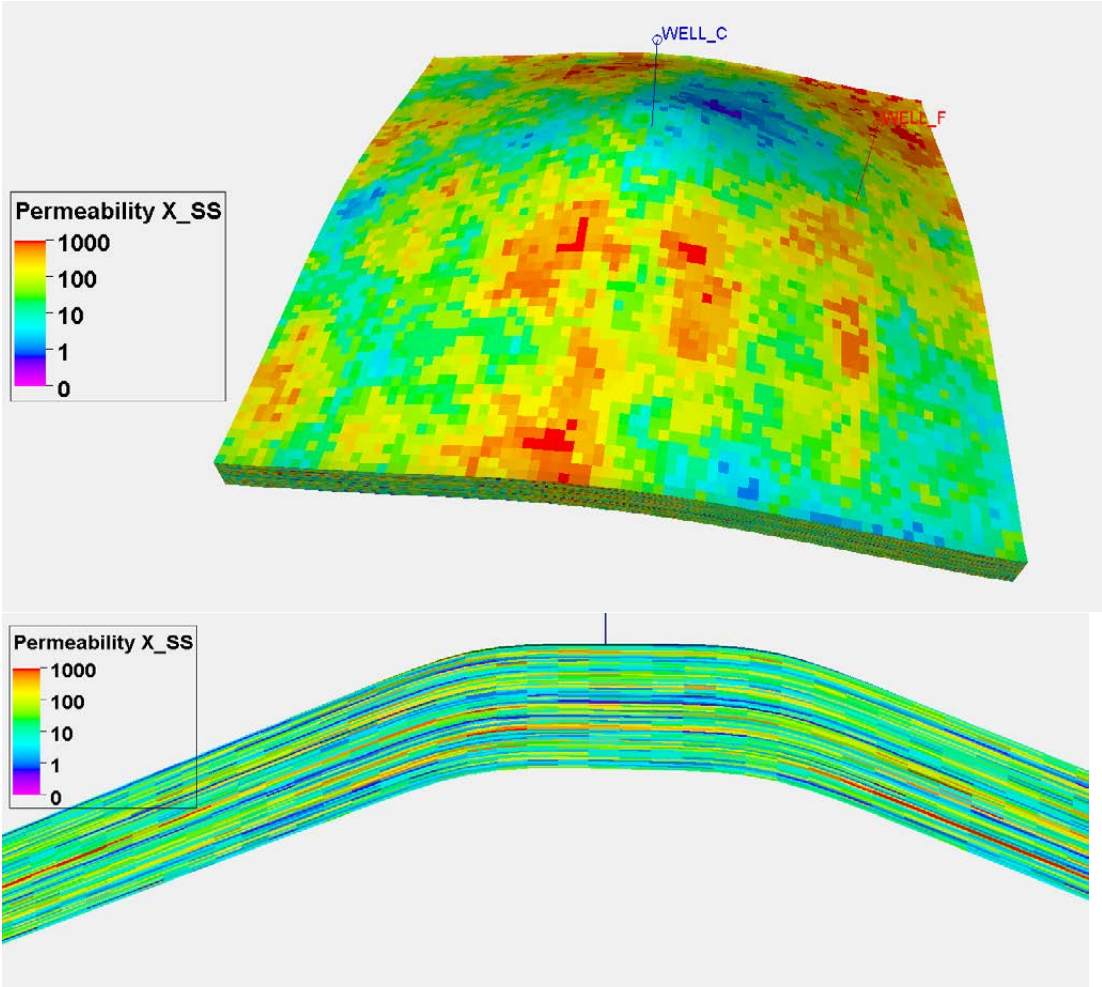


Figure 19. Horizontal permeability of the model populated with properties from the shallow-shelf environment of IEAGHG (2009) as used in the dipping aquifer model.

For the dome model, properties were taken from data collected from Deltaic environments by IEAGHG (2009). An additional geological model was created using data also collected by IEAGHG (2009) from the shallow shelf environment (Figure 19). The data used for each of these models is discussed in Section 5.1. In summary, the shallow shelf has higher porosity and permeability with a greater range. The impact of porosity and permeability on the storage coefficient is shown in Figure 20. The storage efficiency is higher for both injection into the dome and into the flank in the Deltaic environment than the shallow shelf.

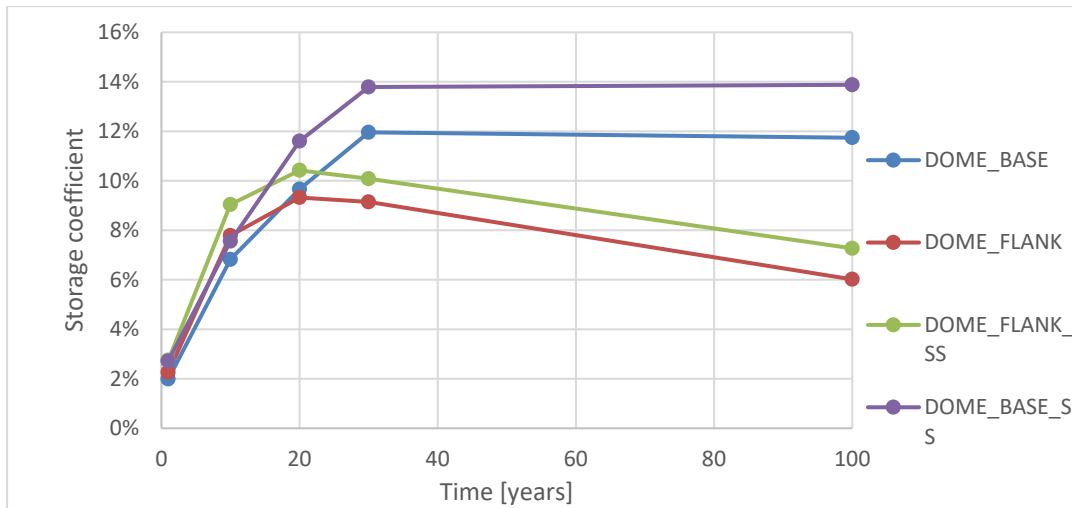


Figure 20. Comparison of results using properties from the Deltaic environment (DOME_BASE and DOME_FLANK) and from the shallow shelf environment (DOME_BASE_SS and DOME_FLANK_SS).

5.3.4 Injection rate

High injection rates force CO₂ to utilise more of the deeper pore space, hence giving a higher storage coefficient. At lower injection rate buoyancy forces are higher relative to injection pressures and therefore the deeper pore space is less utilised and the resulting storage coefficient smaller. Gorecki et al. (2009) tested different injection rates, keeping the total amount of CO₂ fixed at 1 Mt. In this study, we have an injection period of 30 years but cases with injection rate 0.5, 1 and 2 Mt/yr. For the case of high injection rate, twice the total amount of CO₂ is injected. For injection under a dipping caprock (or the flank of a structural dome) simulations achieve very high storage coefficients for high injection rates (up to 13%) but only just over half the efficiency for the lower injection rate (Figure 21).

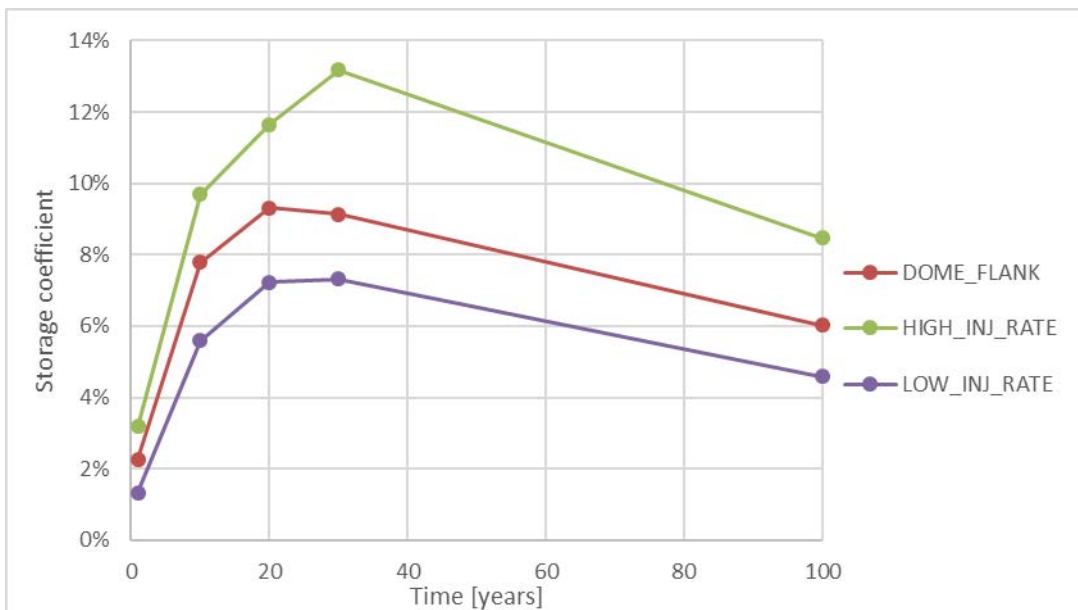


Figure 21. Storage coefficient calculated for cases with high and low injection rates. For case details see Tables 11 and 12.

5.3.5 Water production

Water production is an important factor for CO₂ storage, particularly when estimating the storage resource of a site/complex. The idea of water production to enhance CO₂ storage is widely studied (Bergmo et al., 2011; Birkholzer et al., 2012; Buscheck et al., 2012). The removal of resident brine from a reservoir can greatly increase the amount of pore space available for CO₂ storage and alleviate problems of total increased pressure and/or increased pressure adjacent to a neighbouring site or area of higher risk such as near faults or historical wellbores. The impact of water production on storage coefficients is less studied because it has less influence. Very high rates of water production are required if the buoyancy forces are to be overcome and a plume steered away from its natural up-dip migration path (Vosper et al., 2018). Storage coefficients, as defined in this project, are based solely on the lateral area of the CO₂ plume and do not significantly account for the pressure in the reservoir. In real projects, reservoir pressure is another important factor which must also be considered.

For the case of CO₂ injection into a structural trap, with water production down-dip from the CO₂ injection site, there is no influence on the location of the CO₂ plume and therefore the storage coefficient, as defined in this report, remains unchanged (Figure 22). An additional case was run, where twice the reservoir volume of injected CO₂ was removed through water production. This results in an overall depletion of the reservoir of 1 Mt CO₂ equivalent volume per annum and is not a realistic scenario. Even in this extreme case, the storage coefficient is identical to the case without water production. This is not surprising, as it is intuitive that a large force would be required to overcome buoyancy and remove CO₂ from the structural trap. Water production does, however, have a significant impact on reducing pressure in the reservoir. This can be used to remove barriers such as over pressure (particularly in closed systems) which would otherwise limit the storage resources.

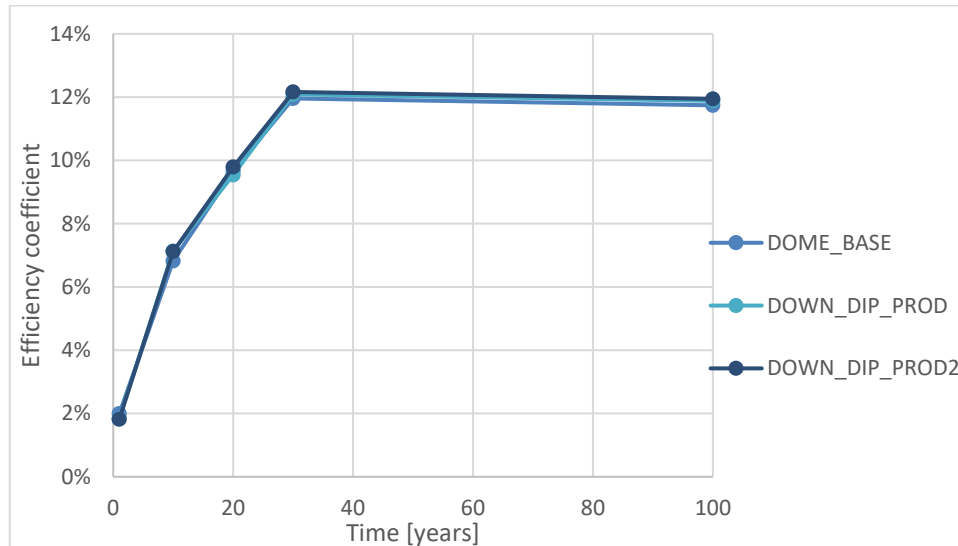


Figure 22. Influence of water production on storage coefficient when CO₂ is injected into a structural dome. For case details see Tables 11 and 12.

For the case of dipping aquifer geometry, case 6 (see Table 11) comprises CO₂ injection into the flank of the dome, and water production of an equivalent volume from the crest of the dome. This effectively creates a hydraulic gradient flowing towards the crest of the dome. Overall, the lateral extent of the plume is not affected by the water production (Figure 23), however the distribution of the plume in the deeper layers of the model is influenced by the water production. This is highlighted by a comparison of cases 2 (no water production) and 8 (double water production)

shown in Figure 24. The storage coefficient therefore doesn't record any impact from the water production, but overall conditions in the site are significantly different. This includes the pressure, which after 100 years (and therefore when local variations in the vicinity of each well have dispersed) does not increase from hydrostatic when water production is included. An additional simulation was run (#8, Table 11) where a volume of brine equivalent to twice the injected CO₂ volume was produced from WELL_C (at the crest of the dome), resulting in an overall depletion of the reservoir. The overall storage efficiency was slightly increased as a result. This is because there was less down-dip travel of CO₂ around the injection well, due to lower pressures, and the increased up-dip travel of CO₂ occurred more in the deeper part of the reservoir, rather than the leading nose at the top of the reservoir just under the caprock on which the storage coefficient is mostly based (Figure 23).

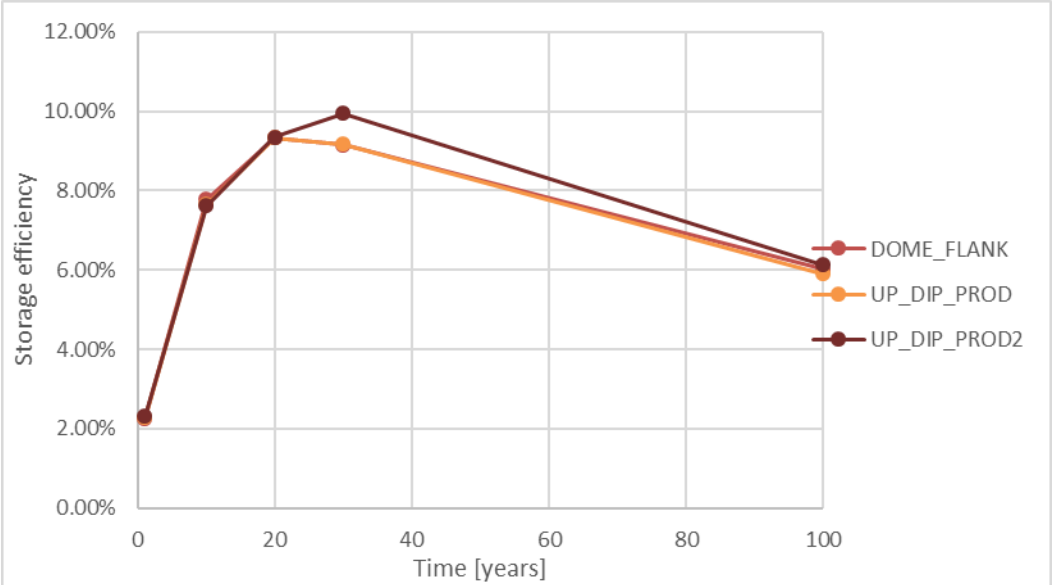


Figure 23. The impact of water production from WELL_C on storage coefficient of a plume injected through WELL_F. For case details see Tables 11 and 12.

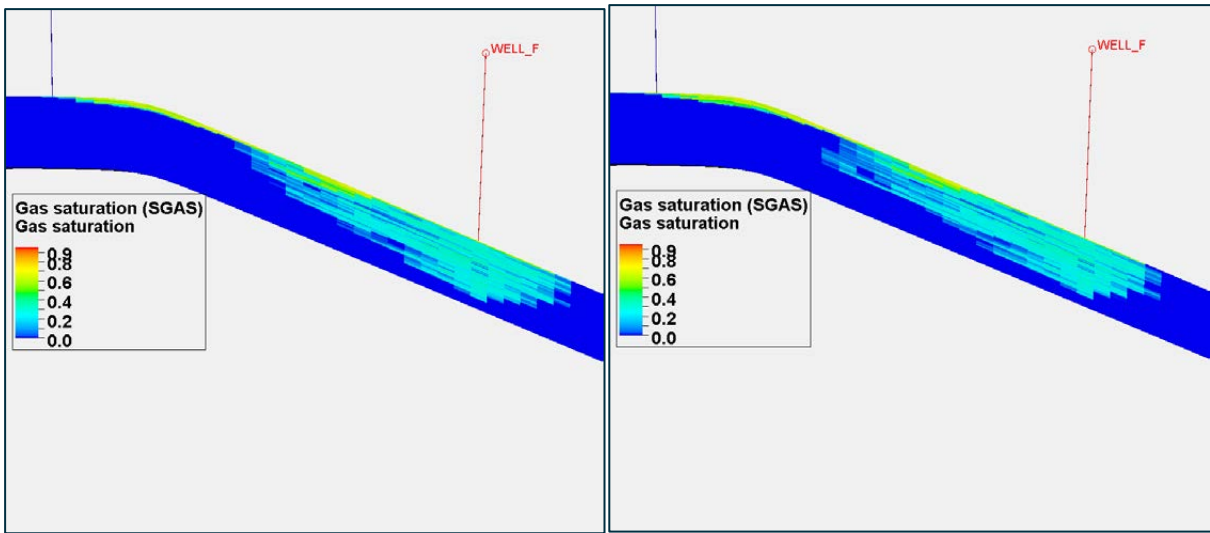


Figure 24. A cross-sectional view of the gas saturation after 100 years of simulation. (a) with no water production (b) with a water production ratio 2:1, i.e. cases 2 and 8 in Table 11. For case details see Tables 11 and 12.

5.3.6 Hysteresis

As CO₂ is injected into the reservoir and begins to travel, resident brine is displaced in a drainage process. The CO₂ will find it easier to travel at higher saturations (see Section 5.2.1 on relative permeability). The trailing edge of the plume represents an imbibition process where different relative permeability relationships apply due to hysteresis. These are described in depth in Section 5.2.2. Therefore, hysteresis is expected to have an impact on cases where the CO₂ plume migrates away from the initial injection site, such as the dipping aquifer.

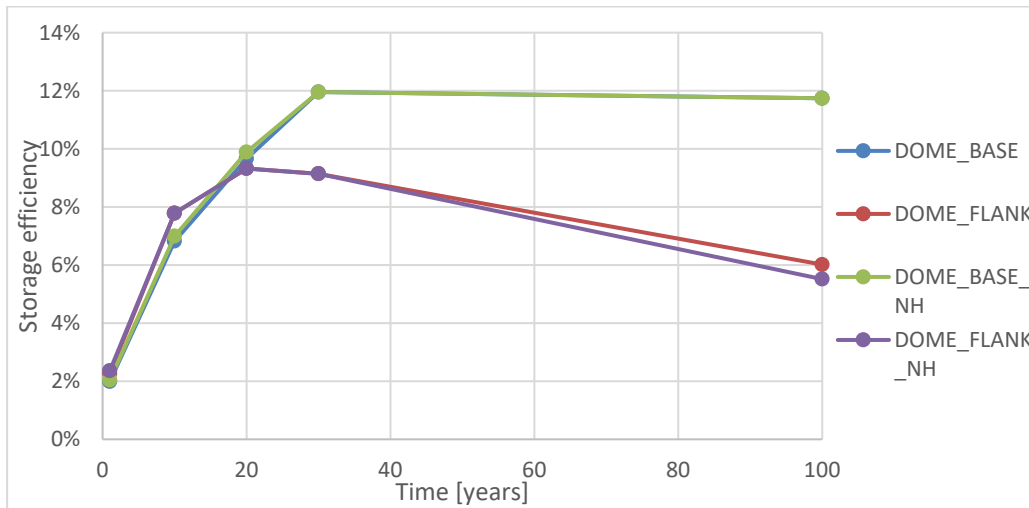


Figure 25. The impact of hysteresis on the storage coefficient for the base cases of injection into the crest and the flank of the dome. For case details see Tables 11 and 12. Note that results for DOME_BASE and DOME_BASE_NH are identical.

All the simulations (cases 1-8 in Table 11) were repeated but without hysteresis to identify how important it is to include hysteresis in modelling studies and what influence it has on the storage coefficient. Little impact on the storage coefficient is seen from cases 1 and 2; hysteresis slightly

increases the storage efficiency in the dipping aquifer case after a long timescale (Figure 25). This result is consistent when the injection rate is varied (Figure 26). Hysteresis works to residually trap gas in the deeper layers of the model, and this leaves less gas in the mobile layer at the top. Therefore, a smaller lateral area is swept by the plume and consequently the storage efficiency is slightly higher when hysteresis is included.

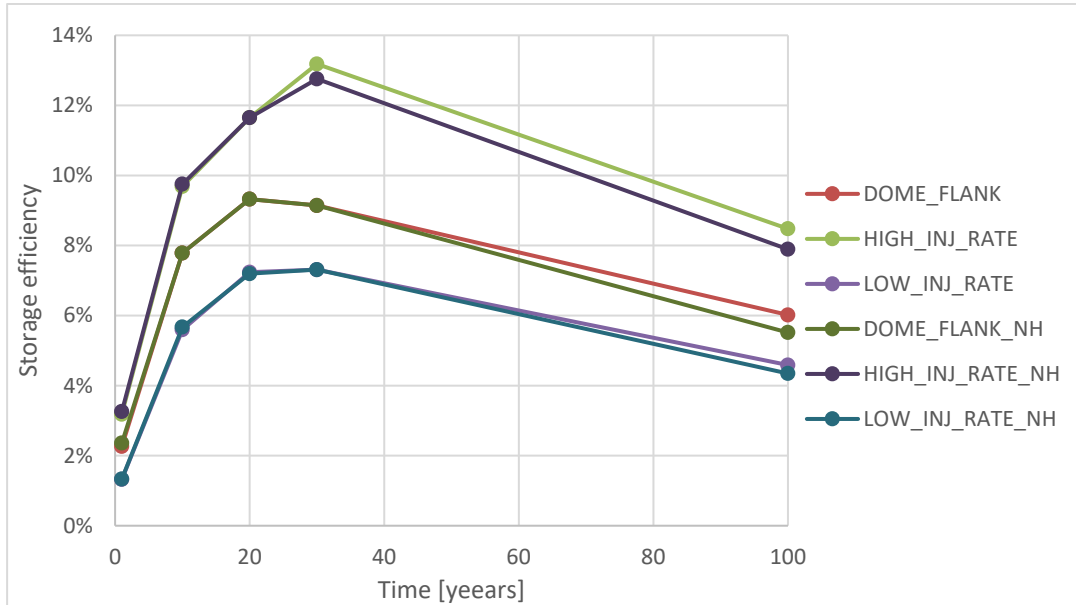


Figure 26. Variation in storage coefficient over time for high, medium and low injection rates, both with and without hysteresis. For case details see Tables 11 and 12.

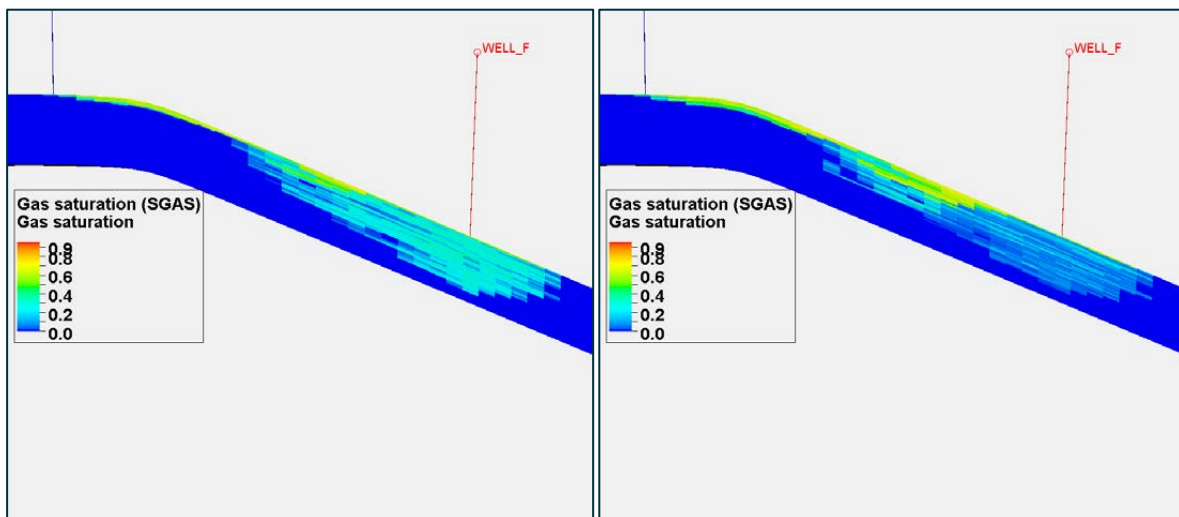


Figure 27. Cross-sectional view of the gas saturation after 100 years of simulation (a) with hysteresis and (b) without hysteresis, corresponding to case #2 and #10 respectively.

Although hysteresis in these simulations has little impact on the storage coefficient, this doesn't mean that hysteresis has little impact on the flow and trapping of the CO_2 . When hysteresis is neglected (Figure 27b) a significantly greater proportion of the CO_2 remains in a free, mobile state even after 100 years of simulation. When an estimation of hysteresis is included in the modelling, much of the CO_2 becomes residually trapped through the trailing edge of the plume (Figure 27a).

Only a small amount in this case remains free and mobile at the leading edge. As well as being more realistic, this is a scenario with much better security of storage – residually trapped CO₂ does not carry the same risk of leakage as mobile, buoyant CO₂ and therefore is desirable to operators and regulators.

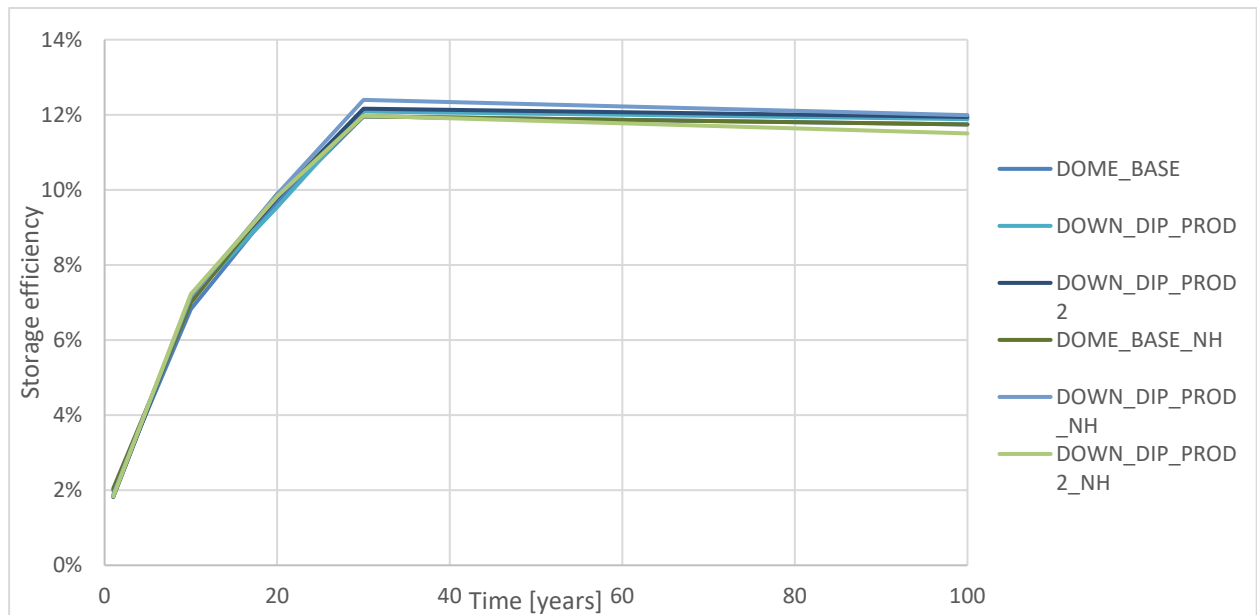


Figure 28. Comparison of all cases with injection into the crest of the dome, with and without hysteresis and water production. For case details see Tables 11 and 12.

A comparison of all cases where CO₂ was injected into the crest of the dome is given in Figure 28. All cases estimate to storage to be around 2% after 1 year of injection, rising to around 12% at the end of the injection period and thereafter. There is no significant impact due to hysteresis or water production – this is an intuitive result as there is no migration of CO₂. Some of the variability shown may possibly be due to inaccuracies in the fitting of an ellipse to the lateral extent of the plume.

Although the impact of hysteresis on the storage coefficient (as defined in this report) is limited, the real impact of hysteresis can be seen in the trapping state of the stored CO₂, i.e. mobile, dissolved, residually trapped etc. Figure 29 shows the total volume of injected CO₂ and the volume which is mobile, dissolved and residually trapped, when the CO₂ is injected into the crest of the dome model. Likewise, for CO₂ injected into the flank of the dome the results are shown in Figure 30.

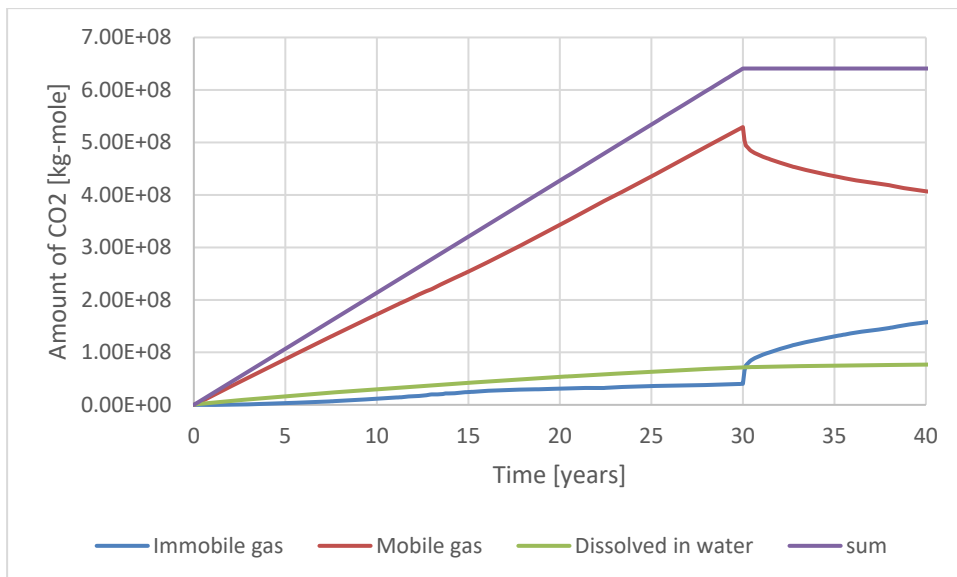


Figure 29. Breakdown of the trapping states of CO₂ for case 1 (injection into crest).

For the case of injection into the flank, representing flow in a dipping aquifer, after 40 years an extra 9% of the CO₂ is residually trapped than in the case of injection at the crest (structural trap). The migration of CO₂ up the flank of the dome gives much greater opportunity for residual trapping than direct injection into a structural trap.

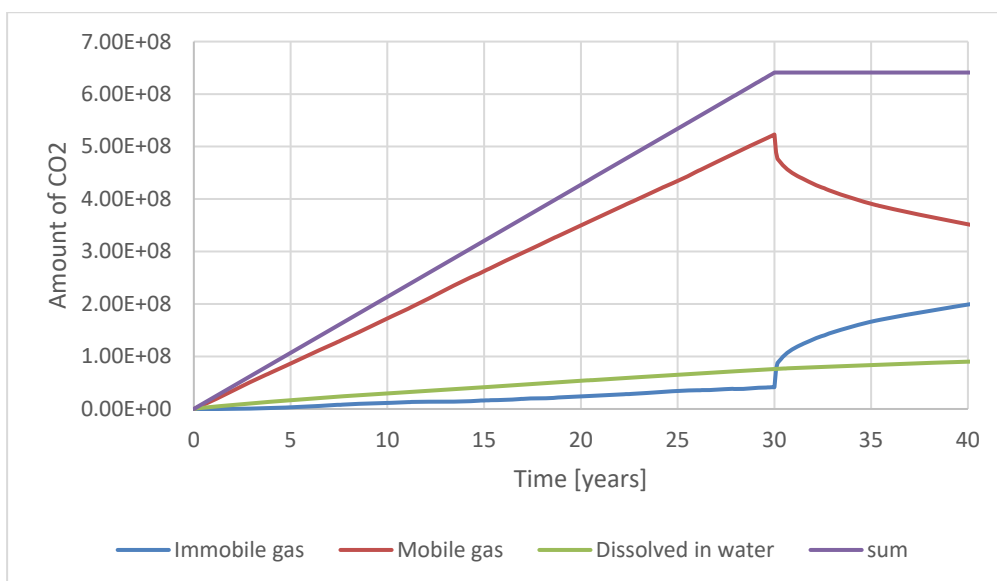


Figure 30. Breakdown of CO₂ trapping states of CO₂ for case 2 (injection into flank).

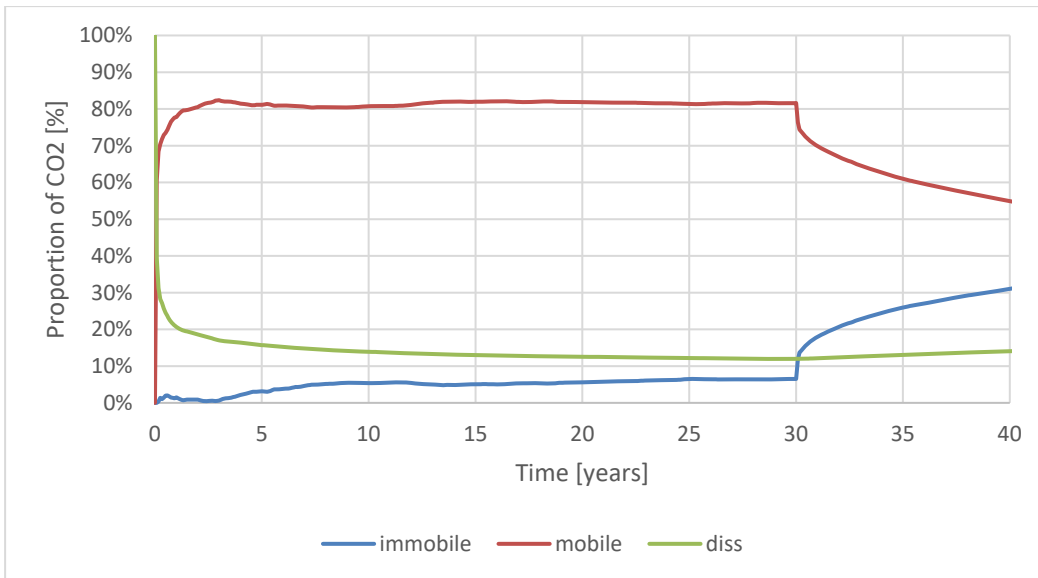


Figure 31. Proportion of CO₂ in each trapping state for case 2 (injection into flank).

The proportion of CO₂ which is mobile, residually trapped, and dissolved is shown in Figure 31 and Figure 32 for cases with and without hysteresis modelling respectively. The amount of CO₂ dissolved in brine is not affected by hysteresis and increases steadily. As a proportion of the cumulative injected CO₂ this increases after the end of injection. A sudden change is seen after 30 years in terms of the proportion of immobile gas when the system changes from injection to post-injection.

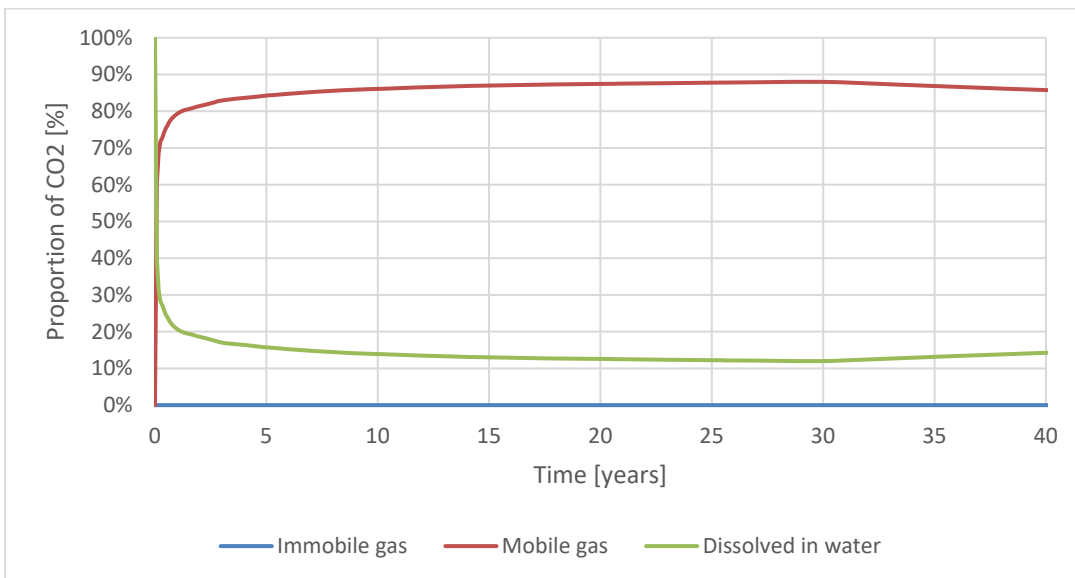


Figure 32. Proportion of CO₂ in each trapping state for case 10 (no hysteresis modelled).

5.3.7 Impact of shape fitting

In the literature there is not a well-established methodology for evaluating the area of a CO₂ plume in a numerical model for the purpose of calculating dynamic storage coefficients. Gorecki et al. (2009) highlight four distinct methods for calculating the volume of the plume and choose a minimum area rectangle. Ideally there would be an internationally agreed definition of storage coefficient that could be applied on site and regional scales. In this study an ellipse has been fitted to each plume, whether captured using seismic data or numerical modelling, and used to calculate the storage coefficient. This section aims to highlight the variance in storage coefficient calculated from identical plumes using two different shapes fit to the plume; an ellipse and a rectangle. In addition, modelling is performed using a purpose-built dipping aquifer model to verify the dome-based model used in the previous section for representing flow in a reservoir with a simple, sloping caprock. This was chosen to add verification to using the dome model to represent a dipping aquifer, and to compare results with a different angle of dip whilst at the same time investigating the impact of shape fitting.

Storage efficiency factors calculated following 1, 10, 20 and 30 years of injection are tabulated in Tables 14 and 15 below. A final storage efficiency for each model was calculated 100 years following the start of CO₂ injection (70 years after the cessation of injection). Long-term results are discussed in Section 5.3.2. The efficiency factors in Table 13 were computed by fitting a 2D ellipse to a map of the net reservoir CO₂ saturation at each time step of interest (e.g., Figure 33a). The 2D saturation surface was constructed by computing the net saturation (Net_{SG}) over the whole reservoir interval, for each grid cell in the model, using the equation:

$$\text{Net}_{\text{SG}} = \text{Sum} [\text{SG}(k) * H(k)] \quad (3)$$

Where SG(k) is the cell gas saturation at Z index k and H(k) the thickness of the kth cell. The bounding polygon of the resulting saturation distribution (blue line in Figure 33a) was then fitted with an ellipse (orange polygon in Figure 33a). The storage efficiency factor (S) was then defined as:

$$S = \text{RV}_{\text{CO}_2} / \pi * a * b * h * \varphi \quad (4)$$

Where RV_{CO₂} is the volume of CO₂ stored in the reservoir, a, b are the elliptical radii, h is the reservoir thickness (in this case 200 m) and φ is the average porosity (in this case c. 0.15).

Table 13. Storage efficiencies calculated by fitting an ellipse to the modelled CO₂ plume extents (see text for an explanation). All cases used the dipping aquifer model.

Case	Description	1 year	10 years	20 years	30 years	100 years
1	CO ₂ injection only; no hysteresis	3.95%	10.47%	13.29%	14.62%	8.06%
2	CO ₂ injection only; hysteresis	4.30%	10.70%	13.53%	15.06%	9.55%
3	1x water production; no hysteresis	4.30%	10.87%	13.89%	14.94%	8.62%
4	1x water production; hysteresis	4.30%	10.87%	13.89%	14.94%	9.36%
5	2x water production; no hysteresis	4.30%	10.80%	13.67%	15.45%	8.59%
6	2x water production; hysteresis	4.30%	10.80%	13.67%	15.45%	9.38%

Using an elliptical function to describe the reservoir volume contacted by the CO₂ plume results in an upper bound estimate for the storage efficiency factor. An alternative approach is to fit a minimum bounding rectangle (Figure 33b, Table 14) enclosing the whole CO₂ plume and use this to estimate the area of the reservoir swept by the plume. Because most CO₂ plumes will be elliptical in plan, this approach will lead to lower storage efficiencies compared to an elliptical bounding surface (compare the results in Tables 13 and 14). The area of the bounding rectangle (A) can be used to calculate S using the following relationship:

$$S = RV_{CO_2} / A \cdot h \cdot \phi \quad (5)$$

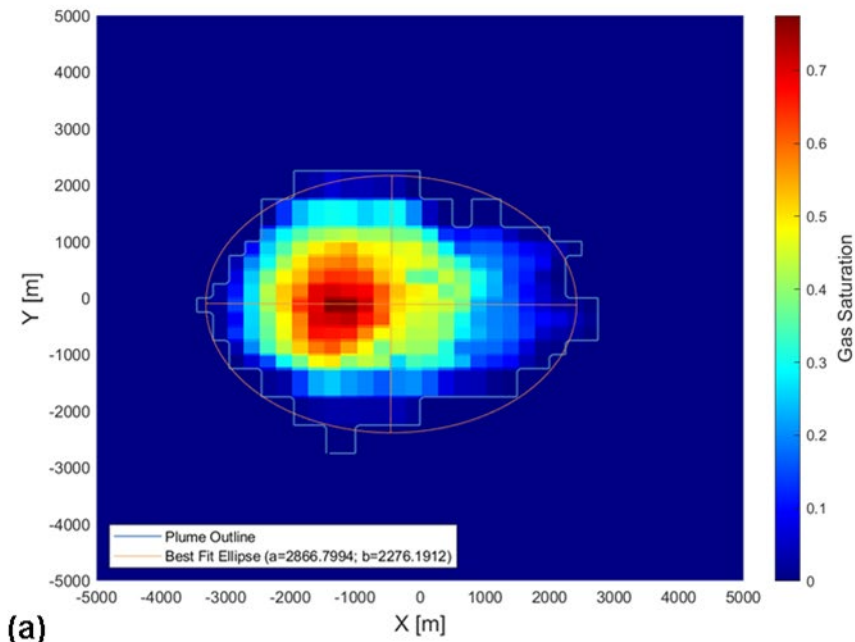
Table 14. Storage efficiencies calculated by fitting a rectangle to the modelled CO₂ plume extents (see text for an explanation). All cases used the dipping aquifer model.

Case	Description	1 year	10 years	20 years	30 years	100 years
1	CO ₂ injection only; no hysteresis	2.53%	8.16%	9.83%	10.46%	5.33%
2	CO ₂ injection only; hysteresis	3.06%	8.16%	9.83%	11.16%	6.44%
3	1x water production; no hysteresis	3.06%	8.99%	9.83%	10.46%	6.17%
4	1x water production; hysteresis	3.06%	8.99%	9.83%	10.46%	6.17%
5	2x water production; no hysteresis	3.06%	8.16%	9.12%	11.16%	6.17%

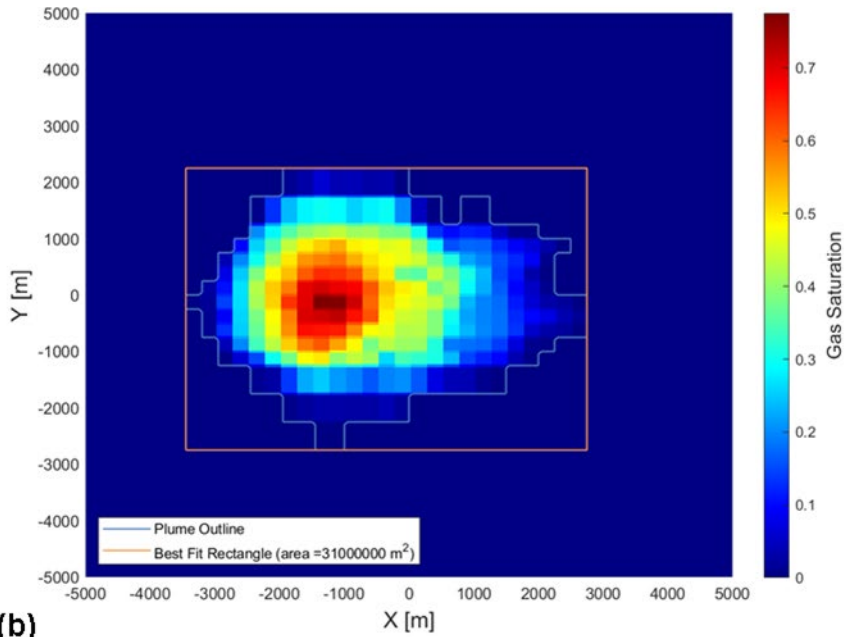
6	2x water production; hysteresis	3.06%	8.16%	9.12%	11.16%	6.44%
---	------------------------------------	-------	-------	-------	--------	-------

Plots showing the evolution of storage efficiency with time are shown in Figure 34. The storage efficiency factor shows an approximate linear increase with time during the injection phase, peaking in each case at the cessation of injection (Figure 34a, b). Storage efficiency then declines as the plume spreads out and migrates up-dip, effectively sweeping a greater volume of the reservoir. The values of storage efficiency in this section are higher than the previous section and this is because a different model has been used. The dome model used in Sections 5.3.1 – 5.3.5 was based on average properties from the deltaic environment in Gorecki et al. (2009), and the dipping aquifer model in this section was based on the shallow shelf properties of the same source. The results of Section 5.3.3 highlight this difference. This shows that the porosity/permeability values are also an important parameter when determining the storage efficiency.

Figure 34c, d shows that hysteric effects act to slightly increase the storage efficiency in this model. This effect is particularly pronounced 70 years after injection ceased, because any trapped gas cannot move and there is consequently less gas in the upper mobile layers of the plume. The plume thus sweeps a smaller volume of reservoir than the models without any residual trapping, and Equations 4 and 5 consequently predict an increased storage efficiency. Finally, Figure 34e, f shows that water production acts to slightly increase the storage efficiency factor, although this effect is negligible.



(a)



(b)

Figure 33. (a) Elliptical fit to the CO₂ plume developed 100 years after the onset of injection for Case 1 in Tables 14 and 15. The minimum bounding ellipse used to define the reservoir area swept by the CO₂ plume is shown as an orange polygon. The blue polygon denotes the boundaries of the gas plume. (b) Minimum bounding rectangle (orange polygon) enclosing the CO₂ plume developed 100 years after the onset of injection for Case 1 in Tables 14 and 15: the blue polygon denotes the boundaries of the gas plume.

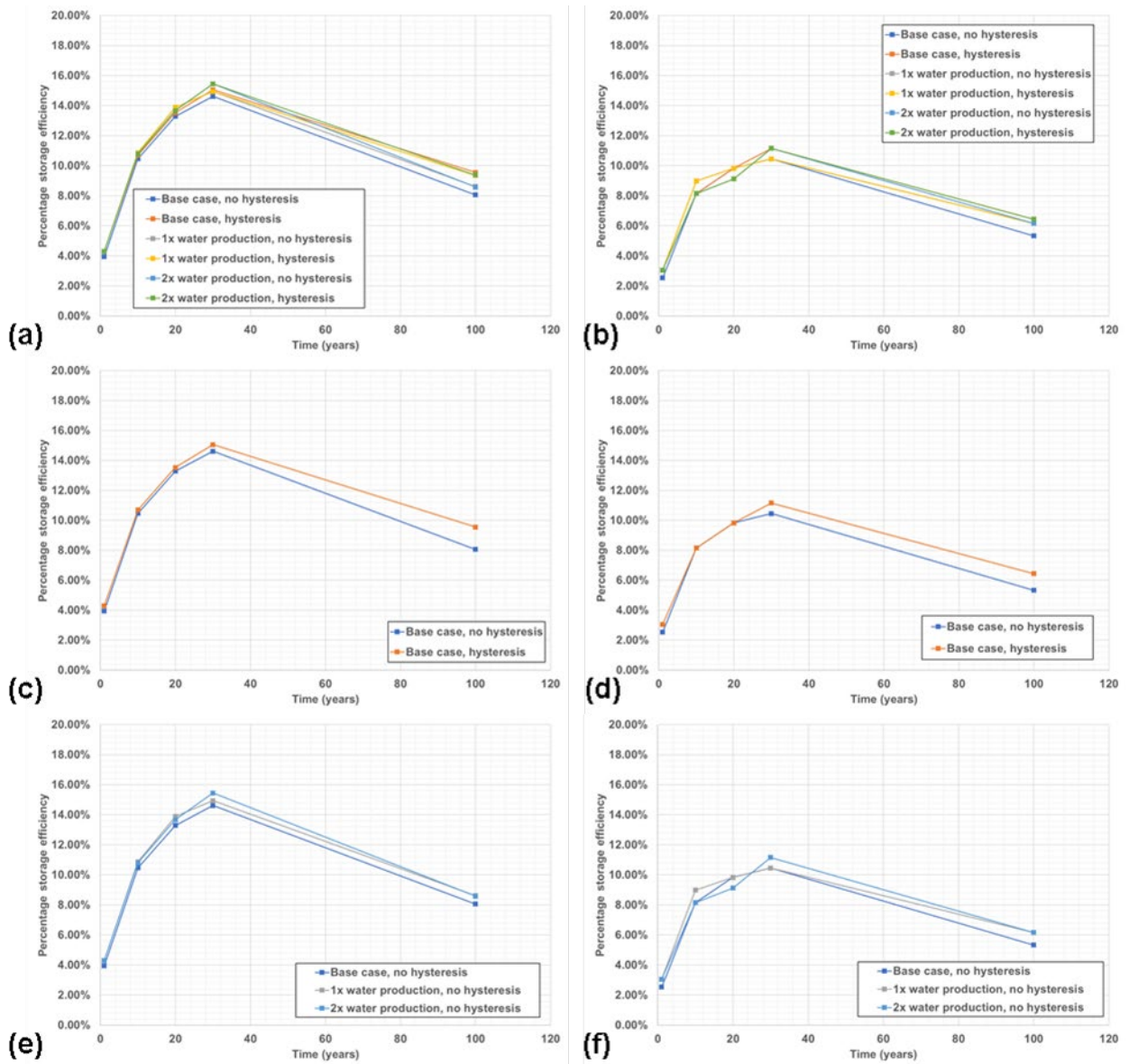


Figure 34. Storage efficiency evolution with time calculated by fitting an ellipse (a, c, e) and a minimum bounding rectangle (b, d, f) to the growing CO₂ plume. All based on the dipping aquifer model.

5.4 SENSITIVITY TO GRID SIZE

Additional simulations were run to test the dependence of the results on the size of the numerical grid used.

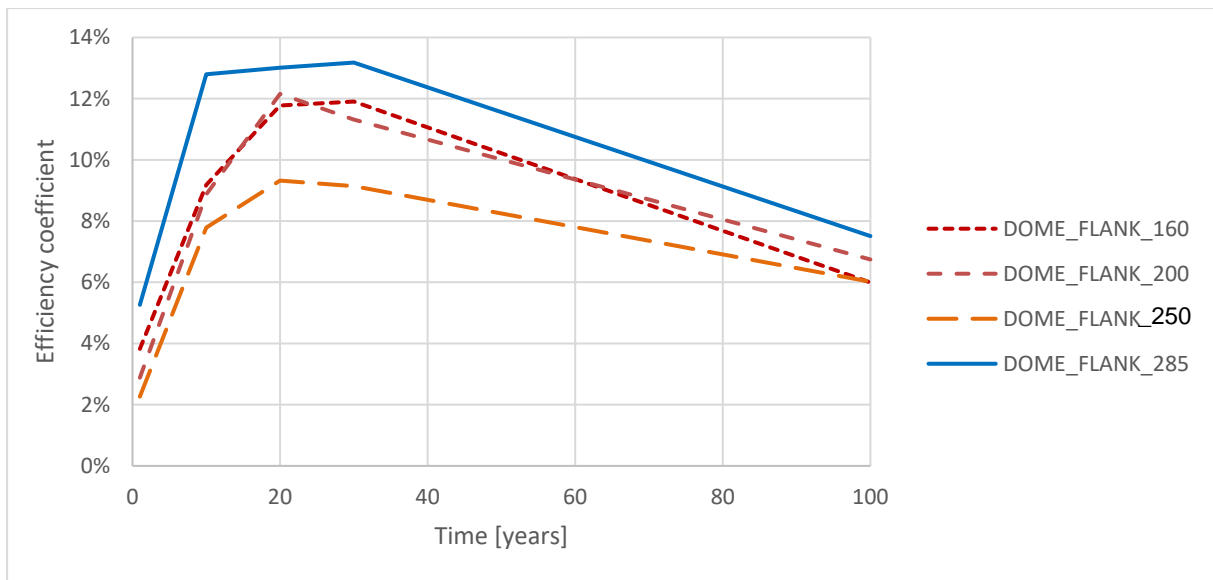


Figure 35. Variations in efficiency coefficient with grid size. Numbers in the legend correspond to the lateral size of cells in the grid (in metres)– 285 is the coarsest and 160 is the finest.

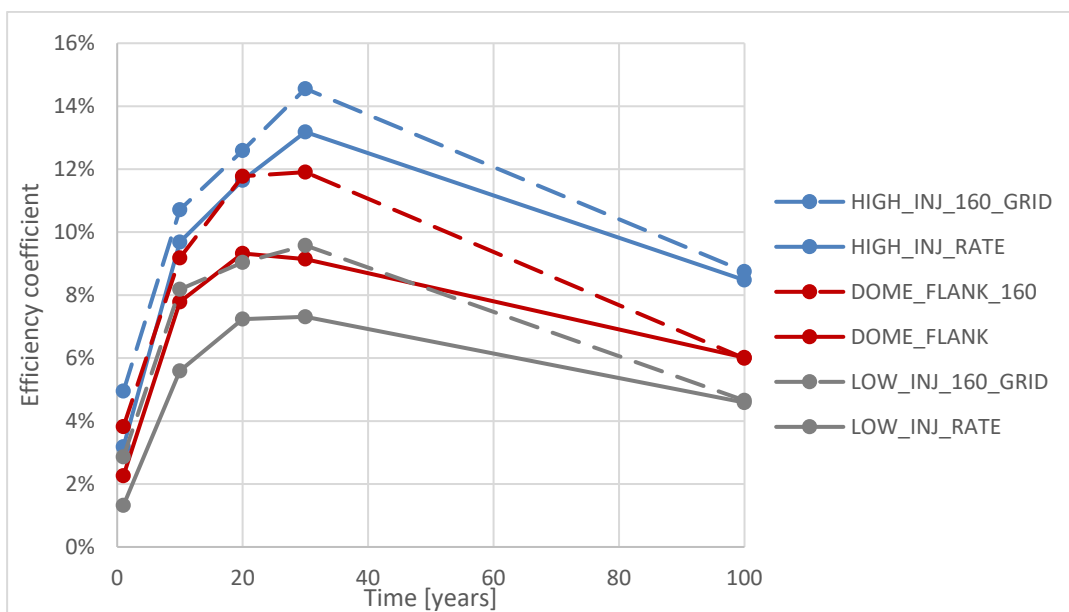


Figure 36. Impact of grid size on the efficiency coefficient for cases of different injection rates.

5.5 SUMMARY OF THE MODELLING STUDY

Numerical flow simulations were undertaken in two structural settings: a structural dome and a dipping aquifer (represented by injecting into the flank of a large dome). The parameterisation was mostly taken from IEAGHG (2009) who used average data from a wide database of reservoirs. The dipping aquifer model utilised data from the Shallow Shelf depositional environment, and the dome model primarily used data from the Deltaic environment, with additional cases representing the shallow shelf presented in Section 5.3.3. A CO₂ injection rate of 1 Mt/yr was maintained for 30 years (a total of 30 Mt CO₂) and simulations continued for a further 70 years. Storage coefficients were calculated by fitting an ellipse to the maximum lateral extent of the free CO₂ plume after 1, 10, 20, 30 and 100 years of simulation.

Injection into a structural trap gave the highest values of storage efficiency in this study, 12%. In this case CO₂ is pooled in a dome structure as a thick layer with lateral spread constrained by the topography. Storage efficiency is unlikely to reach this high value without significant structural trapping or containment.

In the case of flow in a dipping aquifer, storage efficiency increased throughout the injection period, reached a peak of 9% after 20-30 years and gradually reduced post-injection to around 6% at the end of the 100-year simulation. Higher injection rates led to higher storage coefficients, reaching a peak of 13% when twice the CO₂ was injected (2 Mt/yr for 30 years). This trend is also evident from previous literature.

Water production was modelled and its impact on the storage coefficient evaluated. Water production can have a very significant impact on a CO₂ storage operation. The pressure is reduced, which may allow for increased CO₂ injection and/or reduce risks associated with high overpressure. The impact of water production on the location of the CO₂ plume is more limited, large volumes of water must be produced to have a significant effect on the location or migration path of the CO₂ plume. This means that water production has very little effect on the storage efficiency, but this is only one factor of many to be considered when planning a CO₂ storage operation. Water production can have a big impact on the pressure in a model and the total amount of CO₂ that can be injected into a site, but not on the efficiency as defined in this report.

Hysteresis and residual trapping increase the security of CO₂ storage by reducing the amount of CO₂ which is free, mobile and buoyant. This is a factor not considered in storage coefficients as defined in this project, which are purely based on the lateral extent of the plume compared to its injected volume. All simulations were run both with and without an estimation of hysteresis included and large amounts of the CO₂ were residually trapped in deep layers of the model when hysteresis was included. There was still a small layer (on the order of 1 m) of free CO₂ under the caprock which dictated the lateral extent of the plume and therefore the storage coefficient. This was even the case after extending the simulation to 8000 years. A very small amount of CO₂ remained residually trapped even without modelling hysteresis. As a result, hysteresis had only a limited impact on the value of the storage coefficient – hysteresis acts to slightly increase the storage efficiency at late times (i.e., after the plume has started to migrate up-dip). A larger effect would be expected for longer migration distances. This is because so much of the free CO₂ has been trapped in lower layers of the model and there is a smaller amount that is still free to migrate. For cases where the CO₂ is expected to migrate a long way, this residually trapped CO₂ will remain in place near the injection well and along the migration pathway. Compared to cases without residual trapping, eventually this would give a lower storage efficiency.

All the cases modelled in this study were chosen such that there was sufficient injectivity for the volumes of CO₂ required. Issues with injectivity are likely to have a significant influence on the storage coefficient but will be very site-specific.

6 Analytical approximations of storage coefficients

Analytical expressions can be a powerful, quick, and cheap approach to making estimations. In the context of storage coefficients, this section aims to produce simple analytical or semi-analytical models to quantify the storage coefficient of plumes of buoyant CO₂ injected under an impermeable caprock. Two different caprock geometries are studied: a flat caprock and a dipping aquifer. Structural traps are discussed qualitatively. Average geological properties are used to provide a first estimate of the storage coefficient. Analytical expressions for the storage coefficient clearly display how each factor affects the value of the storage coefficient.

Detailed numerical simulations can be expensive and time-consuming, and require significant amounts of input data, including a static geological model. Analytical approximations are based on averaged data for bulk properties and can be applied very quickly and cheaply. Simplified models might not give a result as accurate as more detailed methods, but at the lower SRLs and resource classifications (see Section 2) detailed site-specific data may not be available. This leads to assumptions about the storage site that are in fact utilised in analytical approximations, for example homogeneous properties such as porosity and permeability.

Volumetric calculations of storage efficiency are generally based around analytical methods but the application of analytical techniques to dynamic (changing with time) storage coefficients is currently very limited.

There is a significant amount of literature which utilises analytical methods to predict the size, shape, and position of a plume of buoyant CO₂ injected into a porous reservoir under an impermeable caprock (Mathias et al., 2009; Neufeld and Huppert, 2009; Nordbotten et al., 2005a; Okwen et al., 2010). This section draws on existing models and makes the application to storage coefficients, as defined in previous sections of the current report.

Okwen et al. (2010) built an analytical model based on the shape of plume derived by Nordbotten et al. (2005a). The authors showed that during the injection phase, the storage efficiency depends on three dimensionless groups: S_r , the residual brine saturation following displacement of brine by CO₂; λ , the ratio of CO₂ mobility to brine mobility; and a dimensionless group (Γ) that quantifies the importance of CO₂ buoyancy relative to flow rate.

$$\Gamma = \frac{2\pi\Delta\rho g k \lambda_b B^2}{Q}$$

In the above equation, $\Delta\rho$ is the difference in density between the CO₂ and brine, g the gravitational acceleration (9.81 ms⁻²). k the permeability. The mobility of the brine λ_b is calculated as the relative permeability of brine divided by its viscosity, B is the thickness of the reservoir and Q the CO₂ injection rate. Juanes et al. (2010) extend this idea to incorporate a post-injection period, groundwater flow, and capillary trapping. The maximum distance travelled by a CO₂ plume before complete capillary trapping is calculated and therefore the storage efficiency of a plume immobilised by capillary trapping alone. An additional output is the time taken for the plume to be entirely trapped, under the influence of a continuous groundwater flow.

6.1 STORAGE COEFFICIENT UNDER A FLAT CAPROCK

A basic model is set up consisting of a plume of buoyant CO₂ injected into a single point under an impermeable caprock at a constant rate into a porous medium initially filled with brine (Figure 37). The two fluids are regarded as immiscible. Since the caprock is flat, the plume is expected to spread radially from the injection point and the system is modelled as axisymmetric.

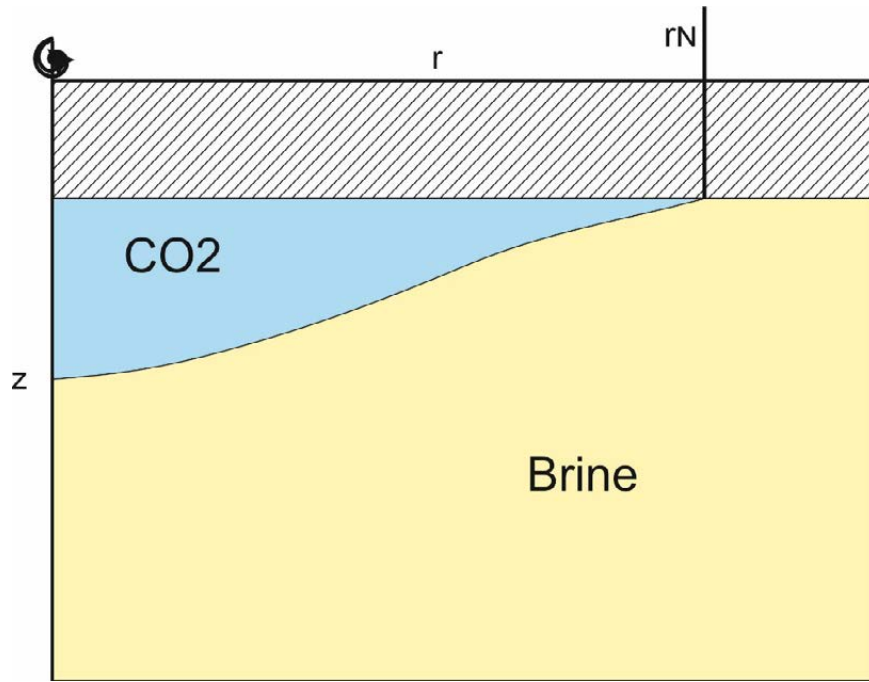


Figure 37. Diagram of a CO₂ plume spreading under a flat caprock. The plume is axisymmetric about the z-axis and extends horizontally a radial distance, r_N .

The following common assumptions used to represent a CO₂ plume with analytical expressions are applied:

- The geological properties of the reservoir are homogeneous and isotropic, including porosity and permeability;
- Resident brine in the reservoir and injected CO₂ are each of constant, uniform density and viscosity;
- CO₂ is injected at a constant rate, Q [m³/s] from directly under the caprock (near-well effects are not incorporated);
- Motion of the brine is neglected;
- Capillary forces and surface tension are neglected;
- The thickness of the reservoir is much greater than that of the plume.

A basic shape of plume is defined by Nordbotten et al. (2005a). Lyle et al. (2005) define the maximum extent of an axisymmetric buoyancy-driven gravity current injected at constant rate Q from a point source to be:

$$r_N(t) = \eta_N(\alpha) \left(\frac{\gamma Q}{\phi} \right)^{1/4} \sqrt{t} \quad (6)$$

Note that a modification has been made, correcting the equation by a factor of the porosity (ϕ), following Bickle et al. (2007). Where r_N is the radius of the plume, η_N is a function of α alone, where α denotes the type of input flux - in this case of a constant injection rate, $\alpha = 1$. The function η_α is presented by Lyle et al. (2005) in their Figure 3, and from this figure it is taken that $\eta_N = 1.15$. The constant γ is defined as $\gamma = \frac{\rho k g \Delta \rho}{\rho \phi \mu}$, where ρ is the density of CO₂, k is the permeability of the porous medium, g the gravitational acceleration 9.81 ms⁻², $\Delta \rho$ the density difference between the brine and CO₂, ϕ the porosity and μ the dynamic viscosity of the CO₂. Q is the rate of CO₂ injection (kg/s). Figure 3 within Lyle et al. (2005) shows that for a constant rate

of CO₂ injection ($\alpha = 1$) then $\eta_N = 1.15$. Substituting these data into Equation 6 gives the expression:

$$r_N(t) = 1.15 \left(\frac{Qkg\Delta\rho}{\phi^2\mu} \right)^{1/4} \sqrt{t}$$

A similar study was undertaken by Nordbotten et al. (2005b), in which the maximal radial extent of the plume was expressed as proportional to the square root of the total volume of injected CO₂ ($Qt = V$). The result here is similar because the injection rate (Q) is a constant. The constant may look different as the Nordbotten et al. (2005b) study considered injection from a line source (i.e. a well) and Lyle et al. (2005) use a point source but both solutions increase with \sqrt{t} .

The current study defines the storage efficiency E as defined by Oldenburg (2021), the ratio of the volume of CO₂ injected to the pore volume of a cylinder encompassing the plume:

$$E = \frac{Qt}{\phi H \pi r_N(t)^2} \quad (7)$$

This is valid for all time. Where H is the thickness of the reservoir. Substituting for r_N (Lyle et al., 2005) gives

$$E = \frac{1}{H\pi 1.15^2} \sqrt{\frac{Q\mu}{kg\Delta\rho}} \quad (8)$$

This is a constant. Despite the numerical pre-multiplicative constant, it is not unit dependent, only consistent units are required. This result shows that in this simplified case the storage efficiency is not expected to change with time throughout the injection phase. The efficiency as a proportion of total storage resources obviously increases as more CO₂ is injected into the reservoir. The most influential factor is the thickness of the reservoir, a thick reservoir will yield a low efficiency, as defined in this report. This does not mean that a thinner reservoir is more desirable but that it can be difficult to utilise the deepest parts of a reservoir, especially when the injection point is at the shallowest depth. The efficiency increases with the square root of the injection rate, this agrees with Section 5 where a high injection rate was found to give a higher storage efficiency.

The parameters gathered in Section 4 for the case studies of Sleipner, Snøhvit and Ketzin (Table 15) can be input into Equation 8 and the results compared to test the accuracy of the analytical approximations (Table 16). A Sleipner permeability value of 2 Darcy was taken from Williams and Chadwick (2021). The Snøhvit permeability value of 600 mD taken from White, J et al. (2018). At Ketzin a permeability value of $90 \times 10^{-15} \text{ m}^2$ (91 mD) and temperature of 34 °C was used (Lengler et al., 2010).

In the case of Sleipner, the plume collected in a series of layers underneath low permeability strata. This would act to increase the storage efficiency as more of the deeper pore space is utilised. This is reflected in the results. The simple analytical approximation gives a storage efficiency lower than that observed from the seismic data. At Snøhvit, the reservoir is compartmentalised and there are lateral barriers to flow. As shown in Figure 9, the plume was very much still focussed around the injection well and the pore space immediately above. This gives a very high storage efficiency, especially compared with analytical models injecting CO₂ into a single point directly underneath the caprock. For Ketzin, the analytical approximation also underestimates the storage coefficient – the observed CO₂ plume covered a smaller lateral area than predicted by an analytical approximation. The use of analytical approximations is primarily applied at a very early stage of site appraisal.

Table 15. Parameters used to calculate the analytical approximation of the storage efficiency for the base case using the dome model. Brine density is taken as 1055 kg/m³.

Parameter, symbol [unit]	Numerical simulations (base case, dome model)	Sleipner	Snøhvit	Ketzin (2009)	Ketzin (2012)
Reservoir thickness, H [m]	200	200	80	37 (70)	37 (70)
Injection rate, Q [m ³ /s]	0.052 (1 Mt/yr)	0.040 (0.9 Mt/yr)	1.49x10 ⁻³ (0.42 Mt/yr)	1.5x10 ⁻³ (0.0125 Mt/yr)	1.8x10 ⁻³ (0.0125 Mt/yr)
Dynamic viscosity of CO ₂ , μ [Pa s]	1.54x10 ⁻⁵	1.61 x10 ⁻⁵	1.61x10 ⁻⁵	1.54x10 ⁻⁵	1.54x10 ⁻⁵
Permeability, k [m ²]	9.87x10 ⁻¹⁴ (100 mD)	1.97x10 ⁻¹² (2000 mD)	5.92x10 ⁻¹³ (600 mD)	9.0x10 ⁻¹⁴ (91 mD)	9.0x10 ⁻¹⁴ (91 mD)
Density of CO ₂ [kg/m ³]	610	720	712	266	215
Porosity, φ	0.15	0.37	0.175	0.2	0.2
Angle of dip, θ [degrees]	4.56	-	-	-	-

Table 16. Comparison of storage coefficients measured from operational data and analytical approximation for three case studies: Sleipner, Snøhvit and Ketzin. The difference between 2009 and 2012 analytical estimations at Ketzin is the density of the CO₂. Parameters used for analytically derived solutions at Sleipner and Snøhvit are not time dependent.

Case study	Analytically derived storage coefficient (year)		Storage coefficient from seismic data (year)			
	Sleipner	1.2%		1.8% (2001)	2.1% (2004)	1.9% (2006)
Snøhvit	3.7%		7.8% (2011)	10% (2012)		
Ketzin (70m thick)	2.0% (2009)	2.1% (2012)	3.9% (2009)	6.6% (2012)		
Ketzin (37m thick)	3.73% (2009)	4.02% (2012)	7.5% (2009)	12.5% (2012)		

6.2 STORAGE COEFFICIENT IN A DIPPING AQUIFER

Vella and Huppert (2006) describe an analytical solution for a gravity plume spreading under a dipping caprock. Dimensional analysis shows the approximate scales of the downslope and cross-slope extent of a plume at both short and long timescales. At short times, only a small adjustment from the axisymmetric results of Lyle et al. (2005) is required. At later times, the flow of CO₂ up the slope becomes dominant. The asymptotic scaling factors for the extent of a buoyant CO₂ plume travelling up-dip are given by (Vella and Huppert, 2006) as

$$\begin{array}{ll} Vt & \text{Downslope} \\ \left(\frac{Q}{\phi \tan \theta}\right)^{1/3} t^{1/3} & \text{Cross-slope} \end{array}$$

Where $V = \frac{kg\Delta\rho \sin \theta}{\mu\phi}$. Note that this is not valid for a flat caprock. This is because it is based on up-dip migration of the plume defining the dominant length scale in the up-dip direction. When θ is small, the axisymmetric approximation becomes more appropriate, and flow is dominated by radial spreading.

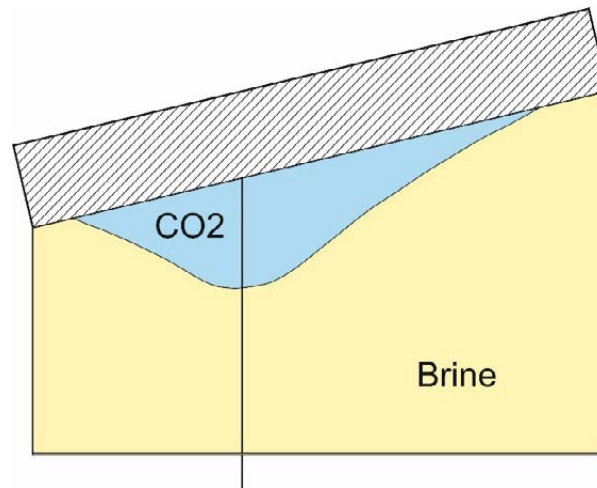


Figure 38. Diagram of a buoyant CO₂ plume spreading under a dipping caprock. Note that injection is modelled as a point source directly beneath the caprock.

Defining the area of the plume as that of an ellipse, πab , where a and b are the scaling factors for downslope and cross-slope migration as above, the storage efficiency can be calculated as per Equation 7 (where $r_N = ab$):

$$E = \frac{Q^{2/3} \mu (\phi \tan \theta)^{1/3}}{H \pi k g \Delta \rho \sin \theta} t^{-1/3} \quad (9)$$

As time increases, the area of the plume increases as driven by both the continued CO₂ injection and the buoyancy forces acting to migrate the CO₂ up-dip. The thickness of the plume at long timescales (after ~2.5 years) is proportional to $t^{-1/3}$, and therefore decreases with time. This is generally observed in numerical simulations of CO₂ storage, the plume spreads laterally and forms a thin layer under the caprock, continuing to travel up-dip according to the topography of the seal. This thinning of the CO₂ layer and continued up-dip migration means that the storage efficiency decreases with time (Figure 39). A simple model has been used in this formulation which only covers the injection period.

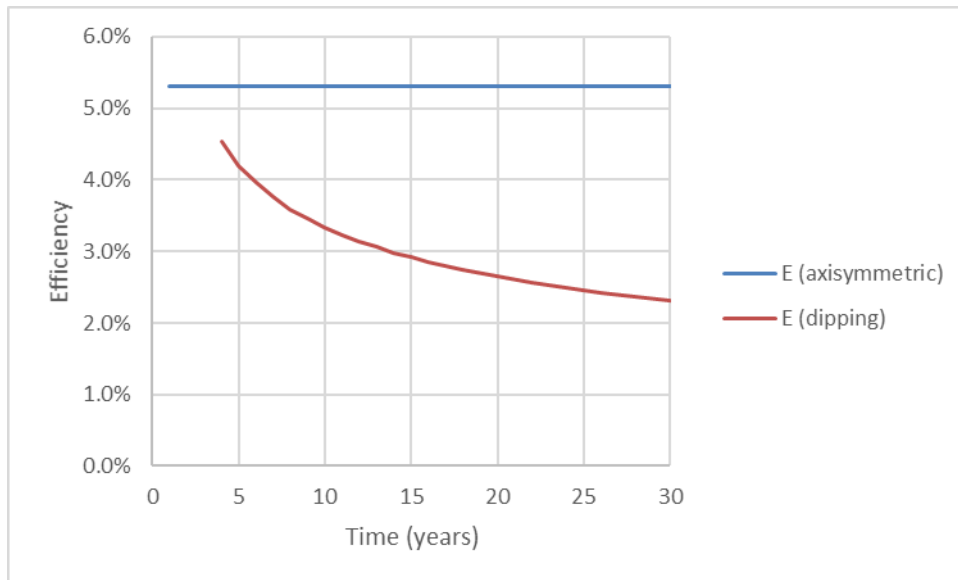


Figure 39. Comparison of analytical storage efficiency values with a caprock of no dip (blue) and a dip angle of 4.5 degrees (corresponding to the dome model in Section 5). A constant injection rate of 1 Mt/yr is assumed.

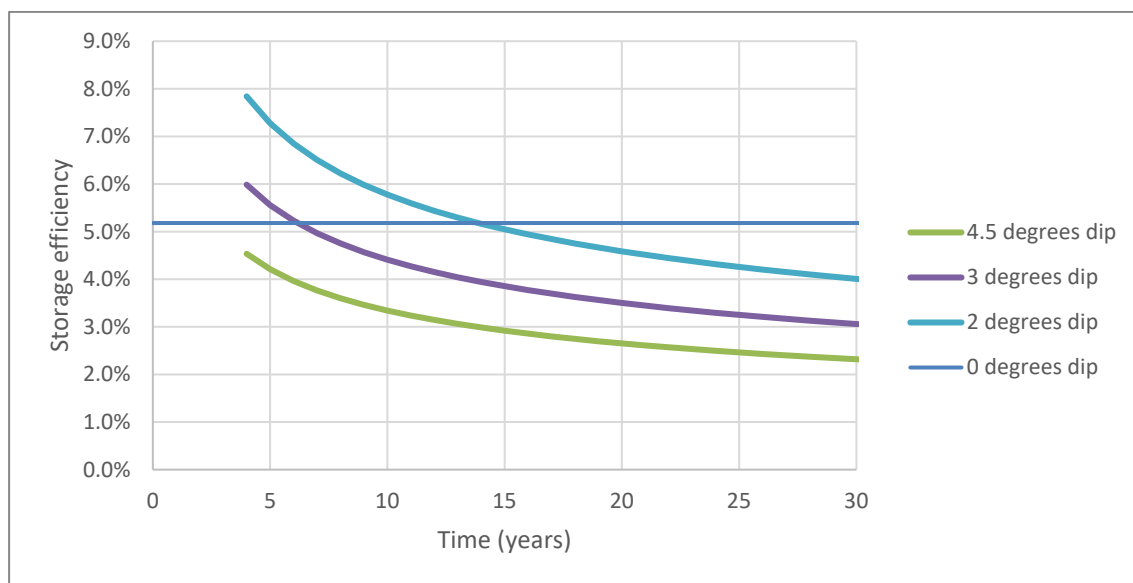


Figure 40. Influence of the angle of dip on the value of the storage coefficient calculated from Equation 9.

Due to the complicated relationship, it is not easy to visualise the dependence of the storage coefficient on the angle of dip from Equation 9. Figure 40 shows that a greater angle of dip results in a lower storage efficiency. This is not an unexpected result as a steeper angle of dip encourages faster migration of CO₂. A dip of 4.5 degrees represents the model in Section 5.1.1 and only the injection period is modelled.

The values of storage coefficients presented in Figure 39 are significantly lower than those calculated from the numerical simulations in Section 5 (Figure 18). One of the main differences between the two models is the location of the CO₂ injection. In the numerical modelling the middle half of the reservoir was modelled as perforations of an injection well and CO₂ entered the model

throughout this whole interval. This means that some of the deeper pore space is utilised right from the start. On the contrary with the analytical modelling, CO₂ enters the model from a single point directly beneath the caprock and immediately begins to spread laterally. This gives a much lower storage coefficient. The results could be more directly compared with additional numerical simulations where CO₂ is injected through a single cell.

The analytical model of CO₂ under a dipping caprock suggests that the storage coefficient decreases throughout the injection period (after the early stages). This is because the layer thickness is decreasing. The numerical simulations suggested that the storage coefficient for the same geological geometry increases to a peak after 20-30 years of injection. This is because the CO₂ is spreading through the deeper layers of the reservoir, primarily radially and making its way up to the top, and vertical travel does not increase the lateral area of the plume.

Despite using the same set of parameters, simple analytical approximations do not yield the exact same results calculated using more detailed numerical methods. The analytical solutions in this study give more conservative estimates of the storage efficiency coefficient than the numerical modelling. This does not mean that they do not have value. Analytical approximations like the ones used here are most relevant at the early stages of site screening and appraisal where only limited data is available. Secondly, these solutions clearly show how each of the included parameters impacts the storage coefficient. This is shown in a simple equation which would otherwise require numerous runs of numerical simulations to determine.

6.3 DISCUSSION OF STRUCTURAL TRAPS

In a geological setting with a structural trap, the geometry acts to increase the storage coefficient. Buoyancy forces drive the CO₂ into the trap and the thickness of the plume increases at the trap is filled. This gives the highest storage efficiency of any geological geometry and is highly dependent on the local topography. A simple way to calculate storage efficiency in this situation is not with analytical approximations but by defining a flat CO₂-water contact and calculating the available pore volume between this and the caprock. This is a standard procedure in industry. In this approach utilisation of deeper pore space, for example through residual trapping, is not included. Since this method requires such site-specific geometry of the caprock it is applicable to sites at higher resource classification stages and higher storage readiness levels. Generic modelling becomes less relevant as more detailed site information is available.

7 Discussion

The classification of resources for the geological storage of CO₂ has been developed over many years. Many different resource management schemas follow a similar pattern: increasing data and understanding in site characterisation and operation leads to greater certainty in storage resource. The classifications of resources within each system and the terms used for each category vary, but the broad structure and approach remains similar. Over time schemes have developed to include more complexity, and most recently schemes are becoming more aligned with project development and economics. The main two groups that have worked on developing schema in the past are the CSLF and the US DOE/IEAGHG.

The SRMS (developed by the Society of Petroleum Engineers) is based on and analogous to the PRME and is currently becoming the industry standard resource management system and is appropriate for the developing industry. Projects globally can now be compared using the SRMS classification. There has been a clear shift, with operators now using these ideas and methodologies when developing projects. However, having reviewed a series of national databases that assess storage potential on a regional or basin scale, it would be useful if the project-based SRMS could be extended to incorporate an internationally recognised classification scheme that is relevant for a wider range of Storage Readiness Levels. There is a requirement for additional funding to ensure that large scale characterisation studies in developed and developing countries are utilised and brought into alignment with one another globally. This would provide a clear framework when evaluating storage resource and expanding CCS more widely around the globe.

The idea of using storage efficiency for resource estimation is well established. Estimates of total storage resources are based on the available pore volume and a storage coefficient. Methods to estimate storage coefficients include several factors and the accuracy of it depends on the quality/quantity of site-specific data available. Initial estimates might only include estimates of parameters such as irreducible water saturation, more involved analysis might incorporate numerical modelling, and storage coefficients can even be calculated from operational data such as seismic. Where the site sits in terms of the resource classification scheme may be directly linked to how informed the estimate of the storage coefficient is. It is important when comparing storage coefficients to be aware of which data they are based on and also the precise definitions used.

There are some discrepancies between published methods of defining the storage coefficient, especially the denominator – i.e. the volume of storage resources it is based upon. The distinguishing feature of two main groups defining storage coefficients is whether to include irreducible water saturation within the storage coefficient or to apply it as a separate factor. This is a parameter that is easy to apply. Another source of uncertainty arises from how the denominator is defined. In this study the storage coefficient is based upon the lateral area of a CO₂ plume. This definition leads to an estimation of the volumetric displacement efficiency. Therefore it is based initially on the near-well area, and over time becomes more dependent on the topography and migration of the plume. The result gives an indication of the amount of pore space within the area of the plume that is utilised. Features such as low permeability shale layers work to increase the efficiency coefficient as the CO₂ pools in multiple layers. An alternative definition is to base the storage coefficient on the total storage resources of the entire site/model/aquifer. A previous study (IEAGHG 2018) used this definition and simulated injection through numerous wells. This allowed investigation of how the number of wells can be used to maximise CO₂ injection. Neither of these definitions are ideal, both could be considered as academic exercises and the storage coefficients with the most value are those based on real,

project-specific storage capacity and operational data. At the least, detailed numerical modelling is required for the most meaningful estimates of storage capacity.

This report has focussed on volumetric displacement efficiency but there are other factors to consider in parallel, including pressure limits. Volumetric displacement efficiency is based around a single plume of CO₂, and there are often multiple injection wells in a given CO₂ storage project.

There have been numerous studies on the estimation of storage coefficients and the parameters that have the most influence. A notable example being the EERC report (IEAGHG 2009) who present a comprehensive list of storage coefficients for a wide parameter space. It is noted that the bulk of this work using generic reservoir models has already been completed and links to observed data and the role of site-specific heterogeneities and variabilities are of most interest to project developers/operators. However, there is still scope within the community to apply these data sets and compare with cost effective tools to extend the scope of CCS to areas of undiscovered/theoretical resource potential. In addition, further links can be made between the classification of storage resources and the estimation of storage resources using coefficients. The quality of storage coefficient estimation is directly linked to the data (and therefore classification) that it is based upon. This will result in a clearer alignment of techniques and enable broader discussion between expert and interested stakeholders.

The use of analytical approximations of CO₂ injection to estimate storage coefficients is novel, albeit using highly simplifying assumptions for the reservoir. Simple approximations of CO₂ spreading under an impermeable caprock were taken from the literature and applied to the concept of storage coefficients. Cases of a flat caprock and a dipping caprock were modelled. Analytical expressions for the storage efficiency were obtained with dependence on injection rate, CO₂ viscosity, porosity, reservoir thickness, permeability, difference in density between CO₂ and brine, time, and angle of dip (the latter two not in the case of a flat caprock). The analytical solutions clearly show the influence of each of these parameters on the storage efficiency. These solutions are particularly useful for sites at a lower storage readiness level where lots of site-specific data are not available and can aid as a screening tool. They are useful for providing initial estimates of total storage resources. They are however much more limited than simple dynamic numerical models which can include any number of parameters.

Storage efficiencies from three types of data were compared: operation data at Sleipner, Snøhvit and Ketzin; numerical simulations of flow in a geological dome and a dipping aquifer; analytical models of flow under a flat and a dipping caprock. Analytical models with a flat caprock gave slightly lower storage efficiencies than operational data. This is due to the simplified models not including geological heterogeneities such as low permeability layers (clearly present at Sleipner) and lateral confinement of the plume. Analytical solutions in a dipping aquifer were also lower than the results of numerical simulations. Injection in the analytical models used in this study is through a point source directly beneath the caprock, whereas the numerical simulations have perforations over the middle half of the reservoir. This injection into deeper parts of the model is expected to significantly increase the storage efficiency because more of the deeper pore space is utilised. An improved analytical model might simulate CO₂ injection through the entire reservoir interval (or a proportion of it) and the storage coefficients would be expected to be higher.

Security of storage is a topic of particular interest to operators and regulators. Trapping mechanisms such as dissolution, residual, capillary, and mineralisation reduce risks associated with CO₂ storage and are desirable. Residual trapping in particular results in CO₂ being trapped throughout any pore space that the plume has swept. The models in this study showed that hysteresis and residual trapping had only a small overall effect on the storage coefficient, although this may be different in larger simulations where CO₂ is expected to migrate a long distance. The location and status of the CO₂ was greatly affected by hysteresis, with a large proportion

becoming residually trapped in the deeper layers of the model, leaving only a thin layer of mobile CO₂ under the caprock.

To quantify the security of storage, trapping efficiency may be used. This is defined as the fraction of total gas trapped in the immobile gas phase and dissolved in brine. This could be used in combination with the storage efficiency and would actually act in an opposite direction in some cases. There may be merit in informing the wider CCS stakeholder community that simply promoting storage coefficients in isolation can be misleading without due attention to other factors.

Estimates of storage coefficients can be made at all Storage Readiness Levels. Where detailed numerical models or operational monitoring data is available these estimates will be more accurate than for sites at lower SRLs where limited site-specific data is available. The usefulness of storage coefficients on any of these classifications is limited. As a site progresses through the classification schemes, detailed numerical models and operational data lead to an informed estimate of the capacity of the site. When there is little information available, e.g. for undiscovered resources that only appear in regional databases, the value of any storage coefficient estimated from such little data is limited.

As the global uptake of CCS increases and more projects come online, it would be valuable to verify the findings of existing modelling work, in order to provide assurance of that body of work for future assessment. The study of storage coefficients in the literature has found that a number of factors influence efficiency factors, including porosity, permeability, structural geometry, injection rate, heterogeneity, vertical flow barriers, and many more. The highest values of storage coefficients are found in structural traps where free CO₂ flow is directed into a laterally confined trap. Injection into deeper areas of a reservoir and at high injection rates also increases the storage coefficient by utilising the deeper pore space. Other factors which need to be considered include the injectivity of the reservoir formation and the pressure increase due to CO₂ injection. These should be evaluated on a site-by-site basis once target storage complexes are identified. This report has started this work in considering Sleipner, Snøhvit and Ketzin and shown that results can be considered alongside the modelled data. It is anticipated that the increase in operational understanding will result in small improvements in the storage efficiency, and the wide sharing of key findings is an important requirement for mutual optimisation of the wider storage resource.

7.1 FURTHER WORK

The task of global alignment of classification of total storage resources continues. An extension of the SRMS to include regional/undiscovered resources before they reach the project status would be useful. This would provide a more complete classification system. If this is to be undertaken then it is suggested that it is built onto the existing SRMS, rather than starting a new classification scheme or having two separate ones to work in parallel to one another. It is noted that the SRMS is project-based, but a way to make it applicable to a wider range of resources may lead to the discovery of new potential sites and projects. This may take the form of further classifying the total storage resource.

Numerical modelling is the basis of storage resource estimation and continues to be an essential part of CO₂ storage site appraisal and assessment as well as an invaluable tool for monitoring and conformance. Wherever possible numerical models form the basis of storage resources estimations and are more reliable than volumetric or analytical approximations of storage coefficients. This is expected to continue as the implementation of CCS expands around the globe.

Storage coefficients are not useful for projects at high SRLs, but efficiency coefficients calculated from these sites with lots of data can be used to inform achievable estimates for sites without so

much information available. To this end, it is proposed to expand the database of storage coefficients obtained using operational data. A starting point for this could be the work of CO₂CRC at the Otway Stage 3 demonstration. Another area with additional information available is Sleipner, where more recent seismic data can be used to calculate storage coefficients.

This report has taken one approach to using analytical methods to estimate storage coefficients. The fundamental physics approximations are particularly relevant to the definition of storage coefficient used in this report. Further work using analytical methods could be attempted from a different angle. The use of dimensionless variables to emulate or build upon some of the numerical modelling work may provide a way to estimate storage coefficients for a cheaper cost than using full dynamic simulations.

8 Conclusions

In this study the classification of storage resources and associated schema has been reviewed. These systems have become more complex over time and more aligned to the requirements of operational CO₂ storage. There is a body of work for new projects and interested stakeholders to utilise to ensure they are best equipped to assess and categorise their storage areas and sites. The SRMS is becoming the industry standard. Storage readiness levels are useful to categorise the level of development of storage sites and the modern methods link geological risks to economic and operational uncertainties.

Within this study the role of storage coefficients (or storage efficiency) have been investigated in the broader topic of geological storage resource estimation. Standard methodologies for calculating coefficients have been presented alongside examples of the usage uses in national and international databases. The key parameters affecting storage coefficients have been identified from the literature and highlighted in the relevant sections.

Real-world operational data at Sleipner, Snøhvit and Ketzin has been used to determine the evolution of “storage coefficients” for the plume area during progressive injection using time-lapse seismic data and published plume outlines. There is significant benefit in understanding real-world operational data from sites such as these. Results show how storage efficiency can develop with time and provide observations that allow the verification of modelled solutions.

A series of numerical simulations were performed addressing key parameters identified from the literature. Storage coefficients were evaluated for each case. The greatest storage coefficients were found in cases where CO₂ was injected into a structural trap, with values approaching around 12%. This structural case limited the lateral spreading of the plume and resulted in a thick layer of CO₂ under the caprock. For cases in a dipping aquifer, the storage coefficient was seen to increase during the injection phase, reaching a peak after 20-30 years of injection then gradually reducing in the post-injection phase. The values calculated are representative of the parameterisation employed in the models, but the results have wider implications for long term behaviour in the subsurface where CO₂ can continue to migrate. In the modelling conducted for this study, a storage efficiency value of around 6% was determined after 100 years of simulation.

It was found that higher injection rates lead to higher storage coefficients. The impact of water production on the storage coefficient as defined in this project was limited. This is because the primary impact of water production is on the pressure of the reservoir and not the position of a plume of CO₂. The position of the plume wasn't greatly affected by the extraction, even when large volumes of brine were produced. The storage coefficient used here is based on an elliptical cylinder enclosing the CO₂ plume. The pressure in the reservoir, however, was significantly reduced by the water production and there are clear operational benefits from producing pore fluids. If using the storage coefficient based on the entire pore volume of a storage site/complex with closed boundaries, then water production will be one of the main influencing parameters on the amount of CO₂ that may be injected.

The impact of hysteresis and residual trapping was investigated. Again, there was only a small impact on the storage coefficient as defined in this project, and this was due to a very thin (of order of 1 m thick) layer of mobile CO₂ just under the caprock and the fact that the storage efficiency here was calculated based on the lateral extent of the plume. The security of storage and the distribution of the CO₂ was greatly affected by hysteretic effects; residual trapping allowed a high proportion of the CO₂ to be trapped in the deeper layers of the reservoir, leaving only a thin layer of mobile CO₂.

Analytical models from the literature were applied in a novel way to estimate storage coefficients. These provide quick and easy estimates, particularly for sites which are at a lower stage of development and have limited data available. It is hoped that these simple tools will benefit the community in the early stages of site appraisal.

There is a substantial basis of work already publicly available on the formation of storage coefficients, together with many example values from generic numerical modelling studies. Opportunities to build on this may come from the increase in operational data available as CCS is rolled out around the globe. This work has begun in this report with data from, amongst others, Sleipner, Snøhvit and Ketzin. Verification of modelling data is key to improving predictions of storage coefficients for new and developing storage sites. The resource classification schemas, for example the SRMS, will continue to evolve to meet the needs of the growing industry.

References

British Geological Survey holds most of the references listed below, and copies may be obtained via the library service subject to copyright legislation (contact libuser@bgs.ac.uk for details). The library catalogue is available at: <https://of-ukrinerc.olib.oclc.org/folio/>.

- AKHURST, M, KIRK, K, NEELE, F, GRIMSTAD, A-A, BENTHAM, M, AND BERGMO, P. 2021. Storage Readiness Levels: communicating the maturity of site technical understanding, permitting and planning needed for storage operations using CO₂. *International Journal of Greenhouse Gas Control*, Vol. 110, 103402.
- ARTS, R, EIKEN, O, CHADWICK, A, ZWEIGEL, P, VAN DER MEER, L, AND ZINSZNER, B. 2004. Monitoring of CO₂ injected at Sleipner using time-lapse seismic data. *Energy*, Vol. 29, 1383-1392.
- BACHU, S. 2008a. Comparison between methodologies recommended for estimation of CO₂ storage capacity in geological media.
- BACHU, S. 2008b. Comparison between methodologies recommended for estimation of CO₂ storage capacity in geological media. *Carbon Sequestration Leadership Forum, Phase III Report*.
- BACHU, S. 2013. Drainage and imbibition CO₂/brine relative permeability curves at in situ conditions for sandstone formations in western Canada. *Energy Procedia*, Vol. 37, 4428-4436.
- BACHU, S. 2015. Review of CO₂ storage efficiency in deep saline aquifers. *International Journal of Greenhouse Gas Control*, Vol. 40, 188-202.
- BACHU, S, BONIJOLY, D, BRADSHAW, J, BURRUSS, R, CHRISTENSEN, N, HOLLOWAY, S, AND MATHIASSEN, O. 2007a. Estimation of CO₂ Storage Capacity in Geological Media, Phase 2. *Work under the auspices of the Carbon Sequestration Leadership Forum (www.cslforum.org). Final report from the task force for review and identification of standards for CO₂ storage capacity estimation*.
- BACHU, S, BONIJOLY, D, BRADSHAW, J, BURRUSS, R, HOLLOWAY, S, CHRISTENSEN, N P, AND MATHIASSEN, O M. 2007b. CO₂ storage capacity estimation: Methodology and gaps. *International Journal of Greenhouse Gas Control*, Vol. 1, 430-443.
- BATZLE, M, AND WANG, Z J. 1992. Seismic Properties of Pore Fluids. *Geophysics*, Vol. 57, 1396-1408.
- BENTHAM, M, MALLOWS, T, LOWNDES, J, AND GREEN, A. 2014. CO₂ STORAge evaluation database (CO₂ Stored). The UK's online storage atlas. *Energy Procedia*, Vol. 63, 5103-5113.
- BERGMANN, P, AND CHADWICK, A. 2015. Volumetric bounds on subsurface fluid substitution using 4D seismic time shifts with an application at Sleipner, North Sea. *Geophysics*, Vol. 80, B153-B165.
- BERGMO, P E, GRIMSTAD, A A, AND LINDEBERG, E. 2011. Simultaneous CO₂ injection and water production to optimise aquifer storage capacity. *International Journal of Greenhouse Gas Control*, Vol. 5, 555-564.
- BICKLE, M, CHADWICK, R A, HUPPERT, H E, HALLWORTH, M, AND LYLE, S. 2007. Modelling carbon dioxide accumulation at Sleipner: Implications for underground carbon storage. *Earth and Planetary Science Letters*, Vol. 255, 164-176.
- BIRKHOLZER, J T, CIHAN, A, AND ZHOU, Q. 2012. Impact-driven pressure management via targeted brine extraction: Conceptual studies of CO₂ storage in saline formations. *International Journal of Greenhouse Gas Control*, Vol. 7, 168-180.
- BOAIT, F C, WHITE, N J, BICKLE, M J, CHADWICK, R A, NEUFELD, J A, AND HUPPERT, H E. 2012. Spatial and temporal evolution of injected CO₂ at the Sleipner Field, North Sea. *Journal of Geophysical Research-Solid Earth*, Vol. 117.
- BRADSHAW, J, BACHU, S, BONIJOLY, D, BURRUSS, R, HOLLOWAY, S, CHRISTENSEN, N P, AND MATHIASSEN, O M. 2007. CO₂ storage capacity estimation: issues and development of standards. *International Journal of Greenhouse Gas Control*, Vol. 1, 62-68.

BRENNAN, S T, BURRUSS, R C, MERRILL, M D, FREEMAN, P A, AND RUPPERT, L F. 2010. A probabilistic assessment methodology for the evaluation of geologic carbon dioxide storage. *US Geological Survey Open-File Report*, Vol. 1127, 31.

BUMP, A P, AND HOVORKA, S D. 2023. Fetch-trap Pairs: Exploring definition of carbon storage prospects to increase capacity and flexibility in areas with competing uses. *International Journal of Greenhouse Gas Control*, Vol. 122, 103817.

BURNSIDE, N M, AND NAYLOR, M. 2014. review and implications of relative permeability of CO₂/brine systems and residual trapping of CO₂. *International Journal of Greenhouse Gas Control*, Vol. 23, 1-11.

BUSCHECK, T A, SUN, Y, CHEN, M, HAO, Y, WOLERY, T J, BOURCIER, W L, COURT, B, CELIA, M A, JULIO FRIEDMANN, S, AND AINES, R D. 2012. Active CO₂ reservoir management for carbon storage: Analysis of operational strategies to relieve pressure buildup and improve injectivity. *International Journal of Greenhouse Gas Control*, Vol. 6, 230-245.

CARLSON, F M. 1981. Simulation of relative permeability hysteresis to the nonwetting phase. *SPE annual technical conference and exhibition*, OnePetro.

CAVANAGH, A, WILKINSON, M, AND HASZELDINE, R. 2020. DELIVERABLE D2. 1 REPORT Methodologies for Cluster Development and Best Practices for Data Collection in the Promising Regions. *Bridging the Gap, Storage Resource Assessment Methodologies, EU H2020 STRATEGY CCUS Project*, Vol. 837754.

CAVANAGH, A J, AND HASZELDINE, R S. 2014. The Sleipner storage site: Capillary flow modeling of a layered CO₂ plume requires fractured shale barriers within the Utsira Formation. *International Journal of Greenhouse Gas Control*, Vol. 21, 101-112.

CHADWICK, R A, AND NOY, D J. 2010. History-matching flow simulations and time-lapse seismic data from the Sleipner CO₂ plume. *Petroleum Geology: From Mature Basins to New Frontiers - Proceedings of the 7th Petroleum Geology Conference, Vols 1 and 2*, 1171-1182.

CHADWICK, R A, WILLIAMS, G A, AND FALCON-SUAREZ, I. 2019. Forensic mapping of seismic velocity heterogeneity in a CO₂ layer at the Sleipner CO₂ storage operation, North Sea, using time-lapse seismics. *International Journal of Greenhouse Gas Control*, Vol. 90.

CHADWICK, R A, ZWEIGEL, P, GREGERSEN, U, KIRBY, G A, HOLLOWAY, S, AND JOHANNESSEN, P N. 2004. Geological reservoir characterization of a CO₂ storage site: The Utsira Sand, Sleipner, Northern North Sea. *Energy*, Vol. 29, 1371-1381.

CONSOLI, C P, HAVERCROFT, I, AND IRLAM, L. 2017. Carbon capture and storage readiness index: comparative review of global progress towards wide-scale deployment. *Energy Procedia*, Vol. 114, 7348-7355.

CONSOLI, C P, WILDGUST, N, AND CAUSEBROOK, R. 2015. *Global storage readiness assessment: an approach to assessing national readiness for wide-scale deployment of CO₂ geological storage projects*. (Melbourne: Global CCS Institute.) ISBN 978-0-9871863-7-9

COWTON, L R, NEUFELD, J A, WHITE, N J, BICKLE, M J, WHITE, J C, AND CHADWICK, R A. 2016. An inverse method for estimating thickness and volume with time of a thin CO₂-filled layer at the Sleipner Field, North Sea. *Journal of Geophysical Research-Solid Earth*, Vol. 121, 5068-5085.

DOE, U. 2008. *Carbon sequestration atlas of the United States and Canada*.

DUAN, Z H, HU, J W, LI, D D, AND MAO, S D. 2008. Densities of the CO₂-H₂O and CO₂-H₂P-NaCl systems up to 647 K and 100 MPa. *Energy & Fuels*, Vol. 22, 1666-1674.

DUAN, Z H, AND SUN, R. 2003. An improved model calculating CO₂ solubility in pure water and aqueous NaCl solutions from 273 to 533 K and from 0 to 2000 bar. *Chemical Geology*, Vol. 193, 257-271.

ETHERINGTON, J, AND RITTER, J. 2008. The 2007 SPE/WPC/AAPG/SPEE Petroleum Resources Management System (PRMS). *Journal of Canadian Petroleum Technology*, Vol. 47.

ETI. 2016a. D10: WP5A – Bunter Storage Development Plan, 10113ETIS-Rep-13-03

ETI. 2016b. D13: WP5D – Captain X Site Storage Development Plan, 10113ETIS-Rep-19-03.

FALCON-SUAREZ, I, PAPAGEORGIOU, G, CHADWICK, A, NORTH, L, BEST, A I, AND CHAPMAN, M. 2018. CO₂-brine flow-through on an Utsira Sand core sample: Experimental and modelling. Implications for the Sleipner storage field. *International Journal of Greenhouse Gas Control*, Vol. 68, 236-246.

FRAILEY, S. 2007. Methodology for development of Carbon Sequestration Capacity Estimates. 90 in *Carbon Sequestration Atlas of the United States and Canada*. UNITED STATES DEPARTMENT OF ENERGY, N E T L (editor).

FREIFELD, B, ZAKIM, S, PAN, L, CUTRIGHT, B, SHEU, M, DOUGHTY, C, AND HELD, T. 2013. Geothermal energy production coupled with CCS: a field demonstration at the SECARB Cranfield Site, Cranfield, Mississippi, USA. *Ghgt-11*, Vol. 37, 6595-6603.

FURNIVAL, S, BROWN, A, ROWBOTHAM, P, WRIGHT, I, AND DESILVA, R. 2017. Planning for Commercial Scale CO₂ Storage in a Massive UK Saline Aquifer.

FURNIVAL, S, WRIGHT, S, DINGWALL, S, BAILEY, P, BROWN, A, MORRISON, D, AND DE SILVA, R. 2014. Subsurface Characterisation of a Saline Aquifer Cited for Commercial Scale CO₂ Disposal. *12th International Conference on Greenhouse Gas Control Technologies, Ghgt-12*, Vol. 63, 4926-4936.

FURRE, A K, KIAER, A, AND EIKEN, O. 2015. CO₂-induced seismic time shifts at Sleipner. *Interpretation-a Journal of Subsurface Characterization*, Vol. 3, Ss23-Ss35.

GAMMER, D, GREEN, A, HOLLOWAY, S, AND SMITH, G. 2011. The Energy Technologies Institute's UK CO₂ storage appraisal project (UKSAP). *SPE Offshore Europe Oil and Gas Conference and Exhibition*, OnePetro.

GOODMAN, A, HAKALA, A, BROMHAL, G, DEEL, D, RODOSTA, T, FRAILEY, S, SMALL, M, ALLEN, D, ROMANOV, V, AND FAZIO, J. 2011. US DOE methodology for the development of geologic storage potential for carbon dioxide at the national and regional scale. *International Journal of Greenhouse Gas Control*, Vol. 5, 952-965.

GORECKI, C D, AYASH, S C, LIU, G, BRAUNBERGER, J R, AND DOTZENROD, N W. 2015. A comparison of volumetric and dynamic CO₂ storage resource and efficiency in deep saline formations. *International Journal of Greenhouse Gas Control*, Vol. 42, 213-225.

GORECKI, C D, LIU, G, BRAUNBERGER, J R, KLENNER, R C L, AYASH, S C, DOTZENROD, N W, STEADMAN, E N, AND HARJU, J A. 2014. CO₂ storage efficiency in deep saline formations. *Energy & Environmental Research Centre, IEAGHG, US DoE*.

GORECKI, C D, SORENSEN, J A, BREMER, J M, KNUDSEN, D J, SMITH, S A, STEADMAN, E N, AND HARJU, J A. 2009. Development of storage coefficients for determining the effective CO₂ storage resource in deep saline formations. *SPE International Conference on CO₂ Capture, Storage, and Utilization*, OnePetro.

GRUDE, S, LANDRØ, M, AND DVORKIN, J. 2014a. Pressure effects caused by CO₂ injection in the Tubåen Fm., the Snøhvit field. *International Journal of Greenhouse Gas Control*, Vol. 27, 178-187.

GRUDE, S, LANDRO, M, AND OSDAL, B. 2013. Time-lapse pressure-saturation discrimination for CO₂ storage at the Snohvit field. *International Journal of Greenhouse Gas Control*, Vol. 19, 369-378.

GRUDE, S, LANDRO, M, WHITE, J C, AND TORSÆTER, O. 2014b. CO₂ saturation and thickness predictions in the Tubæen Fm., Snohvit field, from analytical solution and time-lapse seismic data. *International Journal of Greenhouse Gas Control*, Vol. 29, 248-255.

HAERI, F, MYSHAKIN, E M, SANGUINITO, S, MOORE, J, CRANDALL, D, GORECKI, C D, AND GOODMAN, A L. 2022. Simulated CO₂ storage efficiency factors for saline formations of various lithologies and depositional environments using new experimental relative permeability data. *International Journal of Greenhouse Gas Control*, Vol. 119, 103720.

HANSEN, O, GILDING, D, NAZARIAN, B, OSDAL, B, RINGROSE, P, KRISTOFFERSEN, J B, EIKEN, O, AND HANSEN, H. 2013. Snohvit: The history of injecting and storing 1 Mt CO₂ in the fluvial Tubæen Fm. *Ghgt-11*, Vol. 37, 3565-3573.

HEIDUG, W. 2013. Methods to assess geologic CO₂ storage capacity: status and best practice. *International Energy Agency Workshop Report*.

HUANG, F, JUHLIN, C, HAN, L, KEMPKA, T, LUTH, S, AND ZHANG, F J. 2016. Quantitative evaluation of thin-layer thickness and CO₂ mass utilizing seismic complex decomposition at the Ketzin CO₂ storage site, Germany. *Geophysical Journal International*, Vol. 207, 160-173.

IEAGHG. 2009. Development of storage coefficients for CO₂ storage in deep saline formations. *EERC*.

IEAGHG. 2018. CO₂ Storage Efficiency in Deep Saline Formations - Stage 2.

IFC. 2010. International Formulation Committee of the Sixth International Conference on Properties of Steam.

JEONG, G S, KI, S, LEE, D S, AND JANG, I. 2021. Effect of the flow rate on the relative permeability curve in the CO₂ and brine system for CO₂ sequestration. *Sustainability*, Vol. 13, 1543.

- JUANES, R, MACMINN, C W, AND SZULCZEWSKI, M L. 2010. The footprint of the CO₂ plume during carbon dioxide storage in saline aquifers: storage efficiency for capillary trapping at the basin scale. *Transport in porous media*, Vol. 82, 19-30.
- KETZER, J, MACHADO, C X, ROCKETT, G C, AND IGLESIAS, R S. 2015. Brazilian atlas of CO₂ capture and geological storage, EDIPUCRS.
- KOPERNA, G, PASHIN, J, AND WALSH, P. 2017. Commercial Scale CO₂ Injection and Optimization of Storage Capacity in the South-eastern United States. *U.S. Department of Energy*.
- KOPP, A, CLASS, H, AND HELMIG, R. 2009a. Investigations on CO₂ storage capacity in saline aquifers—Part 2: Estimation of storage capacity coefficients. *International Journal of Greenhouse Gas Control*, Vol. 3, 277-287.
- KOPP, A, PROBST, P, CLASS, H, HURTER, S, AND HELMIG, R. 2009b. Estimation of CO₂ storage capacity coefficients in geologic formations. *Energy Procedia*, Vol. 1, 2863-2870.
- LENGLER, U, DE LUCIA, M, AND KÜHN, M. 2010. The impact of heterogeneity on the distribution of CO₂: Numerical simulation of CO₂ storage at Ketzin. *International Journal of Greenhouse Gas Control*, Vol. 4, 1016-1025.
- LUTH, S, IVANOVA, A, JUHLIN, C, JUHOJUNTTI, N, KASHUBIN, A, BERGMANN, P, AND GOTZ, J. 2012. 4D seismic monitoring of small CO₂ injection - Results from the Ketzin pilot site (Germany). *Harmonising Rock Engineering and the Environment*, 1747-1751.
- LUTH, S, IVANOVA, A, AND KEMPKA, T. 2015. Conformity assessment of monitoring and simulation of CO₂ storage: A case study from the Ketzin pilot site. *International Journal of Greenhouse Gas Control*, Vol. 42, 329-339.
- LYLE, S, HUPPERT, H E, HALLWORTH, M, BICKLE, M, AND CHADWICK, R A. 2005. Axisymmetric gravity currents in a porous medium. *Journal of Fluid Mechanics*, Vol. 543, 293-302.
- MATHIAS, S A, HARDISTY, P E, TRUDELL, M R, AND ZIMMERMAN, R W. 2009. Approximate solutions for pressure buildup during CO₂ injection in brine aquifers. *Transport in porous media*, Vol. 79, 265-284.
- NACAP. 2012. The North American Carbon Storage Atlas
- NATIONAL GRID. 2016. K43: Field Development Report.
- NETL, U. 2012. *The United States 2012 Carbon Utilization and Storage Atlas* (4th Edition edition). DOE/NETL-2012/1589. (Washington, DC.)
- NEUFELD, J A, AND HUPPERT, H E. 2009. Modelling carbon dioxide sequestration in layered strata. *Journal of Fluid Mechanics*, Vol. 625, 353-370.
- NORDBOTTEN, J M, CELIA, M A, AND BACHU, S. 2005a. Injection and storage of CO₂ in deep saline aquifers: Analytical solution for CO₂ plume evolution during injection. *Transport in porous media*, Vol. 58, 339-360.
- NORDBOTTEN, J M, CELIA, M A, BACHU, S, AND DAHLE, H K. 2005b. Semianalytical solution for CO₂ leakage through an abandonen well. *Environmental Science & Technology*, Vol. 39, 602-611.
- NORDEN, B, FORSTER, A, VU-HOANG, D, MARCELIS, F, SPRINGER, N, AND LE NIR, I. 2010. Lithological and Petrophysical Core-Log Interpretation in CO₂SINK, the European CO₂ Onshore Research Storage and Verification Project. *Spe Reservoir Evaluation & Engineering*, Vol. 13, 179-192.
- NORWEGIAN PETROLEUM DIRECTORATE. 2011. *CO₂ Storage Atlas Norwegian North Sea*. (Stavanger.)
- NOY, D J, HOLLOWAY, S, CHADWICK, R A, WILLIAMS, J D O, HANNIS, S A, AND LAHANN, R W. 2012. Modelling large-scale carbon dioxide injection into the Bunter Sandstone in the UK Southern North Sea. *International Journal of Greenhouse Gas Control*, Vol. 9, 220-233.
- OGCI. 2017. Multinational CO₂ Storage Resource Assessment, Availability of CO₂ storage capacity in key markets. INITIATIVE, O A G C.
- OKWEN, R, YANG, F, AND FRAILEY, S. 2014. Effect of geologic depositional environment on CO₂ storage efficiency. *Energy Procedia*, Vol. 63, 5247-5257.
- OKWEN, R T, STEWART, M T, AND CUNNINGHAM, J A. 2010. Analytical solution for estimating storage efficiency of geologic sequestration of CO₂. *International Journal of Greenhouse Gas Control*, Vol. 4, 102-107.
- OLDENBURG, C M. 2021. Radial storage efficiency for CO₂ injection: Quantifying effectiveness of local flow control methods. *Greenhouse Gases: Science and Technology*, Vol. 11, 795-806.

- OSDAL, B, ZADEH, H M, JOHANSEN, S, AND GILDING, D. 2013. CO₂ saturation and Thickness Prediction from 4D Seismic Data at the Snøhvit Field. 75th EAGE Conference and Exhibition. London.
- OSDAL, B, ZADEH, H M, JOHANSEN, S, GONZALEZ, R R, AND WAERUM, G O. 2014. Snøhvit CO₂ Monitoring using Well Pressure Measurement and 4D Seismic. Fourth EAGE CO₂ Geological Storage Workshop. Stavanger.
- REYNOLDS, C A, BLUNT, M J, AND KREVER, S. 2018. Multiphase Flow Characteristics of Heterogeneous Rocks From CO₂ Storage Reservoirs in the United Kingdom. *Water Resources Research*, Vol. 54, 729-745.
- RINGROSE, P. 2020a. Geological storage of CO₂: processes, capacity and constraints. 13-83 in *How to Store CO₂ Underground: Insights from early-mover CCS Projects*. (Springer.)
- RINGROSE, P. 2020b. *How to store CO₂ underground: Insights from early-mover CCS projects*. (Springer.) ISBN 303033113X
- RUTQVIST, J, VASCO, D W, AND MYER, L. 2010. Coupled reservoir-geomechanical analysis of CO₂ injection and ground deformations at In Salah, Algeria. *International Journal of Greenhouse Gas Control*, Vol. 4, 225-230.
- SANGUINITO, S, GOODMAN, A L, AND HAERI, F. 2020. CO₂ Storage prospective Resource Estimation Excel aNalysis (CO₂-SCREEN) User's Manual. *National Energy Technology Lab.(NETL), Pittsburgh, PA (United States)*.
- SANGUINITO, S M, GOODMAN, A, AND LEVINE, J. 2017. NETL CO₂ Storage prospective Resource Estimation Excel aNalysis (CO₂-SCREEN) User's Manual. *National Energy Technology Lab.(NETL), Pittsburgh, PA,(United States)*.
- SAWADA, Y, TANAKA, J, SUZUKI, C, TANASE, D, AND TANAKA, Y. 2018. Tomakomai CCS Demonstration Project of Japan, CO₂ Injection in Progress. *Applied Energy Symposium and Forum, Carbon Capture, Utilization and Storage, Ccus 2018*, Vol. 154, 3-8.
- SNIPPE, J, AND TUCKER, O. 2014. CO₂ fate comparison for depleted gas field and dipping saline aquifer. *Energy Procedia*, Vol. 63, 5586-5601.
- SPAN, R, AND WAGNER, W. 1996. A new equation of state for carbon dioxide covering the fluid region from the triple-point temperature to 1100 K at pressures up to 800 MPa. *Journal of Physical and Chemical Reference Data*, Vol. 25, 1509-1596.
- SPE-SRMS. 2017. *CO₂ Storage Resources Management System*.
- TANAKA, Y, ABE, M, SAWADA, Y, TANASE, D, ITO, T, AND KASUKAWA, T. 2014. Tomakomai CCS Demonstration Project in Japan, 2014 Update. *12th International Conference on Greenhouse Gas Control Technologies, Ghgt-12*, Vol. 63, 6111-6119.
- TANASE, D, SASAKI, T, YOSHII, T, MOTOHASHI, S, SAWADA, Y, ARAMAKI, S, YAMANOUCHI, Y, TANAKA, T, OHKAWA, S, AND INOWAKI, R. 2013. Tomakomai CCS Demonstration Project in Japan. *Ghgt-11*, Vol. 37, 6571-6578.
- TIAN, L, YANG, Z, FAGERLUND, F, AND NIEMI, A. 2016. Effects of permeability heterogeneity on CO₂ injectivity and storage efficiency coefficient. *Greenhouse Gases: Science and Technology*, Vol. 6, 112-124.
- UNITED NATIONS ECONOMIC COMMISSION FOR EUROPE, U. 2020. United Nations framework classification for resources: update 2019.
- VELLA, D, AND HUPPERT, H E. 2006. Gravity currents in a Porous medium at an inclined plane. *Journal of Fluid Mechanics*, Vol. 555, 353-362.
- VINCENT, C J, BENTHAM, M, KIRK, K, AKHURST, M, AND PEARCE, J. 2017. Evaluation of barriers to national CO₂ geological storage assessments. *Energy Procedia*, Vol. 114, 4750-4756.
- VOSPER, H, CHADWICK, R A, AND WILLIAMS, G A. 2018. CO₂ plume migration in underground CO₂ storage: the effects of induced hydraulic gradients. *International Journal of Greenhouse Gas Control*, Vol. 74, 271-281.
- WANG, Y, ZHANG, K, AND WU, N. 2013. Numerical investigation of the storage efficiency factor for CO₂ geological sequestration in saline formations. *Energy Procedia*, Vol. 37, 5267-5274.
- WEATHERFORD LABORATORIES. 2015. National Grid Well 42/25d-3 Conventional Core Analysis final report.
- WHITE, J, WILLIAMS, G, AND CHADWICK, R A. 2018. Seismic amplitude analysis provides new insights into CO₂ plume morphology at the Snøhvit CO₂ injection operation. *International Journal of Greenhouse Gas Control*, Vol. 79, 313-322.

- WHITE, J C, WILLIAMS, G, AND CHADWICK, A. 2018a. Seismic amplitude analysis provides new insights into CO₂ plume morphology at the Snohvit CO₂ injection operation. *International Journal of Greenhouse Gas Control*, Vol. 79, 313-322.
- WHITE, J C, WILLIAMS, G, CHADWICK, A, FURRE, A K, AND KIAER, A. 2018b. Sleipner: The ongoing challenge to determine the thickness of a thin CO₂ layer. *International Journal of Greenhouse Gas Control*, Vol. 69, 81-95.
- WHITE, J C, WILLIAMS, G A, GRUDE, S, AND CHADWICK, R A. 2015. Utilizing spectral decomposition to determine the distribution of injected CO₂ at the SnOhvit Field. *Geophysical Prospecting*, Vol. 63, 1213-1223.
- WIESE, B, NIMTZ, M, KLATT, M, AND KUHN, M. 2010. Sensitivities of injection rates for single well CO₂ injection into saline aquifers. *Chemie Der Erde-Geochemistry*, Vol. 70, 165-172.
- WILLIAMS, G A, AND CHADWICK, R A. 2017. An improved history-match for layer spreading within the Sleipner plume including thermal propagation effects. *13th International Conference on Greenhouse Gas Control Technologies, Ghgt-13*, Vol. 114, 2856-2870.
- WILLIAMS, G A, AND CHADWICK, R A. 2021. Influence of reservoir-scale heterogeneities on the growth, evolution and migration of a CO₂ plume at the Sleipner Field, Norwegian North Sea. *International Journal of Greenhouse Gas Control*, Vol. 106, 103260.
- WIPKI, M, IVANOVA, A, LIEBSCHER, A, LUTH, S, MOLLER, F, SZIZYBALSKI, A, WIESE, B, AND ZIMMER, M. 2016. Monitoring Concept for CO₂ Storage at the Ketzin Pilot Site, Germany -post - injection continuation towards transfer of liability. *European Geosciences Union General Assembly 2016*, Vol. 97, 348-355.
- WU, H, JAYNE, R S, AND POLLYEA, R M. 2018. A parametric analysis of capillary pressure effects during geologic carbon sequestration in a sandstone reservoir. *Greenhouse Gases: Science and Technology*, Vol. 8, 1039-1052.
- ZHANG, G R, LU, P, JI, X Y, AND ZHU, C. 2017. CO₂ plume migration and fate at Sleipner, Norway: Calibration of numerical models, uncertainty analysis, and reactive transport modelling of CO₂ trapping to 10,000 years. *13th International Conference on Greenhouse Gas Control Technologies, Ghgt-13*, Vol. 114, 2880-2895.
- ZHANG, G R, LU, P, AND ZHU, C. 2014. Model predictions via history matching of CO₂ plume migration at the Sleipner Project, Norwegian North Sea. *12th International Conference on Greenhouse Gas Control Technologies, Ghgt-12*, Vol. 63, 3000-3011.
- ZHOU, Q, BIRKHOLZER, J T, TSANG, C-F, AND RUTQVIST, J. 2008. A method for quick assessment of CO₂ storage capacity in closed and semi-closed saline formations. *International Journal of Greenhouse Gas Control*, Vol. 2, 626-639.
- ZHOU, Q, BIRKHOLZER, J T, TSANG, C-F, AND RUTQVIST, J. 2008. A method for quick assessment of CO₂ storage capacity in closed and semi-closed saline formations. *International Journal of Greenhouse Gas Control*, Vol. 2, 626-639.
- ZHU, C, ZHANG, G R, LU, P, MENG, L F, AND JI, X Y. 2015. Benchmark modeling of the Sleipner CO₂ plume: Calibration to seismic data for the uppermost layer and model sensitivity analysis. *International Journal of Greenhouse Gas Control*, Vol. 43, 233-246.

Appendix A. What makes a good geological storage site?

INTRODUCTION

Man-made Carbon Dioxide (CO₂) emissions resulting from the burning of fossil fuels or heavy industry are largely responsible for the increased levels of CO₂ in the atmosphere that have arisen since the industrial revolution, contributing to global warming.

It is possible to capture CO₂ at fossil fuel-burning power plants and inject it via wells and store it deep under the ground in geological formations. This prevents it entering the atmosphere where it acts as a greenhouse gas.

A GEOLOGICAL STORAGE SITE

The aim of the geological storage of CO₂ is to prevent CO₂ reaching the atmosphere by locking it away deep underground. The CO₂ gas can be captured at the power station after or before the fuel is burnt (pre or post combustion capture). After the CO₂ is captured, it can be compressed and transported by pipelines to a suitable geological storage site, either on- or off-shore where it is then pumped via a well or wells deep underground.

As the storage site may be required to store the CO₂ for tens or hundreds or thousands of years they need to be chosen very carefully on the basis of their geological characteristics. For safe storage in oil or gas fields and aquifers, the storage site must have the geological requirements summarised below.

Reservoir rock, porosity and permeability

A reservoir rock is a layer of rock that is capable of storing fluids within its structure. Nearly all reservoir rocks are sedimentary rocks, and they are commonly composed of individual grains of sand or carbonate (the main building blocks of limestones) cemented together at their edges. A reservoir rock has gaps between the individual grains of rock called pore spaces. These pore spaces need to be connected by pore throats, so that fluid can flow into and out of the rock creating permeability. This is a measure of how efficiently fluids can flow through the rock and depends on the size of the pore throats and how well the pore spaces are connected via the pore throats, and it is essential for the injection of fluids.

Under natural conditions, the pore spaces of reservoir rocks are filled with fluids (sometimes described as native pore fluids), except where they are above the water table in onshore areas. The commonest pore fluids are water (which may be fresh or saline) and then oil and gas. When CO₂ is pumped (injected) into the rock it enters the pore spaces, partially or completely pushing out (displacing) the fluids that were originally present. There is usually a small amount of the native pore fluid left in the pore spaces, held in place by capillary forces, or adsorbed onto the rock grains. This is known as the residual saturation.

Cap rock or seal

This is a rock layer above the reservoir that will form a barrier between the reservoir rock containing CO₂ in its pore spaces, and the surface, preventing the CO₂ moving out of the storage site. Cap rocks/seals need to have a low to zero permeability, so liquids and gases cannot pass through them and escape. Cap rocks can be divided into two categories; essentially impermeable strata such as thick rock salt layers (known as aquicludes) and those with low permeability such

as shales and mudstones, known as aquitards, through which fluids can migrate, albeit extremely slowly.

Appendix B. Techno-economic resource pyramid from Bachu et al. (2007)

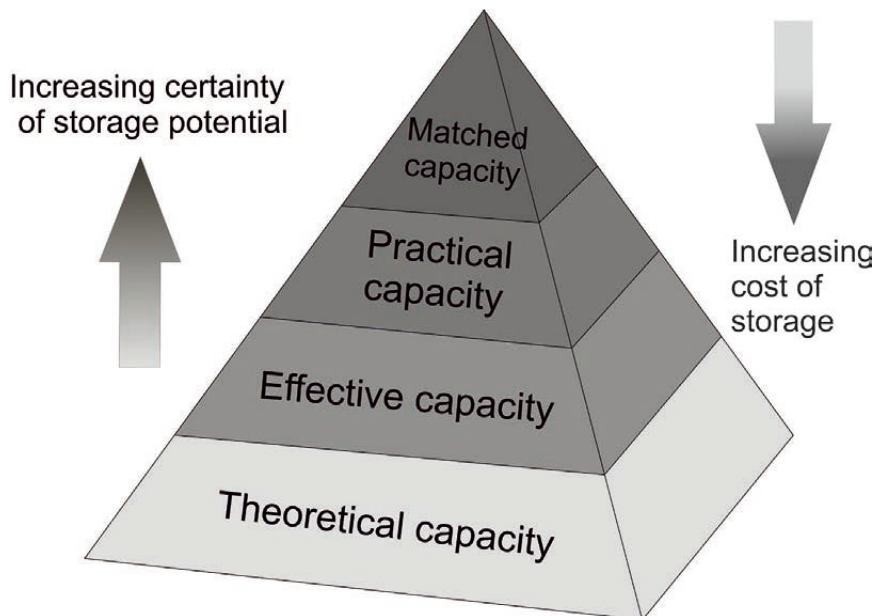


Figure A2. Techno-Economic Resource-Reserve pyramid for CO₂ storage capacity in geological media within a jurisdiction or geographic region. The pyramid shows the relationship between Theoretical, Effective, Practical and Matched capacities (from CSLF, 2007)

The pyramid indicates the accuracy of the storage capacity estimate based on the level of detail available to undertake the capacity estimation. The main issues with determining the CO₂ storage capacity are the availability of data; the availability of time and resources to interpret the available data; the necessary skills to undertake storage capacity estimates. This can be expressed through the levels of the Techno-Economic Resource-Reserve pyramid.

Theoretical Storage Capacity is the total resource. It encompasses the whole of the resource pyramid. It is the physical limit of what the geological system can accept. It assumes that the system's entire capacity to store CO₂ in pore space, or dissolved at maximum saturation in formation fluids, or adsorbed at 100% saturation in the entire coal mass, is accessible and utilized to its full capacity.

Effective Storage Capacity represents a subset of the 'theoretical' capacity and is obtained by considering that part of the theoretical storage capacity that can be physically accessed and which meets a range of geological and engineering criteria.

Practical Storage Capacity is that subset of the 'effective' capacity that is obtained by considering technical, legal and regulatory, infrastructural and general economic barriers to CO₂ geological storage. The 'Practical' Storage Capacity corresponds to the term 'reserves' used in the energy and mining industries.

Matched Storage Capacity is that subset of the 'practical' capacity that is obtained by detailed matching of large stationary CO₂ sources with geological storage sites that are adequate in terms of capacity, injectivity and supply rate to contain CO₂ streams sent for storage from that source or sources. This capacity is at the top of the resource pyramid and corresponds to the term 'proved marketable reserves' used by the mining industry.



IEA Greenhouse Gas R&D Programme

Pure Offices, Cheltenham Office Park, Hatherley Lane,
Cheltenham, Glos. GL51 6SH, UK

Tel: +44 1242 802911

mail@ieaghg.org
www.ieaghg.org